

ABSTRACT

Title of Thesis: DYNAMICS OF NITROGEN AND
METHANE IN GROUND AND SURFACE
WATERS

Dana Elizabeth Bunnell-Young, Master of
Science, 2020

Thesis Directed By: Professor Thomas R. Fisher, Department of
Marine Estuarine Environmental Science

Methane and nitrogen have critically important biogeochemical cycles. Methane is a strong greenhouse gas, while nitrogen is a eutrophication agent in estuarine and coastal systems. This thesis investigates the presence of methane and nitrogen in groundwater and streams as well as any linkages between these biogeochemical cycles. In agricultural groundwater with elevated nitrogen concentrations, dissolved methane concentrations ranged from 0 to over 400 μM . Restored streams in forested and urban watersheds had a range of methane concentrations from 0 to 5.37 μM . The impact of land use was investigated as well, finding that within 3-5 years after the cessation of intensive grain production, groundwater nitrate concentrations in the top of the surface unconfined aquifer dropped from 11 mg $\text{NO}_3^- \text{-N L}^{-1}$ to 0.5 mg $\text{NO}_3^- \text{-N L}^{-1}$. Biogeochemical methods were used to investigate the process of anaerobic oxidation of methane coupled to denitrification in agricultural soils and groundwater.

DYNAMICS OF NITROGEN AND METHANE IN GROUND AND SURFACE
WATERS

by

Dana Elizabeth Bunnell-Young

Thesis submitted to the Faculty of the Graduate School of the
University of Maryland, College Park, in partial fulfillment
of the requirements for the degree of
Master of Science
2020

Advisory Committee:
Professor Thomas R. Fisher, Chair
Professor Jeffrey Cornwell
Dr. Thomas Jordan

© Copyright by
Dana Elizabeth Bunnell-Young
2020

Dedication

To Miles.

Acknowledgements

I feel like it has been a lifetime since I started this journey (well technically it has been 2 lifetimes for my son). I never would have gotten started if it wasn't for my undergraduate mentor, Dr. Jeffrey Simmons. Dr. Simmons pushed me to learn outside of the classroom and books. He gave me my first opportunity to conduct research in the field and the lab. At first, I was skeptical about Dr. Simmons's excitement over the phosphorus cycle, but I eventually came around and found my own love for environmental chemistry. I am eternally grateful the start that I received with Dr. Simmons at Mount St. Mary's University.

Upon starting the MEES program, I have been surrounded by an amazing community of faculty, research assistants, post-docs, and students. Each class and seminar have pushed me to think further and ask more questions. There are too many individuals to list, but a few that I would like to mention are Dr. Laura Lapham, Dr. Laura Murray, Dr. Judy O'Neil, Dr. Walter Boynton, Dr. Mark Castro, Becky Swerida, Dr. Katherine Slater, Dr. Jennifer Webster, and Allison Barba.

I owe a great deal of thanks to the Fisher lab group and all of the help that I received. Anne Gustafson and Dr. Rebecca Fox offered great guidance, friendship, and assistance in troubleshooting in the lab and the field. Dr. John Gardner, Keota Silaphone, and Lindsay Tempinson were always up for helping with field work, to talk over thesis ideas, or just to lament on the life of a graduate student (much appreciated to each of you). In terms of field work, I received great guidance and

help from several individuals, including Tim Rosen, Drew Koslow, Tucker Moorshead, Kalla Kvalnes, Dr. Karen Knee, Dr. Joshua Thompson, and Ryan Saba.

Clearly, none of this is possible without the guidance and support of my advisor, Dr. Tom Fisher. Tom loves his work, and it shows with the care he takes with his graduate students. Tom has supported me as a graduate student, a wife and mother, a new teacher, and a developing scientist. Thank you, Tom for all that you have done. I would also like to thank my other two committee members, Dr. Jeffrey Cornwell and Dr. Tom Jordan. I have enjoyed our scientific discussions and the excitement that you both show when looking at new data.

I would be remiss if I did not mention my family. From a young age, my parents have encouraged me to dream big. They always knew that I would end up being a scientist, even if I didn't always believe them. Thank you, Mom and Dad, for all your love and support. Finally, I don't think I ever would have finished if it wasn't for my husband, Taylor. We started this journey together and have celebrated many milestones along the way, including the birth of our son, Miles. It hasn't always been easy, but I have never been alone. From staying home with a screaming newborn while I worked evenings in the lab, to helping me collect field samples, to encouraging me every step of the way. You have always been there for me. I love you.

Table of Contents

Dedication.....	ii
Acknowledgements	iii
Table of Contents.....	v
List of Tables	viii
List of Figures.....	ix
List of Abbreviations	xi
Chapter 1: Dynamics of Nitrogen and Methane Cycling	1
Introduction	1
Nitrogen and Methane	1
Nitrate and Methane in the Environment	1
Nitrate	1
Methane	2
Cycling of Nitrate and Methane	3
Nitrogen Cycle.....	3
Classic Biological Methane Cycle.....	4
Anaerobic Oxidation of Methane (AOM)	5
Anaerobic Oxidation of Coupled to Denitrification	7
Land Use Changes Associated with Changes in Nitrate and Methane.....	9
Nitrate	9
Methane	9
Thesis Goals	11
Overarching Themes.....	11
Spatial Distribution of Methane in Groundwater and Streams.....	11
Dynamics of Nitrate and Methane in Shallow Groundwater Following Land Use Conversion from Agricultural Grain Production to Conservation Easement.....	12
Biogeochemical Investigation of Simultaneous Metabolism of Nitrogen and Methane	12
Figures	13
Chapter 2: Spatial Distribution and Efflux of Methane in Groundwater and Streams	18
Introduction	18
Landscape Methane Overview	18
Groundwater Methane	19
Fluvial Methane	20
Hypotheses and Experimental Design	22
Methods	23
Agricultural Watershed Field Sampling	23
Urban Streams Field Sampling	24
Analytical Methods.....	24
Urban Stream Flux Sampling	25
Calculating Stream Fluxes.....	25
Statistics	26
Results	26
Agricultural Watershed Comparisons	26

Groundwater Relationships	27
Fluvial Methane and Land Use.....	27
Stream Fluxes	28
Discussion.....	28
Agricultural Watershed Comparisons	28
Groundwater Relationships	29
Stream Relationships	30
Urban Stream Fluxes	31
Test of the Hypotheses	32
Landscape Methane	33
Acknowledgements	33
Tables.....	34
Figures	35
Chapter 3: Dynamics of Nitrate and Methane in Shallow Groundwater Following Land Use Conversion from Agricultural Grain Production to Conservation Easement	42
Introduction	42
Materials and Methods	47
Study Sites	47
Piezometer Installation	49
Groundwater Sampling.....	49
Groundwater and Climate Data	50
Analytical Methods.....	51
Statistics.....	51
Results	52
Temperature, Rainfall, and Groundwater Levels	52
General Groundwater Chemistry.....	53
Seasonal Nitrate Variability.....	54
Nitrate Chronosequence	55
Seasonal Methane Variability.....	56
Methane Chronosequence.....	57
Discussion.....	57
Temporal Variations in Nitrate.....	57
Groundwater Nitrate Model.....	61
Temporal Variations in Methane	65
Acknowledgements	67
Tables and Figures.....	68
Tables.....	68
Figures	72
Chapter 4: Biogeochemical Investigation of Simultaneous Metabolism of Nitrogen and Methane	82
Introduction	82
Methanogenesis	82
Aerobic Methane Oxidation	83
AOM Coupled to Sulfate Reduction	84
AOM Coupled to Manganese or Iron Reduction.....	85

AOM Coupled to Denitrification.....	86
AOM as a Potential Methane Sink	87
Methane Production and Oxidation in Soils and Groundwater	88
Hypotheses and Experimental Design.....	89
Methods	90
Study Sites	90
Sampling Methods.....	90
Soil Slurry Incubations	91
Soil Core Incubations	92
<i>In-Situ</i> Additions.....	93
Statistics.....	93
Results	94
Soil Slurry Incubations	94
Soil Core Incubations	95
<i>In-Situ</i>	97
Discussion.....	98
Soil Slurry Incubations	98
Soil Core Incubations	99
<i>In-Situ</i>	102
Hypotheses.....	103
Acknowledgements	104
Tables and Figures.....	105
Tables.....	105
Figures	108
Bibliography	118

This Table of Contents is automatically generated by MS Word, linked to the Heading formats used within the Chapter text.

List of Tables

Chapter 2.

Table 1. Summary of methane data.....	34
Table 2. Urban sampling sites.....	34
Table 3. Average watershed outlet stream concentrations.....	35
Table 4. Average concentrations of dissolved gases at urban sampling sites..	35

Chapter 3.

Table 1. Sampling location descriptions.....	68
Table 2. Summary of average groundwater chemistry.....	69
Table 3. Seasonal variability of nitrate concentrations.....	70
Table 4. Denitrification and nitrogen uptake rates from literature.....	71

Chapter 4.

Table 1. Slurry data statistics.....	105
Table 2. Soil core incubation data statistics.....	106
Table 3. Comparison of growth coefficients for soil incubations.....	107

List of Figures

Chapter 1.	
Figure 1. Nitrogen cycle in anoxic and oxic environment with AOM-D.....	13
Figure 2. Methane pathway processes.....	14
Figure 3. Oxidation of organic carbon and methane in groundwater with sequence of electron acceptors.....	15
Figure 4. Percent oxygen saturation and nitrate concentrations in groundwater and methane and excess N ₂ in vadose zone at an agricultural site.....	16
Figure 5. Methane concentrations, nitrate concentration, and oxygen saturation for groundwater and vadose zone samples collected on the Eastern Shore of Maryland.....	17
Chapter 2.	
Figure 1. Methane transport pathways from groundwater.....	35
Figure 2. Distribution of terminal electron acceptors in groundwater.....	36
Figure 3. Map of sampling sites.....	36
Figure 4. Conceptual diagram of methane transport in streams.....	37
Figure 5. Stream and groundwater averages for methane and nutrients.....	38
Figure 6. Groundwater methane and nitrogenous-compound concentrations in agricultural watersheds.....	38
Figure 7. Stream methane concentrations in 16 watersheds and percent soil class.....	39
Figure 8. Watershed outlet methane vs. percent urban.....	40
Figure 9. Methane fluxes in urban streams.....	40
Figure 10. Stream carbon dioxide concentrations at Wilelinor Creek.....	41
Chapter 3.	
Figure 1. Map of study sites.....	72
Figure 2. Weather data for Trappe, MD.....	73
Figure 3. Groundwater temperature and depth below ground.....	74
Figure 4. Seasonal groundwater nitrate variability.....	75
Figure 5. Groundwater nitrate chronosequence.....	76
Figure 6. Season variability of dissolved methane.....	77
Figure 7. Groundwater methane chronosequence.....	78
Figure 8. Methane and nitrate in groundwater.....	79
Figure 9. Conceptual model of nitrogen processes.....	79
Figure 10. Annual groundwater nitrate concentrations.....	80
Figure 11. Projected groundwater nitrate concentrations.....	81

Chapter 4.

Figure 1. Conceptual model of methane and nitrate in groundwater.....108

Figure 2. Conceptual diagram of experimental design for soil incubations..109

Figure 3. Oxygen levels in incubation chambers.....110

Figure 4. Diagram of closely spaced piezometer nest.....110

Figure 5. Expected patten of results for soil incubations.....111

Figure 6. Average headspace methane for slurry incubations.....112

Figure 7. Average headspace methane for forest soil core incubations.....113

Figure 8. Average headspace methane for wetland soil core incubations....114

Figure 9. Average headspace methane for crops soil core incubation.....115

Figure 10. Headspace methane and CO₂ for segmented soil cores.....116

Figure 11. Groundwater conductivity, temperature, and depth below ground
for closely spaced piezometer nest.....117

Figure 12. Methane and oxygen levels for forested soil core incubations with
leaking chamber lids.....117

List of Abbreviations

Anammox-Anaerobic ammonium oxidation

AOM-Anaerobic oxidation of methane

AOM-D: Anaerobic oxidation of methane coupled to denitrification

MCR: Methyl-coenzyme M reductase

MIMS: Membrane inlet mass spectrometry

DOC: Dissolved organic carbon

CRP: Conservation reserve program

CREP: Conservation reserve enhancement program

A: Surface nitrogen applications

D: Denitrification

U: Plant nitrogen uptake

E: Export

ANME: Anaerobic methanotrophic Archaea

SRB: Sulfate-reducing bacteria

GC-FID: Gas chromatography-flame ionization detector

CSPN: Closely spaced piezometer nest

ANOVA: Analysis of variation

NS: Not significant

MS: Marginally significant

*: Significant

** : Highly significant

Chapter 1: Dynamics of Nitrogen and Methane Cycling

Introduction

Nitrogen and Methane

In the Chesapeake Bay region, a primary concern is eutrophication and the role of land use in nutrient releases to the environment. On a global scale, a more pressing concern is for climate change and the anthropogenic emissions of greenhouse gases. Although these two environmental dilemmas are typically considered isolated from one another, they both involve the cycling of elements (predominately nitrogen and carbon, respectively) and can be connected through biogeochemical interactions. This thesis will evaluate the dynamics of a primary eutrophication agent, nitrate, and a primary climate change agent, methane, in an agricultural landscape.

Nitrate and Methane in the Environment

Nitrate

Nitrate (NO_3^-) is a primary concern in estuaries for its role in eutrophication. Nitrogen is a limiting nutrient for phytoplankton in coastal areas for the majority of the year (Fisher et al. 1992), so when excess nitrate enters aquatic systems, algal blooms become common. These algal blooms lead to a cascade of events, culminating in the establishment of anoxic regions, called ‘dead zones’ (Ryther and

Dunstan 1971, Smith et al. 1999, Kemp et al. 2005). The Chesapeake Bay has been plagued with seasonal hypoxia and anoxia since the 1950s (Kemp et al. 2005).

In an environment undisturbed by human activity, nutrient levels are low and the ecosystem has a balance of the nitrogen that it needs. The largest pool of nitrogen is triple-bonded dinitrogen gas (N_2) in the atmosphere. This triple-bond is not easily broken and is only fixed naturally by the high temperatures of lightning and a select group of nitrogen-fixing microbes (Galloway et al. 1995, Galloway et al. 2004).

Anthropogenic activities, though, have vastly changed concentrations of nitrogen and phosphorus in soils and water. The Haber-Bosch process is the synthetic production of ammonia (NH_3) from N_2 and became the primary source of ammonia for agricultural use in the 1930s (Galloway et al. 2004). Synthetic fertilizers are now used widely, and this increase in nitrogen applications to land has led to an increase in nitrogen (NO_3^- and NH_3) concentrations in waterways (Vitousek et al. 1997). While agriculture is not the only land use that releases excess nutrients, it is a primary cause for eutrophication in regions dominated by agriculture, such as the Eastern Shore of Maryland, within the Chesapeake Bay watershed (Kemp et al. 2005).

Methane

Methane (CH_4) is the second most important greenhouse gas in terms of radiative forcing in the atmosphere. On a molar basis, CH_4 is about 20 times more effective at heating the atmosphere than carbon dioxide (CO_2), which is the leading greenhouse gas. Although methane is not long-lived in the atmosphere, photo-oxidation converts methane to carbon dioxide. Atmospheric methane concentrations have increased

50% since 1750, which is more than the greenhouse gases carbon dioxide and nitrous oxide (IPCC 2014).

Methane is produced geologically through thermogenic and abiotic processes, and biologically through microbial metabolism (Kietavaine and Purkamo 2015, Reeburgh 2007). Natural sources of methane include animals (e.g. termites), wetlands, methane hydrates, oceans, and freshwaters. Anthropogenic sources of methane include animal agriculture (e.g. cows), rice agriculture, landfills, biomass burning, and coal and natural gas production. The largest contributors of methane emissions are freshwater wetlands and rice production, respectively. The major environmental sinks of methane include soils and photo oxidation in the atmosphere (Le Mer and Roger 2001, Reeburgh 2007, IPCC 2014).

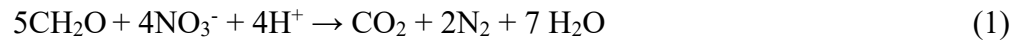
Cycling of Nitrate and Methane

Nitrogen Cycle

The nitrogen cycle is considered complex, but it is also highly studied and well understood. I will start my discussion of the nitrogen cycle with the dominant atmospheric gas, N_2 , which is highly stable but can be converted to ammonium (NH_4^+) by lightning or bacterial nitrogen fixation. Ammonium can be assimilated by organisms to form organic nitrogen, released as gaseous NH_3 , or nitrified to NO_3^- , which can also be denitrified to N_2 . Nitrite (NO_2^-), nitric oxide (NO), and nitrous oxide (N_2O) are intermediates of nitrification or denitrification (Galloway et al. 2004). Nitrification is an aerobic process, while denitrification is anaerobic, but anaerobic ammonium oxidation (anammox) couples ammonium oxidation and nitrite

reduction to produce N₂ (Canfield et al. 2010). This dissertation will connect the nitrogen cycle, particularly denitrification, to methane oxidation in the anoxic environment (Fig 1 and 2).

Denitrification is the most efficient process for removing nitrate from the environment. Although this process does convert nitrate to N₂ gas (eq. 1; Berner 1980, Hedin et al. 1998), it can release nitrite and nitrous oxide as byproducts of incomplete denitrification.



$$\Delta G^\circ = -448 \text{ kJ mol}^{-1} \text{ CH}_2\text{O}$$

Denitrification is highly thermodynamically favorable, and nitrate is typically the first electron acceptor to be depleted in the anaerobic environment (Fig. 3; Berner 1980).

Classic Biological Methane Cycle

There have been many recent discoveries about new biogeochemical processes involving the oxidation of methane (Fig 2). The “classic” biological methane cycle involves the anaerobic production and aerobic consumption of methane. Methane is produced by methanogenic archaea through 3 pathways of methanogenesis: carbon dioxide reduction (eq. 2), acetate fermentation (eq. 3; Thauer 1990, Reeburgh 2007), and methanol reduction (eq. 4; Thauer 1990):



$$\Delta G^\circ = -131 \text{ kJ mol}^{-1} \text{ CH}_4$$



$$\Delta G^\circ = -36 \text{ kJ mol}^{-1} \text{ CH}_4$$



$$\Delta G^\circ = -107 \text{ kJ mol}^{-1} \text{ CH}_4$$

Methanogenesis is not highly energetically favorable and typically takes place after the depletion of other terminal electron acceptors (Fig 3).

In the presence of oxygen, methane is consumed by methanotrophs through the energetically favorable process of methane oxidation (Segers 1998). Methane oxidation canonically occurs in aerobic conditions with oxygen as the electron acceptor (eq. 5; Berner 1980, Caldwell et al. 2008):



$$\Delta G^\circ = -859 \text{ kJ mol}^{-1} \text{ CH}_4$$

Aerobic oxidation of methane is not typically associated with anaerobic processes, but Modin et al. (2007) found that methanotrophs can supply carbon compounds to denitrifiers in a coupled aerobic methane oxidation and denitrification metabolism.

Anaerobic Oxidation of Methane (AOM)

More recent research indicates that methane oxidation also takes place anaerobically coupled with alternate electron acceptors (Fig 3) such as sulfate, manganese, iron, and nitrate (Martens and Berner 1977, Islas-Lima et al. 2004, Raghoebarsing et al. 2006, Beal et al. 2009, Ettwig et al. 2016). Little is known about anaerobic oxidation of methane (AOM) in freshwater, but this process could be an important sink for methane. According to Valenzuela et al. (2017), AOM potentially contributes to suppressing up to 1,300 Tg CH₄ y⁻¹ in global wetlands.

AOM was first discovered due to concave-up methane depth distributions in marine sediments. Methane was consumed in the zone of sulfate reduction leading to

the conclusion that anaerobic oxidation of methane was performed by sulfate reducing bacteria (Barnes and Goldberg 1976, Reeburgh 1976, Martens and Berner 1977). Sulfate acts as the electron acceptor and methane as the electron donor. Although this process has low thermodynamic favorability, this reaction (eq. 6) occurs when sulfate levels are high (Beal et al. 2009):



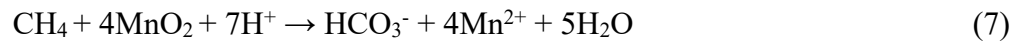
$$\Delta G^\circ = -14 \text{ kJ mol}^{-1} \text{ CH}_4$$

Evidence for this process is concentrated in high sulfate environments (Reeburgh 2007, Knittel and Boetius 2009, Schubert et al. 2011). Although this process is typically associated with marine systems, evidence for AOM coupled to sulfate reduction has also been found in freshwaters with high sulfate levels (Schubert et al. 2011).

Solid-phase oxides could be another source of electron acceptors for microbes that perform AOM (Sivan et al. 2011). Manganese (bernessite) and iron (ferrihydrate) can be used as electron acceptors in marine AOM. Although large amounts of manganese and iron are deposited to continental margins from rivers, these electron acceptors are typically underestimated as potential alternate electron acceptors since they are mostly found in the solid phase. Soluble Fe^{3+} and nanoparticulate Fe^{3+} and Mn^{4+} supports methane oxidation, producing CO_2 and Fe^{3+} (Ettwig et al. 2016). When iron and sulfate are abundant, like in the Black Sea, AOM is found to be integral in the dynamics of iron and sulfur in sediments (Egger et al. 2016). Iron and manganese have the potential to be oxidized and reduced up to 300 times before they are buried (Canfield et al. 1993), and they should be considered as

playing a role in AOM. Sediment incubations with ^{13}C -enriched methane displayed evidence of AOM coupled with sulfate, iron, and manganese reduction (Beal et al. 2009).

Although few studies have been conducted on manganese- and iron-dependent AOM, there is a lot of potential for these reactions to occur. There is high energetic favorability for both of these reactions (eq. 7 and 8):



$$\Delta G^\circ = -556 \text{ kJ mol}^{-1} \text{ CH}_4$$

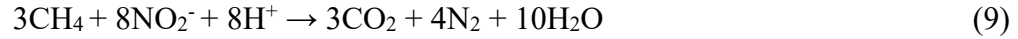


$$\Delta G^\circ = -270 \text{ kJ mol}^{-1} \text{ CH}_4$$

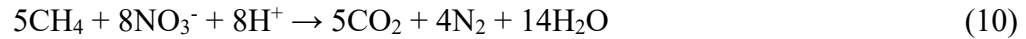
Although the potential energy yield is more favorable for these forms of AOM than sulfate-dependent AOM (eq. 6), sulfate was found to oxidize more methane than manganese and iron in marine sediments (Beal et al. 2009). The metabolic pathway for iron-dependent AOM was found to be similar to AOM coupled to sulfate reduction. Microbes that perform these metabolisms do so through the reverse methanogenesis pathway (Cai et al. 2018, Timmers et al. 2017). This is most likely due to the high concentration and availability of sulfate (28 mM) in the marine environment (Holland et al. 2011).

Anaerobic Oxidation of Coupled to Denitrification (AOM-D)

Theoretically, AOM coupled to denitrification is a thermodynamically favorable reaction. The electron acceptor in this metabolism can either be nitrite (NO_2^-) or nitrate (NO_3^-), shown in equations (9) and (10; Raghoebarsing et al. 2006):



$$\Delta G^\circ = -928 \text{ kJ mol}^{-1} \text{ CH}_4$$



$$\Delta G^\circ = -765 \text{ kJ mol}^{-1} \text{ CH}_4$$

These high Gibbs free energy values for AOM-D reveal that this process is more thermodynamically favorable than all other forms of AOM (Figure 3). As confirmed in several studies, nitrite is preferred over nitrate as the electron acceptor for AOM-D (Shima and Thauer 2005, Raghoebarsing et al. 2006, Ettwig et al. 2008, Hu et al. 2009). This nitrite preference is due to the properties of methyl-coenzyme M reductase (MCR; Shima and Thauer 2005). Although AOM-D has been theorized to exist for decades, the microbes that perform this process were not cultured until recently.

Smith and others (1991) found evidence of anaerobic oxidation of methane (AOM) occurring when methane was pumped into an aquifer. Although the authors stated that nitrate was a likely electron acceptor for freshwater AOM, they did not have evidence that AOM and denitrification were coupled. More recently, AOM-D was detected in reservoir sediments in Poland using $^{13}\text{CH}_4$ isotope markers and added NO_3^- (Szal and Gruca-Rokosz 2019). *In vitro* studies of anoxic sludge (Islas-Lima et al. 2004) and laboratory studies of soils detected AOM-D, with a microbial consortium of a bacterium and an archaeon which perform this coupling (Raghoebarsing et al. 2006).

Land Use Changes Associated with Changes in Nitrate and Methane

Nitrate

Anthropogenic activities are known to release excess nutrients into soils, groundwater, and surface water. As human population increases, nitrate export increases exponentially (Vitousek et al. 1997). The same relationship is found as the percentage of agricultural land within a watershed increases (Fisher et al 2010). Minor increases in the percentage of feeding operations within a watershed also increases the stream ammonium concentrations (Fisher et al. 2010, Beckert et al. 2011). In groundwater, nitrate concentrations over $714 \mu\text{M NO}_3^- \text{-N}$ are considered unhealthy for human consumption (Follett and Follett 2001), but this value is exceeded by much of the groundwater in the United States (Spalding and Exner 1993). In the Chesapeake Bay watershed, agriculture is a dominant land use and a dominant influence in eutrophication (Kemp et al. 2005).

Methane

Like carbon dioxide, atmospheric methane is at record high concentrations since the Industrial Revolution (IPCC 2014). Methane flux measurements show that soils are among the most important biological source and sink of atmospheric methane with saturated wetland soils being the top source of methane at 55% of global emissions (Le Mer and Roger 2001, IPCC 2014). Methane oxidation in soils is inhibited by low pH (under 5.6) and excess nitrogen applications from fertilization (Hütsch et al. 1994). Due to high variability in soils, methane oxidation and production in saturated and unsaturated soils is hard to predict and estimate (Le Mer and Roger 2001). Due

to increased precipitation and soil hydrological flux methane uptake has decreased in forest soils in North American (Ni & Groffman 2018).

Methane oxidation rates do not quickly recover from the impacts of cultivation. It can take over 100 years for methane oxidation to reach pre-cultivation levels (Priemé et al. 1997). Although methane oxidation does decrease with increased nitrogen, nitrogen availability indices do not necessarily correlate with methane fluxes from soil, indicating that oxidation may not be important in explaining the differences in methane fluxes among land uses. Soil water content was found to be a major driver of methane fluxes because methane oxidation is lower in the wet season than the dry season (Verchot et al. 2000).

Methane can be abundant in water-saturated soils. Methane ebullition events have been observed in groundwater (Fig 3; Fisher et al. 2010, Fox 2011). When dissolved oxygen is less than 15 % saturated and nitrate is less than 10 μM in groundwater, methane concentrations can approach 1 mM (Fig 4 and 5). Methane ebullition events could be the result of increased methanogenesis following nitrate depletion or could be due to a decrease in AOM, including AOM-D once the nitrate is depleted.

In anoxic, fresh groundwater, AOM-D should dominate over all other anaerobic oxidation of methane processes due to its high energetic favorability (Fig 3). In groundwater that is high in nutrients, such as in agricultural areas, excess nitrate and nitrite are available to be used as electron acceptors by *M. oxyfera*. This process could have important ecological ramifications since excess nitrogen is a primary cause for eutrophication. AOM-D could be an important removal

mechanism for both the greenhouse gas methane and the eutrophying nutrient nitrate, a pathway that has not been well explored.

Thesis Goals

Overarching Themes

This master's thesis investigates nitrogen and methane dynamics from 3 perspectives: (1) spatial distribution of methane in groundwater and streams, (2) dynamics of nitrate and methane in shallow groundwater following land use conversion from agricultural grain production to conservation easement, (3) biogeochemical investigation of simultaneous metabolism of nitrogen and methane. This research is primarily focused in the agriculturally impacted groundwater and streams of the coastal plains on Maryland's Eastern Shore. The goal of this thesis is to establish the commonalities between nitrogen and methane: temporal variabilities, spatial overlap, and the potential for simultaneous metabolism.

Spatial Distribution of Methane in Groundwater and Streams

In chapter 2, I investigate the distribution of methane, nitrogen, and other chemical parameters in groundwater and streams in the coastal plain. Data from 13 years at 16 sites was analyzed and samples were collected from 15 agricultural, 4 urban, and 1 forested watershed. Methane fluxes from urban streams were calculated and analyzed as well. Dissolved methane concentrations are greater than atmospheric equilibrium (13.65 nM CH_4) in all of the streams, and often reached exceedingly high concentrations ($> 20 \text{ }\mu\text{M}$) in groundwater. My hypothesis for this chapter is: watershed with higher percent hydric soils have higher methane production in

groundwater and flux from streams. This chapter provides an understanding of the spatial distribution of methane throughout the landscape and how it is influenced by land use, soil types, nutrient concentrations, and other factors.

Dynamics of Nitrate and Methane in Shallow Groundwater Following Land Use
Conversion from Agricultural Grain Production to Conservation Easement

In chapter 3, I investigate and discuss the impacts that the cessation of agricultural fields has on shallow groundwater concentrations of nitrate and methane. A chronosequence study is performed using plots of land that were retired from agricultural production over a 16-year period. I propose 2 hypotheses: (1) groundwater nitrate concentrations will decrease as time out of agricultural production increases and (2) methane concentrations would increase over time as the supply of the alternate electron acceptor nitrate decreased, resulting in more methanogenesis in the anaerobic metabolism of the soil. This chapter is used to establish an understanding of the impact of decreasing nitrate inputs to soil on groundwater and methane production.

Biogeochemical Investigation of Simultaneous Metabolism of Nitrogen and Methane

In Chapter 4, I will investigate AOM-D using biogeochemical methods. This study has 2 parts: (1) soil core methods and (2) *in-situ* methods. The soil core procedures will test 2 hypotheses: (1) AOM is detectable in soils and (2) nitrite is the primary electron acceptor used in the reaction. The *in-situ* test was meant to detect AOM-D and investigate these hypotheses in the field using similar methods as in the lab

experiments. This study proved to be methodologically challenging and is a cautionary tale for attempting this type of procedure.

Figures

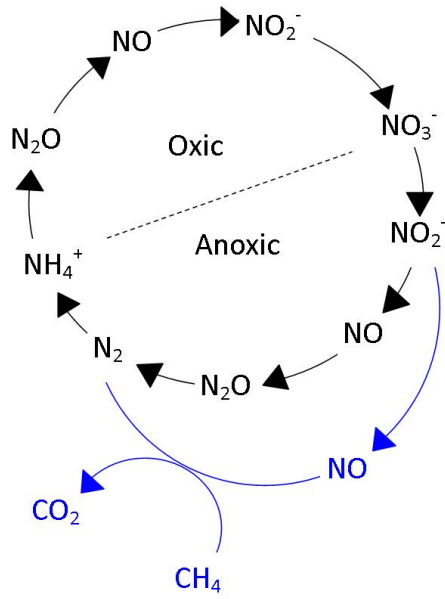


Figure 1. The nitrogen cycle in anoxic and oxic environments (black). Nitrite is reduced to N_2 via anaerobic methane oxidation (blue). Adapted from Karl 2002, Galloway et al. 2004, Ettwig et al. 2010.

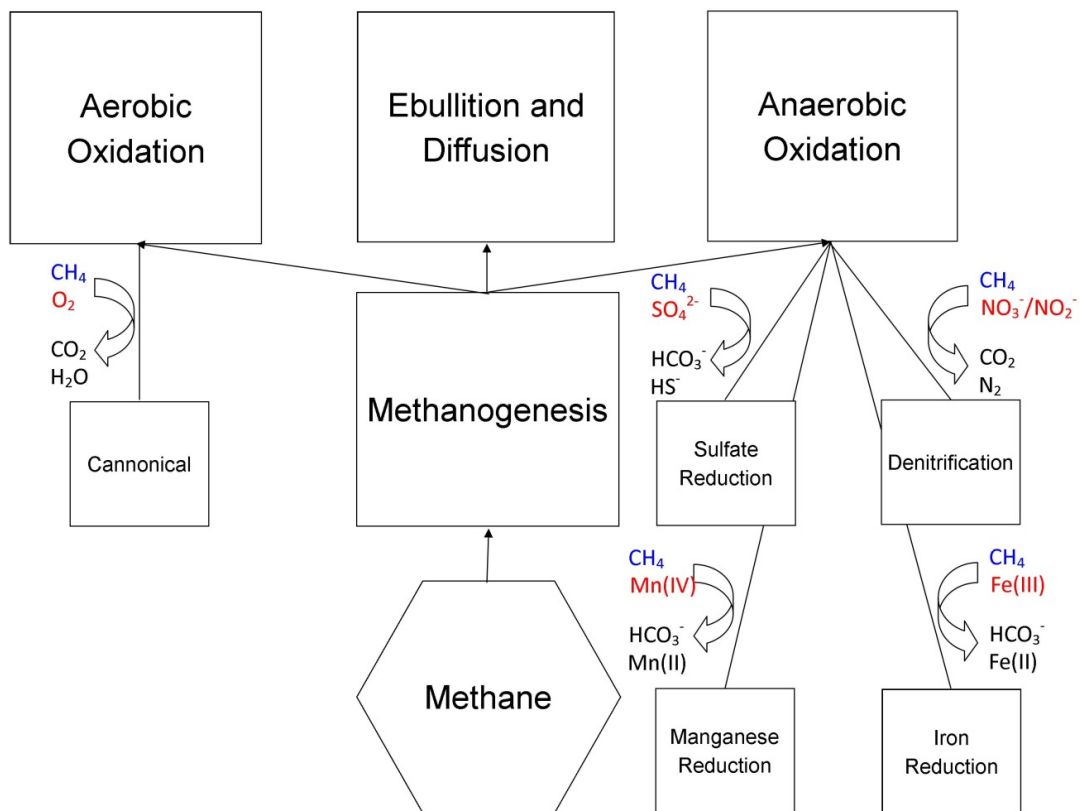


Figure 2. Methane pathway processes. Methane produced via methanogenesis is oxidized aerobically or anaerobically or bubbles into the atmosphere (ebullition). The electron donor (CH_4) is in red, electron acceptors in blue, and products in black.

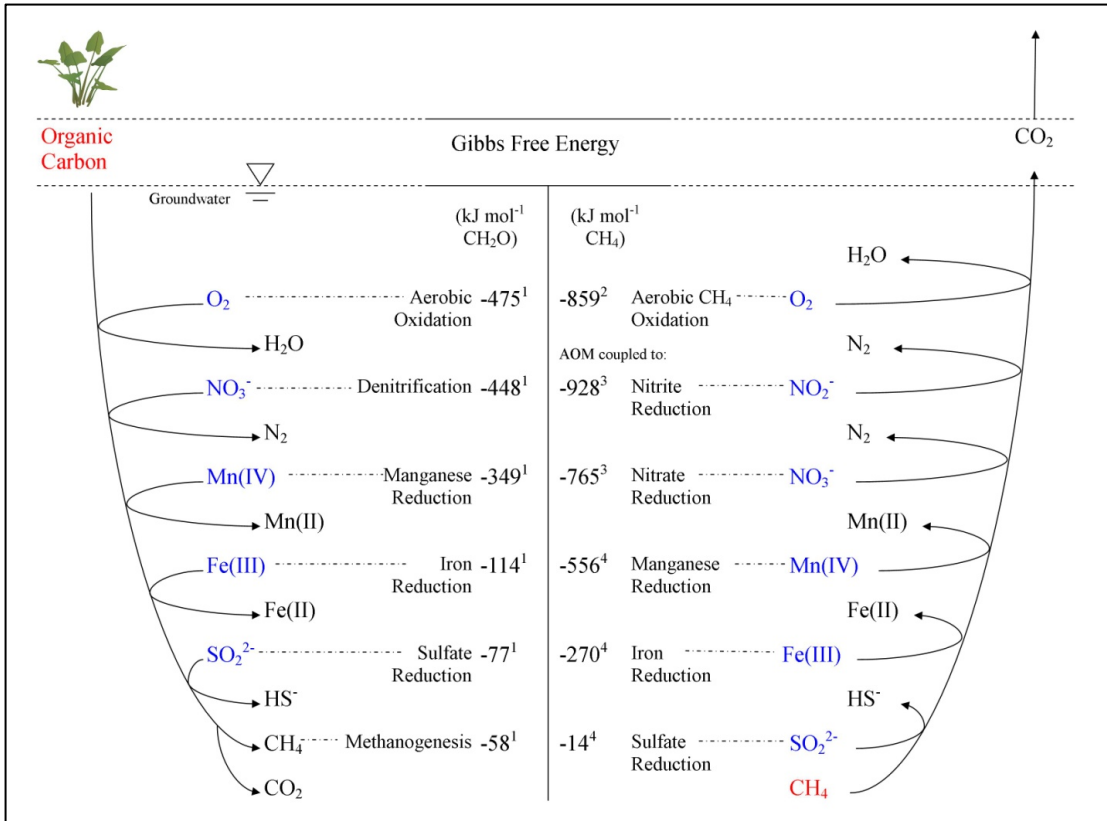


Figure 3. Oxidation of electron donors (red)-organic carbon (left) and methane (right)-in groundwater with the sequence of electron acceptors (blue) and the reduced products (black; adapted from Korom 1992 and Rivett et al. 2008). Gibbs free energy values are from: (1) Berner 1980, (2) Caldwell et al. 2008, (3) Islas-Lima et al. 2004, Raghoebarsing et al. 2006, (4) Beal et al. 2009. Arrow Arum figure is from Tracey Saxby, IAN Image Library (Ian.umces.edu/imagelibrary/).

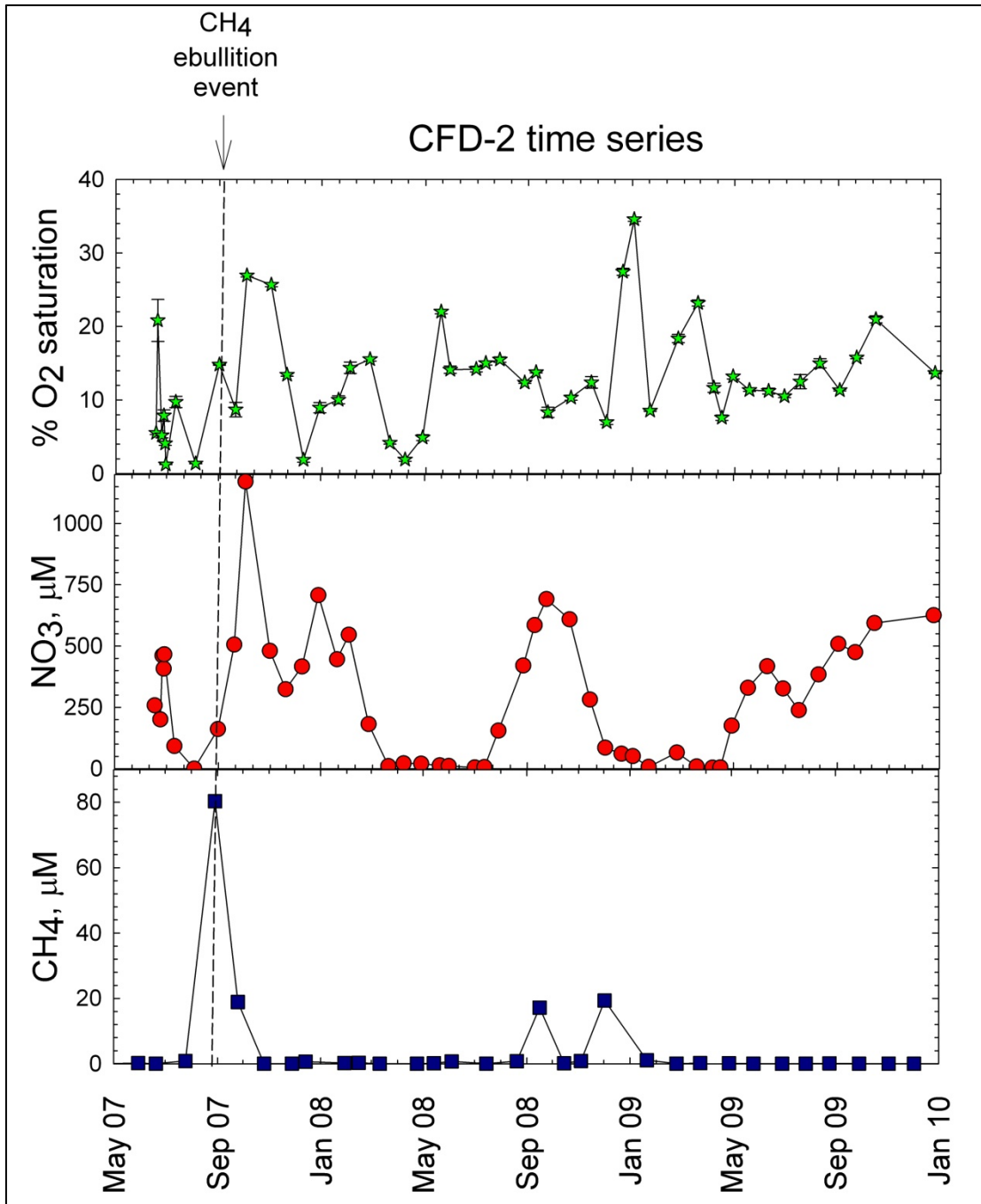


Figure 4. Percent oxygen saturation and nitrate concentrations in groundwater and methane and excess N₂ in the vadose zone at an agricultural site (Fox 2011). In September 2007, the nitrate concentration was below 10 μM and the methane concentration increased to about 80 μM. The high concentration of methane is indicative of a methane ebullition event, when methane bubbles up into the atmosphere.

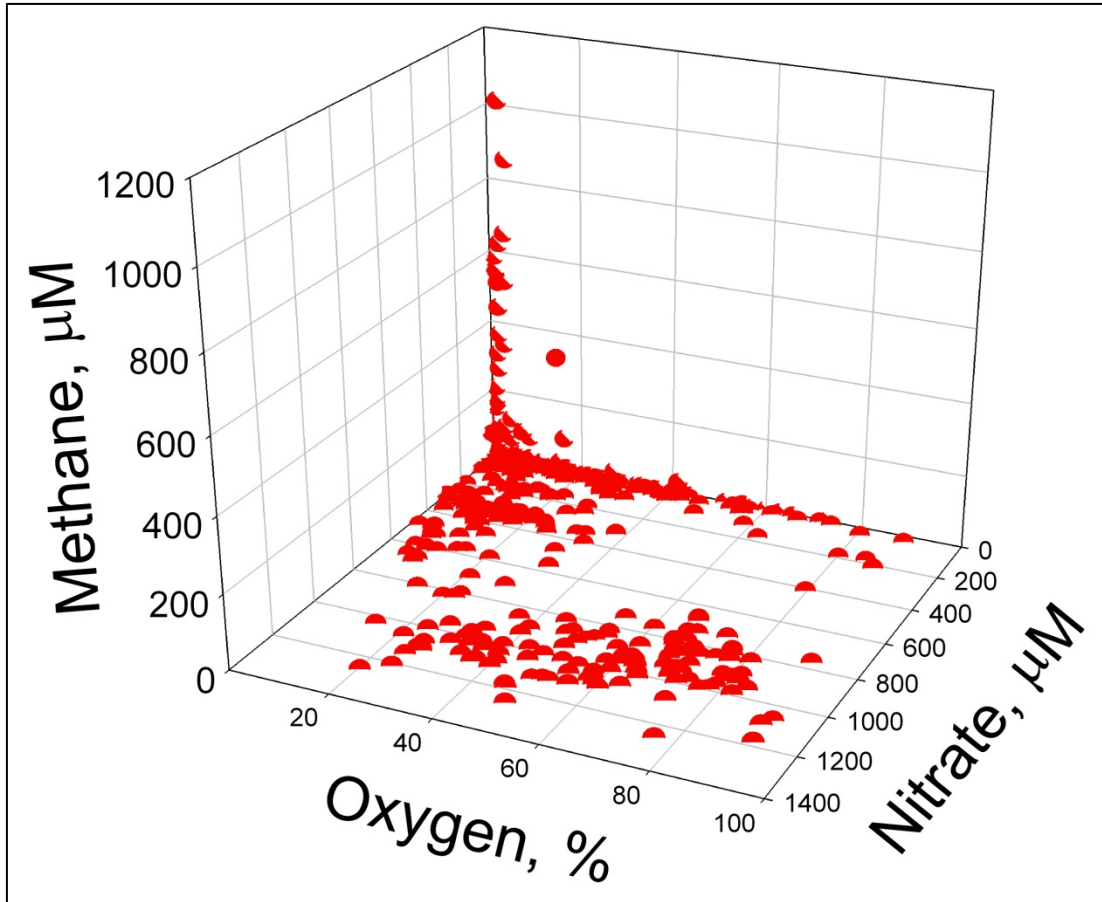


Figure 5. Methane concentration, nitrate concentration, and oxygen saturation for groundwater and vadose zone samples collected on the Eastern Shore of Maryland. Methane primarily occurs when nitrate is below 10 μM and oxygen saturation is below 15%.

Chapter 2: Spatial Distribution and Efflux of Methane in Groundwater and Streams

Introduction

Landscape Methane Overview

Atmospheric concentrations of methane are the second highest of all greenhouse gases. Like carbon dioxide, atmospheric methane has increased exponentially since the Industrial Revolution (IPCC 2014). While the dramatic rise in greenhouse gases is attributed mostly to the burning of fossil fuels, rising global temperatures could be increasing natural emissions of methane via diffusive and ebullitive fluxes (DelSontro et al. 2016). In terms of CO₂-equivalents, global methane emissions are approximately 25% of the estimated terrestrial greenhouse gas sink (Bastviken et al. 2011).

The largest natural source of biogenic methane to the atmosphere is wetlands. Fluvial systems as well as groundwater (and soils) are considered to have negligible or even negative methane emissions resulting from methane oxidation (Reeburgh 2007). Due to intermittent anoxic conditions in groundwater and hyporheic zones of streams, methane is periodically produced in potentially high concentrations and transported to the atmosphere via stream and/or soil fluxes (Fig. 1, Stanley et al. 2016). This methane source is often underestimated with regards to global methane emission estimates. In this chapter, I will assess methane concentrations and fluxes in groundwater and streams.

Groundwater Methane

This chapter focuses on methane that is newly produced through microbial activity in shallow groundwater and soils. As in marine sediments, groundwater has the redox zonation of: oxic (O_2), nitrate-reducing, Mn (IV) and Fe (III)-reducing, sulfate-reducing, and methanogenic (Baedeker and Back 1979, Lyngkilde and Christensen 1992, Lovley et al. 1994). In aquifers contaminated with organic compounds, the redox zonation around the contaminant is in reverse order (methanogenic to oxic conditions; Fig 2, Christensen et al. 2000, Lovley et al. 1994). Anoxic groundwater also has higher concentrations of reduced products (CH_4 , Fe^{2+} , Mn^{2+} , NH_4^+) from anaerobic metabolism (Baedeker et al. 1993). Anaerobic oxidation of methane coupled to iron, manganese, or nitrate reduction is a potential reaction in anoxic groundwater because the methane produced in the methanogenic zone can diffuse into the regions with Fe, Mn, or NO_3^- reduction (Fig 2, Smith et al. 1991, Baedeker et al. 1993).

Soils and groundwater are rich in microbial activity and studies have found evidence of methanogenic bacteria in the coastal plains of Maryland (Chapelle et al. 1987). Groundwater is often considered to have only trace methane concentrations, but in the Choptank Basin, methane has been found to reach concentrations of 310 μM (Table 1, Fox 2011). The upland soil flux to the atmosphere is reported to have a range of 0-1.35 $mmol\ m^{-2}\ d^{-1}$ (Table 1, Le Mer and Roger 2001). This is a low methane emission rate relative to wetlands, but the larger concern is transport of groundwater-produced methane to streams and escape to the atmosphere.

Fluvial Methane

Streams and rivers have long been omitted when considering their contribution to global methane emission distributions (Stanley et al. 2016). Many studies have shown methane concentrations in streams and rivers that are in excess of atmospheric equilibrium (Hope et al. 2001, Jones and Mulholland 1998a, Stanley et al. 2016). Mean fluvial methane concentrations are reported to be 1.35 μM (range of 0-386 μM , Table 1, Stanley et al. 2016). This value is nearly 100 times background atmospheric equilibrium (0.03 μM) with methane.

Fluvial sources are often ignored for methane emissions due to their lack of *in situ* methane production. Since the microbial production of methane (methanogenesis) is an anaerobic process (Vogels et al. 1984), oxic streams and rivers generally do not support the creation of methane. Fluvial methane typically comes from groundwater (Stanley et al 2016), particularly subsurface flow from riparian soils (Jones and Mulholland 1998a). Some streams with seasonal low water velocity and the accumulation of plant beds (such as the macrophyte, *Ranunculus penicillatus*) have been shown to have significant methanogenesis occurring in the stream channel (Sanders et al. 2007). Although the water columns of open stream channels do not have ideal conditions for methanogenesis, stream sediments often have conditions more favorable for CH_4 production. In-stream metabolism, temperature, and organic content are found to influence diffusive and ebullitive methane fluxes (Campeau and Del Giorgio 2014, Crawford et al. 2014). Once in the stream channels, streams can act as conduits of methane transport from the watershed to the atmosphere (Stanley et al. 2016).

Stream methane concentrations vary depending on the landscape of the stream's watershed. Wetland, agricultural, and urban streams are found to have higher methane concentrations than mountain and forested streams (Yavitt et al. 1990, Jones and Mulholland 1998a, Stanley et al. 2016). The geomorphology of the drainage basin also influences stream methane concentrations due to soil types and conditions, such as temperature, organic matter, redox status, and nutrients (Jones and Mulholland 1998b, Stanley et al. 2016). Changes in watershed land use potentially impact methane concentrations and emissions from streams. An example of these changes includes the urbanization of streams that could increase stream temperatures, leading to an increase in methane production in the hyporheic zone.

The methane dissolved in stream water can be transported to the atmosphere in 3 ways: diffusive flux, ebullition, and plant-mediated transport. Estimated global emissions of methane from open freshwater are: 55.3 Tg CH₄ y⁻¹ for diffusive flux, 9.9 Tg CH₄ y⁻¹ for ebullition, and 25.1 Tg CH₄ y⁻¹ for plant-mediated transport (Bastviken et al. 2011). This total flux is higher than Reeburgh's (2007) estimate of the combined freshwater and ocean methane emission (10 Tg CH₄ y⁻¹) and is greater than the global soil sink for methane (-10 Tg CH₄ y⁻¹). Bastviken's (2011) total methane emissions may also be an underestimate due to the difficulty in measuring ebullition events, and this fraction of transport could account for 20-67% of stream methane emissions (Baulch et al. 2011). Stanley et al. (2016) found the mean fluvial diffusive flux to be 8.22 mmol m⁻² d⁻¹ (range of -10.43-432.5 mmol m⁻² d⁻¹, Table 1). This chapter will focus on the diffusive flux of methane to the atmosphere.

Methane's strong potential as a greenhouse gas (30x that of CO₂) makes any emissions a concern (IPCC 2014). Due to the increase in global temperatures, methane emissions from boreal rivers and streams alone could increase 13-68% under plausible climate change scenarios that have been projected over the next 50 years (Campeau and Del Giorgio 2014). Forests and upland soils are typically thought of as methane sinks, capable of absorbing 4-10% of atmospheric methane, but recent studies have shown that tree emissions of methane could be offsetting the soil sinks (Pitz and Megonigal 2017). Leaf litter studies have also shown that decomposing leaves and other biomass are a significant source of methane (Yavitt et al. 2019). All freshwater should be considered to have to the potential to release an increasing amount of methane to the atmosphere.

Methane is not the only gas of concern. N₂O, a byproduct of denitrification, is emitted from forest streams (Audet et al. 2019). Large rivers have also been found to have high saturation of N₂, indicative of denitrification (Ritz et al. 2018). Previous under valuation of dissolved gases and fluxes from streams are due to the methodological challenges of studying gas fluxes.

Hypotheses and Experimental Design

In terms of the global methane budget, soils are methane sinks and wetlands are the largest natural source of methane (IPCC 2014). However, soil properties, including methane production/consumption, have high spatial variability, and hydric soils could be a net methane source with or without overlying surface water (e.g. Fox et al. 2014). When predicting methane emissions, most models focus on wetlands and ignore hydric soils without overlying waters. This approach could underestimate

methane emission because Fox et al. (2011, 2014) found high dissolved methane (up to 1 mM dissolved methane) in groundwater of hydric soils throughout the northern Choptank watershed. Here on the Delmarva Peninsula (Mid-Atlantic region). I investigated groundwater and stream methane concentrations across 16 small watersheds in the upper Choptank Basin. Four small agricultural watersheds were investigated intensively for methane and nitrogen concentrations (Fig 3). I hypothesized that watersheds with slower draining soils have higher methane production in groundwater and streams. Fluvial sources of atmospheric methane are often underestimated (Stanley et al. 2016), so I investigated methane fluxes from three urban streams (Fig 3). I hypothesized that urban streams have methane concentrations above atmospheric equilibrium and are a positive source of methane to the atmosphere. Stream fluxes will be studied using methods described in Gardner et al. 2017.

Methods

Agricultural Watershed Field Sampling

Groundwater samples were collected monthly for nutrient and gas sampling from July 2014 to May 2017 in 4 small watersheds: Spring, South Forge, Old Town, and Broadway. Monitoring piezometers were installed at 1-3 m depth below the surface to sample groundwater. Prior to collecting water at each site, undisturbed instantaneous water depth below the top of the piezometer was measured using a Solinst water level meter (model 102m). After recording water level, groundwater was pumped from the piezometer for 5 minutes or until groundwater was depleted

using a positive displacement pump or peristaltic pump. Water was sampled 24 hours later once the piezometers recovered sufficiently with fresh groundwater.

Sampling of the newly recovered groundwater was completed using the positive displacement or peristaltic pump. Samples for nutrient analyses (nitrate, ammonium, and phosphate) were collected in 75 ml sample bottles that were rinsed 3 times with sample water before filling. Gas sampling was completed after nutrient sampling using only the positive displacement pump. From each site, 8 samples were collected in 12 mL glass exetainer test tubes and capped, ensuring that no air was trapped in the tube. All samples were placed on ice to be transported to Horn Point Laboratory for further analyses.

Urban Streams Field Sampling

Urban streams were sampled for CH₄, N₂O, N₂, CO₂, and radon-222 (Rn²²²). Streams were sampled in 3 locations (upstream, midstream, and downstream). The total length of stream reaches sampled were about 40 m. Piezometers were installed at each stream location to sample for groundwater. Piezometers were pumped out using a positive pressure pump and would recharge within 30 minutes. Samples for dissolved gases were collected from the stream water column and groundwater using the same gas sampling method as described above.

Analytical Methods

Samples were analyzed for pH and conductivity using a VWR SympHony SP70P pH meter and Yokogawa Model SC82 conductivity meter, respectively, in the field.

Samples were filtered at Horn Point Laboratory using GF/F filters for automated

colorimetric analysis of nitrate + nitrite and phosphate on a Technicon AutoAnalyzer II in the Horn Point Analytical Services Lab. Dissolved methane and nitrous oxide were measured using a static headspace equilibrium method (Johnson et al. 1990, Kampbell and Vandegrift 1998) on a Shimadzu GC-8A gas chromatograph with a flame ionization detector. Excess N₂ was measured using the membrane inlet mass spectrometry (MIMS) method (Kana et al. 1994).

Urban Stream Flux Sampling

Stream gas flux measurements were modelled after Gardner et al. (2016) and Demars et al. (2015). Each stream was sampled 2-3 times. Rn²²² was used as a conservative tracer for gas transfer velocity (Table 2). Stream radon was sampled with a RAD-AQUA connected to a RAD7 radon-in-air monitor (DurrIDGE, Billerica, MA). Groundwater was pumped through a submersible pump (Model GP132, Whale Water Systems Inc., Manchester Center, VT) from piezometers in the stream sediment. Stream and groundwater samples were collected in Exetainers and transferred on ice for lab analyses of methane and N₂ (Fox 2011).

Calculating Stream Fluxes

Stream gas fluxes were calculated based on Gardner et al. 2016 (Fig 4). The total flux (F_T , mmol CH₄ m⁻² d⁻¹, eq. 1) was calculated by subtracting the gas loss to the atmosphere and groundwater gas inputs from the stream gas inventory,

Eq. 1

$$F_T = Z \frac{C_t - C_0}{\Delta t} - V \left(C_{rec} - \frac{C_t + C_0}{2} \right) - Z \left(\frac{K_t + K_0}{2} \right) \left(\frac{CE_t + CE_0}{2} - \frac{C_t + C_0}{2} \right)$$

where Z is depth (m), C is methane concentration (μ M), t is time (d), K is gas transfer

velocity (m d^{-1}), and CE is equilibrium methane concentration (μM). The last term in Eq. 1 is the atmospheric flux calculation. Groundwater methane flux (F_{gw} , $\text{mmol CH}_4 \text{ m}^{-2} \text{ d}^{-1}$) was calculated by eq. 2,

Eq. 2

$$F_{\text{gw}} = (C_{\text{gw}} - C_{\text{rec}})V_{\text{gw}}$$

where C_{rec} is recharge methane concentration (μM) and V_{gw} is the groundwater piston velocity (m d^{-1}). Stream flux (F_{st} , μM) is the difference of F_{T} and F_{gw} (Eq. 3),

Eq. 3

$$F_{\text{st}} = F_{\text{T}} - F_{\text{gw}}$$

Statistics

Statistical analyses were run using SigmaPlot 12.5 software.

Results

Agricultural Watershed Comparisons

The four agricultural watersheds that were intensively sampled had variable concentrations of methane in groundwater and stream outlets (Fig 5). While South Forge's average groundwater methane concentrations were near atmospheric equilibrium ($0.03 \mu\text{M}$), the other three watersheds had average groundwater methane concentrations greater than $5 \mu\text{M}$. All of the watershed stream outlets had methane concentrations greater than atmospheric equilibrium, but lower than $0.3 \mu\text{M}$ methane.

Nutrient concentrations were also variable at the four watersheds, but nitrate concentrations ($90\text{-}715 \mu\text{M}$) were the highest nutrient concentrations in groundwater and the outlets of each watershed (Fig 5). Average groundwater nitrate

concentrations at Broadway and South Forge were higher than the outlet concentrations, but the opposite occurred at Spring and Old Town. Average ammonium and phosphate were low at all the agricultural watersheds.

Groundwater Relationships

The nitrogenous compounds have inverse relationships to dissolved methane in the groundwater samples (Fig 6). The nitrate data had a strong inverse hyperbolic relationship to methane concentrations ($p < 0.005$, Fig 6). The ammonium relationship to groundwater methane deviated from the inverse hyperbolic relationship found with the other nitrogen compounds. Groundwater methane and nitrous oxide have a significant inverse hyperbolic relationship ($p < 0.0001$, Fig 6). Groundwater methane and excess nitrogen did not have a significant relationship (Fig 6).

Fluvial Methane and Land Use

A third of the watershed outlet data had methane below detection, but the other data was greater than atmospheric equilibrium ($0.03 \mu\text{M CH}_4$), with 2 values exceeding $30 \mu\text{M}$. The average methane concentration was $1.67 \pm 6.75 \mu\text{M}$ (Table 3). This value is congruent with other literature values (Table 1). There were no significant relationships between watershed outlet methane and percentage hydric soils (Fig 7). When the 2 outliers ($\text{CH}_4 > 30 \mu\text{M}$) were excluded, a positive linear relationship was found between stream methane and percent soil class B ($p = 0.0008$, Fig 8).

Stream Fluxes

All of the urban streams sampled for stream fluxes had methane concentrations above atmospheric equilibrium. Groundwater methane concentrations in the four urban watersheds ranged from 1.60 $\mu\text{M CH}_4$ to 94 $\mu\text{M CH}_4$, with the range in streams being 0.28 $\mu\text{M CH}_4$ to 1.70 $\mu\text{M CH}_4$ (Table 4). The stream methane concentrations were similar to the average fluvial methane concentrations found in Stanley et al. 2016 (Table 1).

Methane fluxes were dominated by the groundwater to stream fluxes (Fig 9). Wilelinor and Church Creeks had the highest methane fluxes to streams ($> 30 \text{ mmol CH}_4 \text{ m}^{-2} \text{ d}^{-1}$). In-stream production of methane was low and ranged from 0.06 to 7.52 $\text{mmol CH}_4 \text{ m}^{-2} \text{ d}^{-1}$. Atmospheric flux ranged from 0.35 to 5.29 $\text{mmol CH}_4 \text{ m}^{-2} \text{ d}^{-1}$. Wilelinor Creek had the highest stream flux, stream production, and atmospheric flux (Fig 9). As expected, atmospheric carbon dioxide concentrations had a diel pattern (Fig 10).

Discussion

Agricultural Watershed Comparisons

The four intensively sampled watersheds have methane and nutrient concentrations similar to literature values for groundwater and streams (Fisher et al 2010, Stanley et al. 2016). South Forge is the only watershed with marginal methane concentrations and this watershed also has the highest concentration of groundwater nitrate (Fig 5). This relationship is not indicative of a pattern as elevated groundwater methane and nitrate is found in other watershed in this study. The Spring Branch watershed had

the highest groundwater methane and highest watershed stream outlet nitrate concentrations (Fig 5). The watershed outlet nitrate value is greater than the average groundwater nitrate concentration. This is indicative that there is a source of groundwater nitrate to the stream that is not being accounted for by the groundwater sampling in this study. More sites are needed to properly assess the groundwater methane and nutrient concentrations in the Spring Branch watershed.

Groundwater Relationships

Groundwater methane concentrations were consistent with what Fox (2011) found in the same sampling area (Table 1). There is a large range in values (0-400 $\mu\text{M CH}_4$), but a low median indicative of the many below detection level measurements. It is clear that elevated methane concentrations in groundwater often occur at low nitrogen levels (Fig 6). This is consistent with laws of thermodynamics that assert low energy yields for methanogenesis (Berner 1980). This is apparent in the data comparing methane and nitrate concentrations (Fig 6). Elevated methane levels were only found with very low nitrate values. This supports the concept that in the presence of nitrate, denitrification is preferred over methanogenesis (Berner 1980). If denitrification is occurring in lieu of methanogenesis, it would be expected that excess N_2 and methane concentrations would have the same relationship with nitrate, but while there is an inverse relationship, excess N_2 and methane do not have a significant relationship. This indicates that methane production and denitrification may not be linked. Nitrous oxide had a similar relationship to groundwater methane as nitrate (Fig 6). In contrast, ammonium levels increased slightly with increased methane concentrations (Fig 6). This could reflect a lack of nitrification as the redox declines.

Methane production has been shown to be related to groundwater depth below ground and temperature (Itoh et al. 2008, Godin et al. 2012). However, in my data, groundwater depth below ground did not have a significant relationship to groundwater methane concentrations. The highest methane concentrations also occurred in the summer months when temperatures were elevated, but there was not a significant relationship.

Stream Relationships

When considering fluvial methane and nutrient concentrations (particularly nitrate), it is expected that methane would have an inverse relationship due to thermodynamic principles of respiratory processes (Stanley et al. 2016). The two stream methane concentrations greater than 30 $\mu\text{M CH}_4$ had very different relationships to nutrient concentrations. These samples were collected in different months and at different locations. In June 2016, the methane concentration at the outlet of North Forge was 38.03 $\mu\text{M CH}_4$ and the nutrient concentrations were all below average for the watershed outlet data (Table 3). In July 2016, the methane concentration at the outlet of Piney watershed was 46.49 $\mu\text{M CH}_4$ and the nutrient concentrations were highly elevated (Table 3). It is hard to assess the connotations of these 2 data points alone, but according to Stanley et al. (2016), while terminal electron acceptors are considered hierarchical and that methanogenesis should only occur after the depletion of nitrate, mixed results have been found in various studies. Nutrient (nitrogen and phosphorus) interactions with fluvial methane have also been found to be variable (Stanley et al. 2016).

Water chemistry was highly variable amongst the watersheds (Table 3). Average values of phosphate, total phosphorus, ammonium, nitrate, and total nitrogen were all elevated relative to forested streams but were within typical ranges for agricultural areas (Fisher et al. 2010). As indicative with low redox, the July 2016 sample showed elevated methane and nutrients. Ammonium in this sample was 29 times the average value for the watershed outlets. Organic matter is a proximate control on fluvial methane concentrations (Stanley et al. 2016), so a working hypothesis for the high methane, phosphorus, and nitrogen concentrations is that there was a high dissolved organic carbon (DOC) level as well. This would increase respiration and provide ample organic matter for multiple respiratory processes. Without supporting DOC values, this is only speculation.

Urban Stream Fluxes

Stream methane concentrations in the urban streams were roughly 1% of groundwater methane concentrations (Table 4). While stream methane is considerably lower than groundwater methane, the concentrations are still greater than atmospheric equilibrium and this study indicates an outward flux of this methane to the atmosphere (Fig 9). Methane fluxes to the atmosphere ranged from 0.35 – 5.29 mmol CH₄ m⁻² d⁻¹, which fall within the same range that was documented in Stanley et al. 2016 (Table 1).

It is clear that the majority of the methane within the stream is supplied through groundwater and only a small fraction comes from in-stream production (about 2% of total flux; Fig 9). The largest methane flux is closely linked to groundwater methane concentration and groundwater piston velocity (Table 2, Fig 9).

Therefore, stream fluxes of methane to the atmosphere are heavily influenced by the influx of groundwater rich in dissolved methane. Flux magnitudes are also influenced by stream hydrology.

High methane concentrations were found in streams with a history of hydrology restoration projects. When streams are reconnected to their floodplains, it has been showed that denitrification rates increase. When hydrologic residence time is increased due to an increase in pools of standing water, there is more time for processing of carbon and nutrients (Kaushal et al. 2008). This explains the increase in methane fluxes from Wilelinor and Church Creeks.

Test of the Hypotheses

One hypothesis for this study asserted that fluvial methane concentrations would be correlated with soil type and land use. No significant relationship was found between fluvial methane concentrations and soil class. When assessing the four soil classes, while excluding the two outliers, the only significant relationship found was a slight direct increase in methane concentrations when soil class B (non-hydric) increased (slope = $0.03 \mu\text{M CH}_4 / \% \text{ soil B}$, $p = 0.0008$, Fig. 7). These data do not support my hypothesis that methane would increase with slower draining soils. In terms of land use, percent urban land was the only significant relationship (Fig. 8). There was an exponential decay in methane concentrations as urban land increased, but urban land only rose to 8%, and this relationship is not fully supported without also looking at higher concentrations of urban lands. Methane concentrations were expected to increase with increasing agriculture, but no significant relationship was found so this hypothesis was not supported nor refuted.

The second hypothesis stated that urban streams have methane concentrations above atmospheric equilibrium and were a positive source of methane to the atmosphere. Nearly all of the streams sampled (agricultural and urban) had methane concentrations above atmospheric equilibrium (Table 1; Table 4). Flux measurements also confirmed that the urban streams have a positive flux of methane to the atmosphere (Fig 9). This data supports this hypothesis.

Landscape Methane

It is clear that while hydric soils may not be a driver of methane concentrations in groundwater and streams, methane concentrations are considerable throughout the landscape. Methane is produced in shallow groundwater and transported to the atmosphere via soils and streams. This study indicates that this methane is not a marginal flux and should be considered more closely when analyzing global methane distribution.

Acknowledgements

I would like to thank Dr. Joshua Thompson (SERC), Dr. Karen Knee (American University), Dr. Thomas Jordan (SERC), Dr. John Gardner (UNC), and Anne Gustafson (UMCES) for their contributions to field work, lab analyses, and data analyses.

Tables and Figures

Tables

Table 1. Summary of methane data.

Environment Type of CH ₄ Data	No. of Data	Mean ± SD	Median	Range	Source
Groundwater Concentration* (μM)	62	7.15 ± 39.56	0.16	0.01 to 310.55	Fox 2011
Groundwater Concentration	232	8.63 ± 41.49	0.005	0 to 407	This Study
Upland Soil Flux to Atmosphere (mmol·m ⁻² ·d ⁻¹)	5	N/A	0.02	0 to 1.35	Le Mer and Roger 2001
Fluvial Concentration (μM)	939	1.35 ± 5.16	0.25	0 to 386 (n = 952)	Stanley et al. 2016
Fluvial Concentration	86	0.63 ± 1.05	0.25	0 to 5.37	This Study
Fluvial Diffusive Flux (mmol·m ⁻² ·d ⁻¹)	385	8.22 ± 25.50	0.86	-10.43 to 432.5 (n = 394)	Stanley et al. 2016
Fluvial Diffusive Flux	4	1.61 ± 2.46	0.40	0.35 to 5.29	This Study

*Mean, median, and range calculated from reported medians of multiple samplings at 62 piezometers

Table 2. Urban sampling sites.

Site	Ave. Depth, m	Stream Temp., °C	Groundwater Temp., °C	Rn, K, s ⁻¹	Groundwater Piston Vel., m s ⁻¹
Wilelinor Cr	0.175	18.6	19.1	0.000126	0.00003169
Church Cr	0.012	13.5	16	0.000393	0.00000984
Dividing Cr	0.082	12.1	14	0.00014	0.00000683

Table 3. Average watershed outlet stream concentrations \pm standard deviation and max concentrations

Methane, μM		Phosphate, μM		Total Phosphorus, μM	
Ave \pm SD	Maximum	Ave \pm SD	Maximum	Ave \pm SD	Maximum
1.67 \pm 6.75	46.49	2.09 \pm 5.07	42.5	3.89 \pm 5.99	49.2
Ammonium, μM		Nitrate, μM		Total Nitrogen, μM	
Ave \pm SD	Maximum	Ave \pm SD	Maximum	Ave \pm SD	Maximum
5.93 \pm 19.91	175	295.6 \pm 196.6	367	336 \pm 203.61	691

Table 4. Average concentrations of dissolved gases at the urban sampling sites

Site	Methane, μM		Nitrous Oxide, μM		Excess N_2 , μM	
	Groundwater	Stream	Groundwater	Stream	Groundwater	Stream
Wilelinor Cr	94	1.70	0.022	0.054	-439	-77
Church Cr	41	0.76	0.047	0.337	-199	-83
Dividing Cr	2.75	0.28	0.311	0.138	59	45

Figures

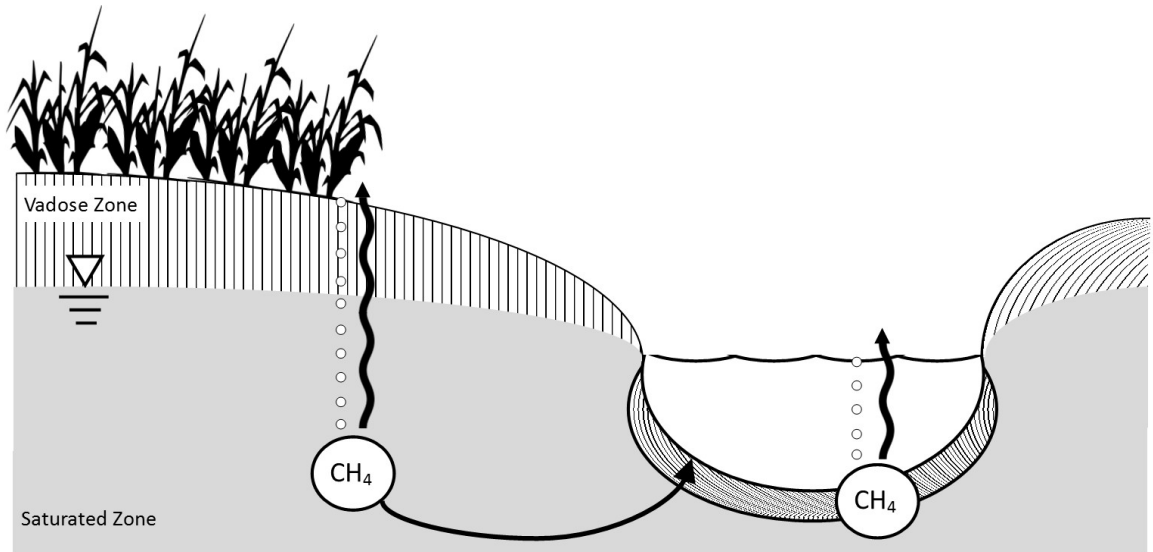


Fig 1. Methane produced in anoxic groundwater (saturated zone) is transported to the atmosphere via the vadose zone and streams through diffusive (arrows) and ebullitive (bubbles) fluxes. Corn outline was downloaded from clipartmax.com.

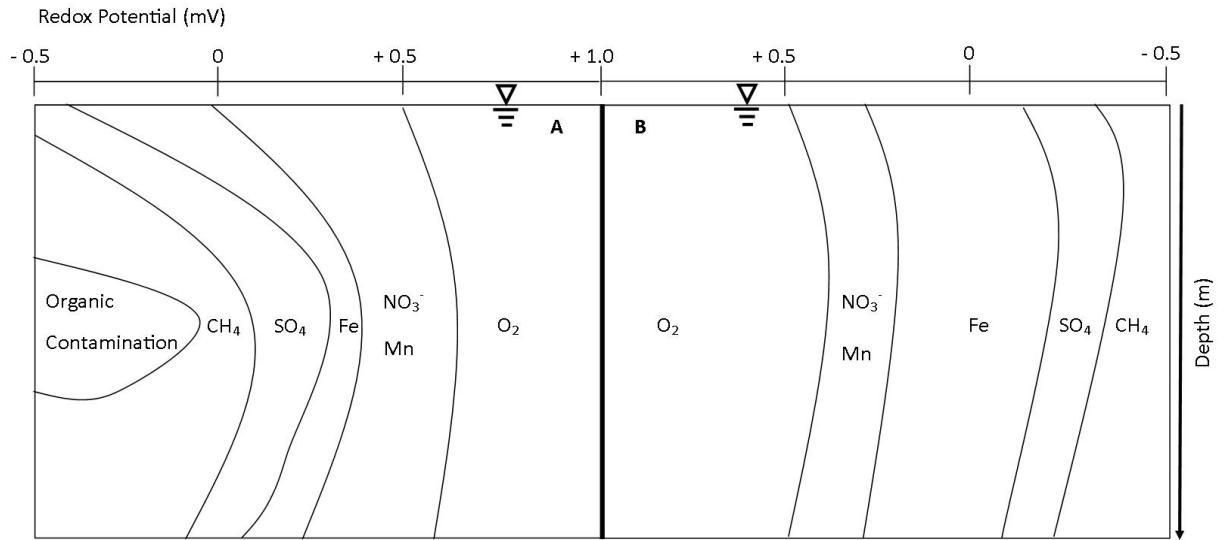


Fig 2. A.) Distribution of terminal electron acceptors in contaminated groundwater. B.) Distribution of terminal electron acceptors in pristine groundwater. Figure adapted from Lovely et al. 1994 and Christensen et al. 2000.

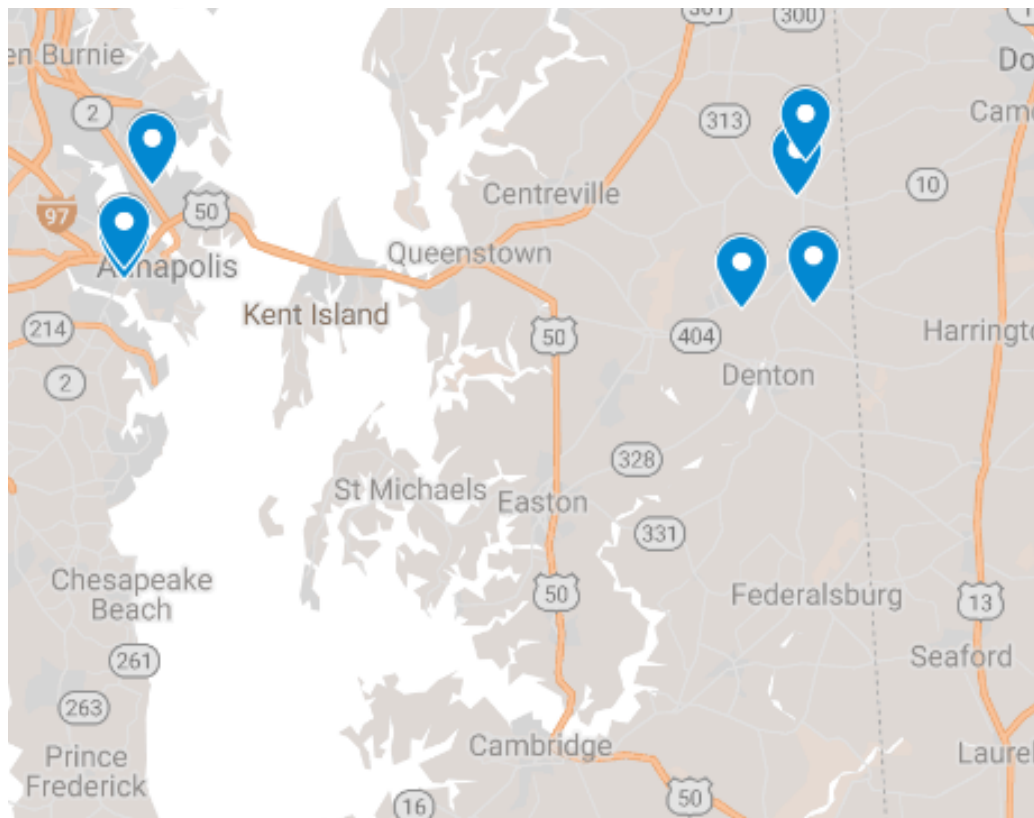


Fig 3. Map of intensive sampling sites. Sites west of the Chesapeake Bay (white) are the urban sampling sites at the Wilelinor Creek, Church Creek, and Dividing Creek. Sites east of the Chesapeake Bay are agricultural sites at Spring, Old Town, South Forge, and Broadway watersheds. Map was made using Google Maps.

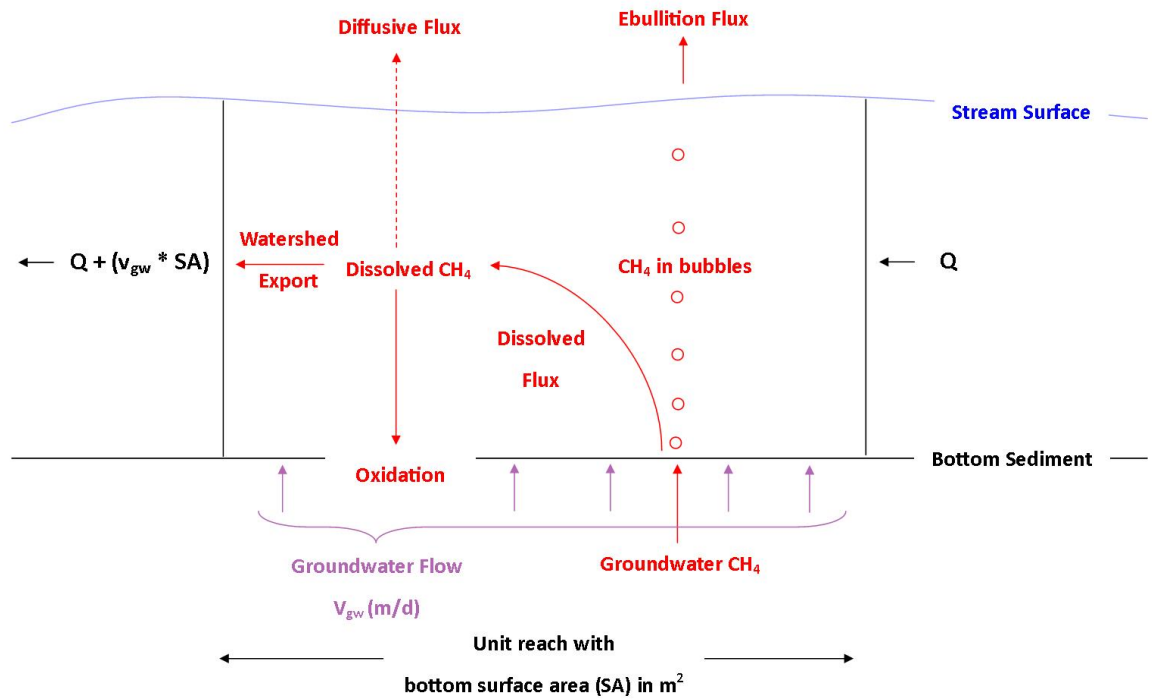


Fig 4. Conceptual diagram of methane transport in streams. Methane is transported into streams via groundwater flow, where it is then transported in bubbles or as dissolved methane. The methane is transported out of the watershed via the stream flow, diffusive flux, and ebullition flux. This model can be used to estimate the fate of watershed methane.

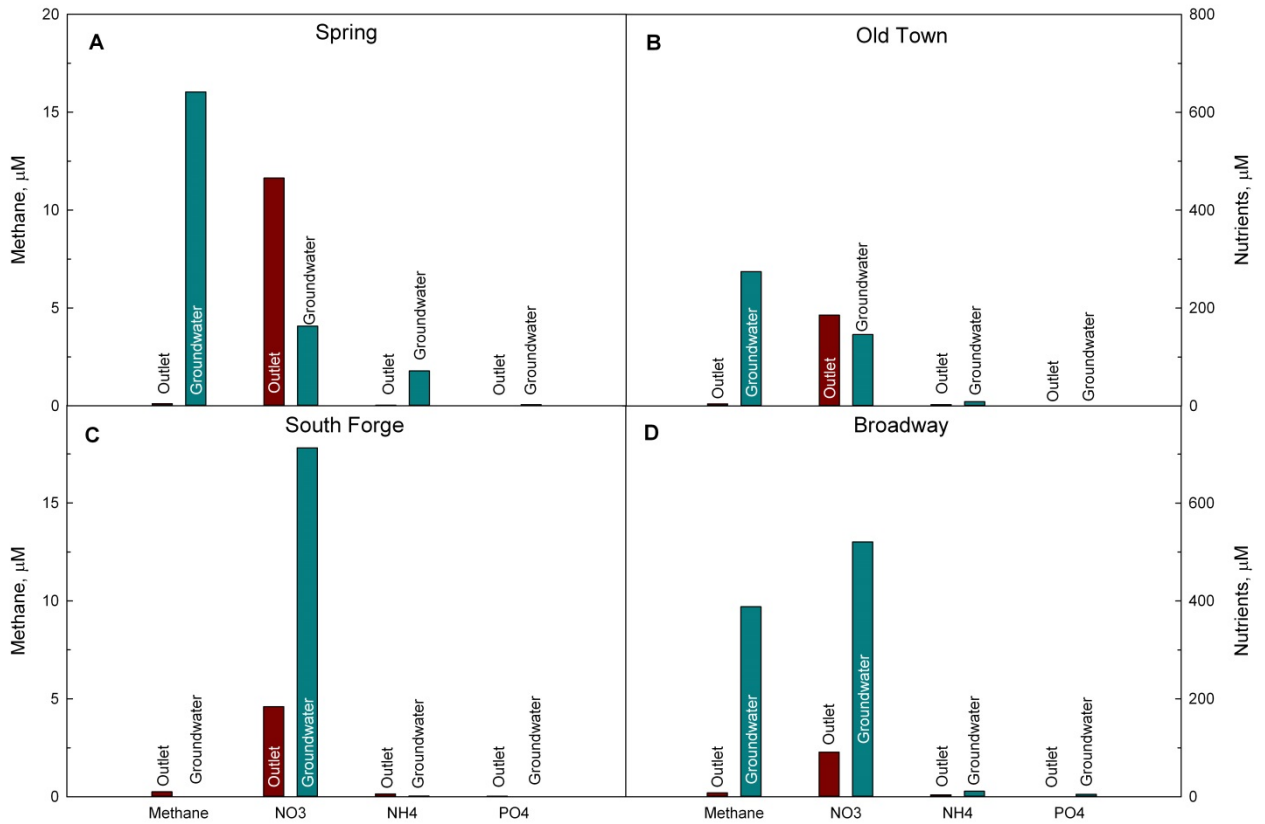


Fig 5. Watershed outlet (stream) and groundwater averages for methane and nutrients in agricultural watersheds.

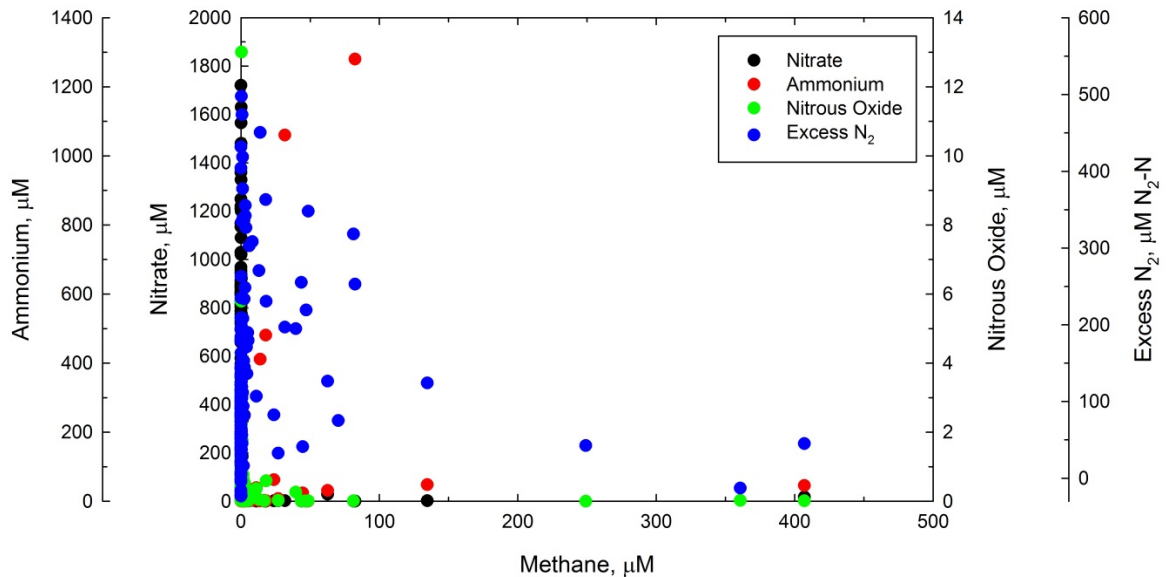


Fig 6. Groundwater methane and N-compound concentrations in agricultural watersheds.

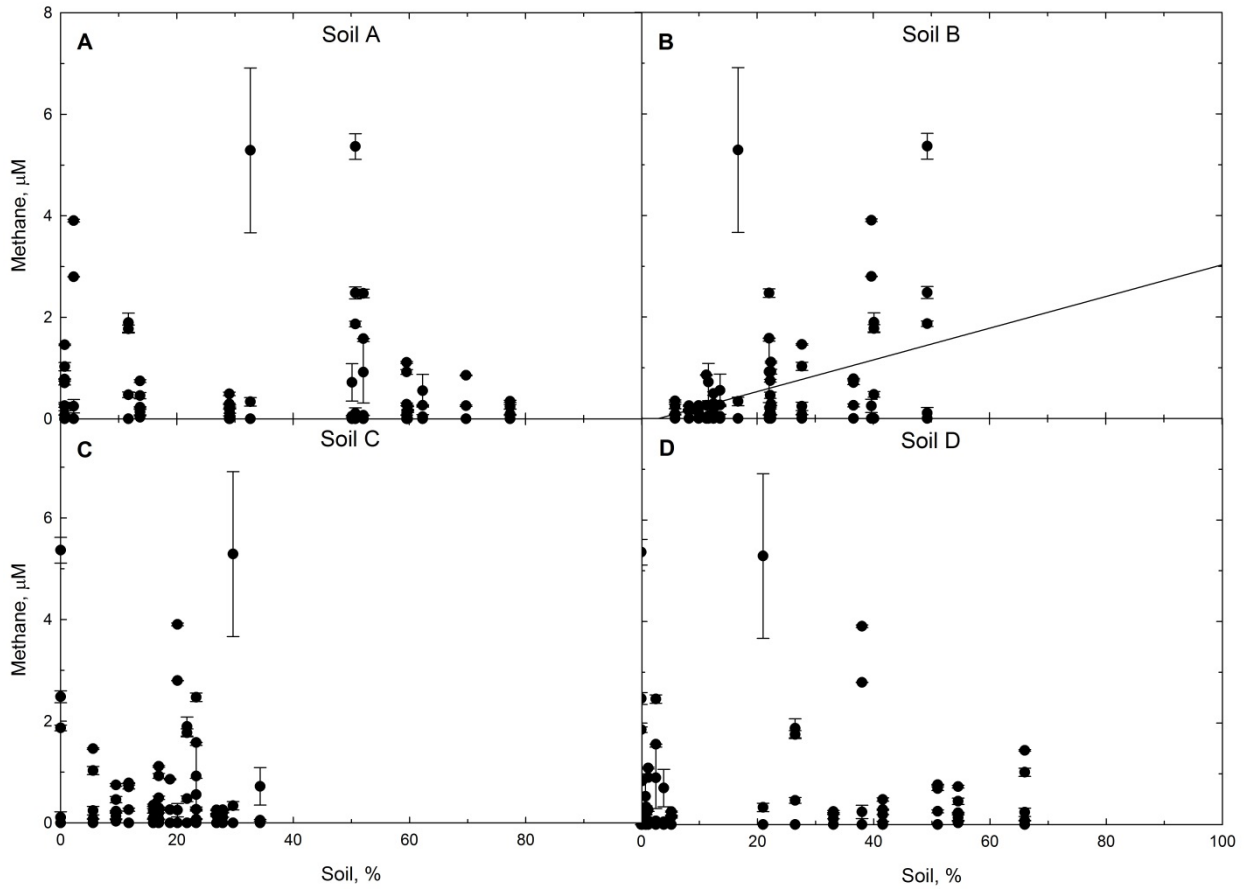


Fig 7. Stream methane concentrations in 16 watersheds and percent soil class. Two outliers (methane > 30 μM) were excluded. Soil class B has a significant positive slope of 0.03 $\mu\text{M CH}_4 / \% \text{ Soil B}$ ($p = 0.0008$).

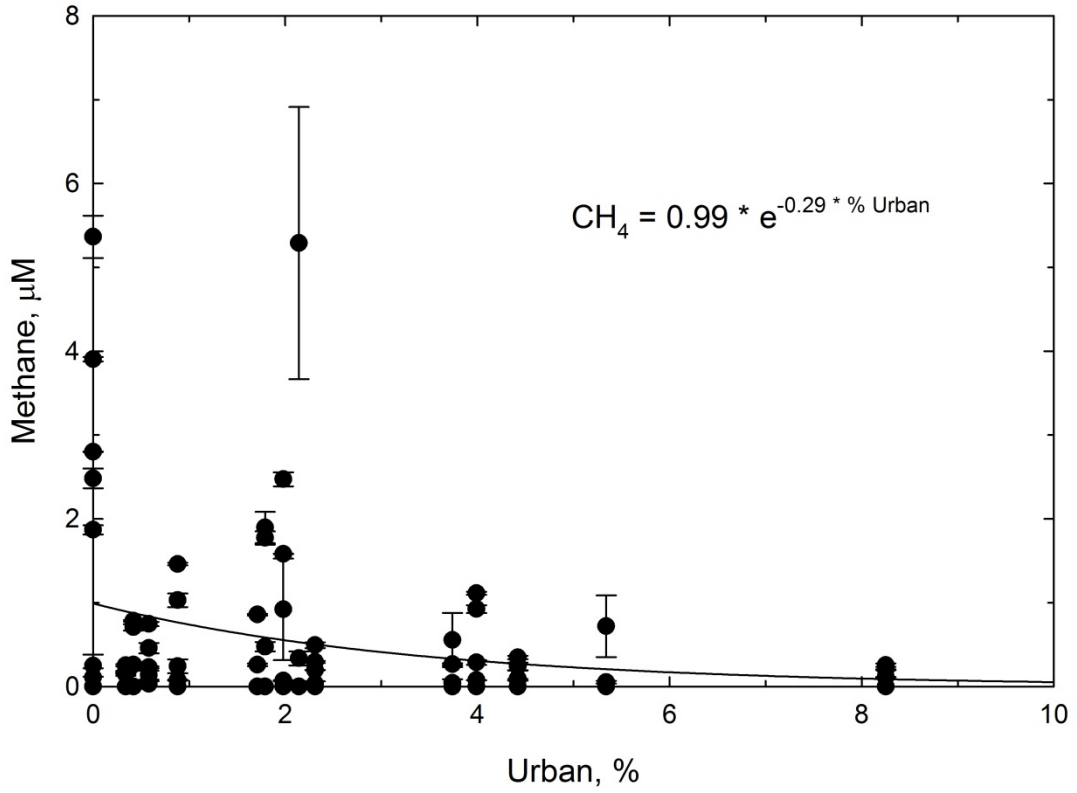


Fig 8. Watershed outlet methane vs percent urban, no outliers.

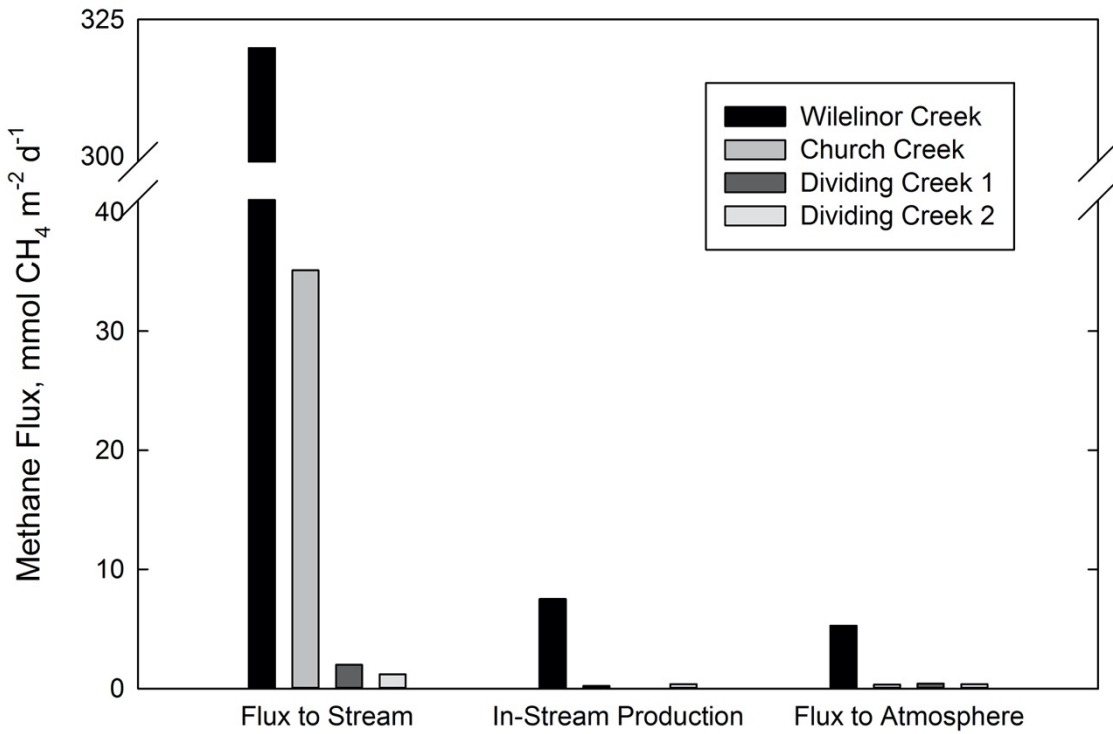


Fig 9. Methane fluxes in urban streams

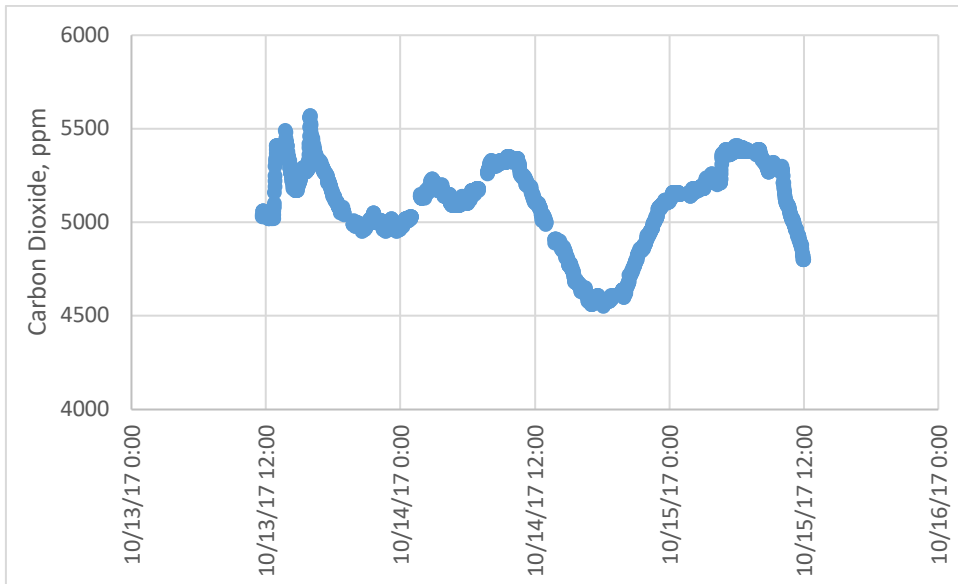


Figure 10. Stream carbon dioxide concentrations (ppm) at Wilelinor Creek over 2 days.

Chapter 3: Dynamics of Nitrate and Methane in Shallow Groundwater Following Land Use Conversion from Agricultural Grain Production to Conservation Easement

Introduction

A common water quality problem around the world is high nitrate (NO_3^-) in shallow ground and surface waters fueling eutrophication (Davidson et al. 2012). Nitrate, which is bioavailable and soluble, is of particular concern since it moves readily with water. Nitrate is naturally present at low concentrations in soils and water; however, in many places ground and surface water nitrate has increased due to fertilizer application to lawns and crop fields and by discharges of wastewater from sewage plants and septic systems (Valiela and Costa 1988, Spalding and Exner 1993, Reay 2004, Dubrovsky et al. 2010). High nitrate concentrations ($> 10 \text{ mg NO}_3^- \cdot \text{N L}^{-1}$) in freshwater also makes the water unfit for human consumption (Follett and Follett 2001). Excess nitrate in groundwater-fed streams and rivers (in conjunction with phosphorus) negatively affects water quality by causing eutrophication in downstream lakes and estuaries, providing suitable conditions for harmful algal blooms, loss of submerged aquatic vegetation due to lack of light penetration, and dead zones (Kemp et al. 2005). The Chesapeake Bay and tributaries is a well-studied eutrophic system that is plagued with annual dead zones due to increased N inputs from mixed land uses within its watershed (Kemp et al. 2005, Fisher et al. 2006).

Conservation practices, such as riparian buffers and wetlands are often used to reduce the water quality impacts of fertilizer. These practices enhance biological

processes which intercept nitrate within an agricultural landscape (Lowrance et al. 1997). The many efforts underway in the Chesapeake Watershed to reduce the impacts of fertilizer and manure applications on agricultural lands and suburban lawns have yielded few improvements in stream and river water quality (Denver et al. 2004, Dubrovsky et al. 2010). This is primarily considered to be the result of long groundwater residence times of years to decades (e.g., Sanford and Pope 2013). However, there are relatively few studies focused on the recovery time of shallow groundwater after agricultural fields are converted to conservation practices (Primrose et al. 1997, Schilling and Spooner 2006, Tomer et al. 2010, Schilling and Jacobson 2010).

Although land use conversion studies are common (e.g., Foley et al. 2005), conversion from agriculture to grassland has few studies with reference to groundwater nitrate concentrations. Time series and chronosequences (artificial time series using similar sites with varying ages since agricultural usage) have both been used to investigate the changes in groundwater nitrate. For example, a chronosequence study performed in Iowa on land use conversion from agriculture to prairie showed nitrate concentrations decreasing at $0.58 \text{ mg NO}_3^- \text{-N L}^{-1} \text{ y}^{-1}$ in the top of the unconfined aquifer (Schilling and Jacobson 2010). A time series analysis of nitrate concentrations in a stream draining the area of the chronosequence study plus additional areas with no land use change showed nitrate decreasing more slowly at $0.12 \text{ mg NO}_3^- \text{-N L}^{-1} \text{ y}^{-1}$ (Schilling and Spooner 2006). These studies show large nitrate reductions in groundwater and streams after agricultural retirement in their study region, but the results are limited geographically and are specific to one soil

class. If similar rates are found in the Chesapeake Bay region, then groundwater residence time may be a smaller factor in nitrate remediation than insufficient adoption or unknown or increasing nitrate sources.

Nitrate is a serious water quality concern, but one confounding problem with conservation efforts may be the production of the greenhouse gas methane due to changing hydrology and encouraging anaerobic conditions that can induce methanogenesis (Reeburgh 2007). Besides improving water quality, converting agricultural land back to natural conditions can have impacts on greenhouse gases that accumulate in water (Huttunen et al. 2003, Hendriks et al. 2007, Reeburgh 2007). The Conservation Reserve Program (CRP) and the Conservation Reserve Enhancement Program (CREP) are voluntary USDA programs that remove sensitive land from agricultural production and substitute plants that improve environmental quality (typically warm and cool-season grasses). Areas taken out of farm production under CRP and the CREP are often those lands that tend to collect water, and these areas are easily converted back to wetlands, which are hotspots for both denitrification and methanogenesis, the production of methane (CH₄). Although wetlands aid in processing nitrogen, about 12% of the global production of the greenhouse gas methane comes from wetlands (Reeburgh 2007). It is well established that methane is the second most important greenhouse gas after carbon dioxide in terms of radiative forcing in the atmosphere. On a molar basis, methane is about 105 times more effective at heating the atmosphere than carbon dioxide over a 20-year period (Shindell et al. 2009, Howarth et al. 2011). The largest contributors of methane emissions are freshwater wetlands and rice production, respectively

(Reeburgh 2007). High levels of methane (up to 20,000 times the atmospheric background) have been detected in groundwater under farm ditches, controlled drainage structures, and wetlands, and these high concentrations could result in ebullition (bubble formation) of methane into the vadose zone and rapid transport to the atmosphere (Fisher et al. 2010, Fox et al. 2014).

One study (Morse et al. 2012) investigated wetland greenhouse gas fluxes after wetland restoration in a former agricultural field in coastal North Carolina. Methane fluxes were found to be highly variable, and the highest fluxes were found in the warm months and at the wettest sites. The wetland sites had significantly higher methane fluxes than the agricultural field, but the agricultural field had higher greenhouse gas fluxes (CO₂-equivalents) due to carbon dioxide and nitrous oxide fluxes (Morse et al. 2012). There appears to be a dual nature to the effects of conversion of active agricultural land to natural or conservation land use. Soil nitrogen declines, groundwater nitrate appears to decrease, and stream nitrate concentrations decrease. However, wetland emissions of greenhouse gases may also increase, posing a potential trade-off between improving water quality and augmenting greenhouse gas emissions. If methane is produced in groundwater at lower concentrations of nitrate, ebullition is a possibility, potentially avoiding methane oxidation in higher, more oxic soil strata.

Methanogenesis is known to be inhibited by the presence of other electron acceptors, such as oxygen (O₂), nitrate, ferric iron (Fe³⁺), and sulfate (SO₄²⁻). Iron- and sulfate-reducers outcompete methanogens for substrate (Acht nich et al. 1995a, b), but the reduction of nitrate suppresses methanogenesis by the presence of toxic

denitrification intermediates: nitrite (NO_2^-), nitric oxide (NO), and nitrous oxide (N_2O , Roy and Conrad 1999). In agricultural fields, nitrate is the dominant electron acceptor after oxygen. Although ferric iron and sulfate also inhibit methanogenesis, these electron acceptors are not found in high concentrations in agricultural areas in our study region (Kasper et al. 2015).

The objective of this study was to evaluate the nitrate and methane impacts of applying conservation practices to agricultural land over time. Harleigh Farms in Talbot County, MD represented a unique opportunity to evaluate reductions in agricultural nitrate and potential methane production in groundwater because of the documented retirement of a series of farms from intensive grain production to conservation planting for wildlife. Groundwater nitrate and methane levels in the surficial aquifer were monitored in a chronosequence of plots with as many as 16 years of post-agricultural conservation land use. We wanted to test the concept that if conservation practices are effective, then improvements in groundwater quality should be observable under the practice. The chronosequence reported here provides information on the time period required for groundwater nitrate concentrations to decrease on the coastal plain in Maryland. We hypothesized that nitrate concentrations would decrease as time out of agricultural production increased, and that methane concentrations would increase over time as the supply of the alternate electron acceptor nitrate decreased, resulting in more methanogenesis in the anaerobic metabolism of the soil.

Materials and Methods

Study Sites

For this chronosequence study, we examined groundwater nitrate and methane concentrations under fields that had been sequentially retired from grain production over 16 years. One field was still in active grain production, and the other six fields were last farmed from 2-16 years prior to the start of the study. The varied land retirement history of these fields provided a 16-year chronosequence of groundwater chemistry conditions after the cessation of fertilization. Sampling was conducted monthly from November 2012-November 2013.

This study was conducted at Harleigh Farms, located in Talbot County on the eastern shore of Maryland (Fig. 1). All of the sites drain to the tidal Trippe Creek, a tributary of the Tred Avon River which drains to the Choptank River (the seventh largest tributary to the Chesapeake Bay by catchment size). The site is in the hydrogeomorphic region “fine-grained lowlands” that is characterized by a shallow water table (generally 0 to 3.0 m below land surface) and poorly drained sediments of low permeability (Hamilton et al. 1993). All sites are between 3 and 7 m above sea level. Soil types and the presence of hydric soils were determined using USDA’s SSURGO dataset (Soil Survey Staff 2015). Due to the limited size of conservation practices at Harleigh Farms, soil type selections were limited. All sites were poorly to somewhat poorly drained, except for the Forest site, which was well drained (Table 1). Forest and agriculture are the two major land uses and represent end members in terms of nitrogen inputs (forests = low, agriculture = high). To provide nitrate data from both well and poorly drained soils outside Harleigh Farms, data from other

nearby sites with a range of soil types on Maryland's Eastern Shore were also used to supplement these forest and agricultural end members of nitrate input (Table 1).

Over the past 17 years, Harleigh Farms has successively acquired fields in intensive grain production (corn, wheat, soy) and put them into conservation easements. The property is managed based on 1/3 forest, 1/3 crop, and 1/3 managed conservation for the enhancement of game species such as quail. The buffers are managed as CREP or CRP and are a mixture of warm season grasses with CREP having additional woody shrubs and some non-tidal wetlands (Table 1). Our sampling locations were chosen based on varying ages (0-16 years) since intensive grain production as documented by Harleigh Farmland records. We designated groundwater piezometers in fields by years since retirement from active grain production and fertilization; e.g., '9a' is the first piezometer in a field with no grain production or fertilizer in nine years since the piezometer installation (not since present day). In addition, there were piezometers installed in a forested site (Forest) and an actively cropped field (Ag). The Forest site is a hardwood forest with a few, very large pine trees that is approximately 100 years old. Three sites (8a, 8b, 9a) are under wetland easements, and these sites exhibit wetland hydrology with hydric soils. Although the post-agricultural conservation practices include CRP, CREP, and wetlands, these land uses are being grouped together in this study as general conservation practices.

Because we had only one agricultural and one forest site at Harleigh Farms, the statistical analyses were run with nitrate data from four supplemental agricultural sites and one supplemental forested site. The agricultural sites (CFC1, EFAg2, HFF1,

BNDS1) are all located within the Choptank Basin and have a range of sand and silt loam soil types similar to those of Harleigh Farms (Table 1, Fox et al. 2014). The supplemental forested site (MHF1) is located in the adjacent Nanticoke Basin and is within a small, completely forested watershed (Gardner et al. 2016, Bunnell-Young unpublished) in the Chesapeake Forest Land Program of MD Department of Natural Resources. The aggrading pine forest in the uplands of the watershed was logged in the 1980s and is now approximately 30 years old. The approximately 30 m wide stream corridor has large trees (0.5-0.8 m diameter) of tulip poplar, beech, and pine.

Piezometer Installation

Fourteen monitoring piezometers were installed at 1-3 m depth below the surface to sample groundwater on Harleigh Farms in areas with different land management practices (agriculture, forested, wetland, grassland). 7.6 cm boreholes were manually dug with a hand auger, and a 5.1 cm inner diameter piezometer was placed in the center of the hole. Coarse sand filled the annulus around the piezometer slots, and bentonite sealed the upper portion of the annulus above the piezometer slots from surface leaks. Similar piezometer installations had previously been made at the supplemental sites.

Groundwater Sampling

Groundwater was sampled from each piezometer monthly for analyses of pH, conductivity, nitrate, and dissolved methane concentrations. Prior to collecting water at each site, undisturbed instantaneous water-table depth below the top of the piezometer was measured using a Solinst water level meter (model 102m). Water-

table depth below ground was obtained by subtracting the above-ground length of the piezometer from the total depth. After recording water level, groundwater was pumped from the piezometer for 5 minutes or until groundwater was depleted using a positive displacement pump or peristaltic pump. Once the piezometers recovered sufficiently with fresh groundwater, usually within 10 minutes, sampling of the newly recovered groundwater was completed using the same positive displacement or peristaltic pump. Samples for nitrate analysis were collected in 75 ml sample bottles that were rinsed 3 times with sample water before filling. Methane sampling was completed after nitrate sampling using only the positive displacement pump. From each site, 2 samples were carefully collected in 22 mL glass test tubes and capped, ensuring that no air was trapped in the tube. Methane could not be sampled from 16b because the positive displacement pump tubing was too short to reach the bottom of the piezometer. All samples were placed on ice to be transported to Horn Point Laboratory for further analyses, with pH and conductivity analyzed in the field when time allowed.

Groundwater and Climate Data

Groundwater temperature and water-level data were collected in 2 piezometers (2a and 14b) at 30-minute intervals using Solinst Leveloggers (model 3001 CE LT F15/M5) sitting at the bottom of the piezometers. The water-level data were corrected for variations in atmospheric pressure using parallel records from a Solinst Barologger (model 3001 CE F5/M1.5). Data were downloaded from the loggers installed in the piezometers at ~6-month intervals, baro-corrected, referenced to depth

below ground using the piezometer depth, and plotted as monthly and annual records of local water table depth and temperature.

Aboveground temperature and precipitation data were obtained from nearby monitoring stations. Precipitation data was accessed from the NOAA National Climatic Data Center's Global Historical Climatology Network-Daily (NOAA NCDC 2014). Average monthly precipitation was calculated using total monthly precipitation from 3 stations: Easton 1.1 SW, MD US, Easton 2.4 SE, MD US, and Trappe 3.5 NE, MD US. Air temperature data was collected from the La Trappe Creek station (KMDTRAPP1, Weather Underground 2014).

Analytical Methods

Chemical analyses (pH, conductivity, nitrate, methane) were conducted at Horn Point Laboratory. Conductivity and pH were measured in the field or in the lab using a portable Yokogawa Model SC82 conductivity meter and a VWR SympHony SP70P pH meter. Conductivity standards and measurements were standardized to a temperature of 25°C, and the pH meter was standardized using pH 4 and 7 buffers. Samples were filtered in the lab using GF/F filters for automated colorimetric analysis of nitrate+nitrite on a Technicon AutoAnalyzer II in the Horn Point Analytical Services Lab. Dissolved methane was measured using a static headspace equilibrium method (Johnson et al. 1990, Kampbell and Vandegrift 1998) and run on a Shimadzu GC-8A gas chromatograph with a flame ionization detector.

Statistics

Graphics and statistics were done using SigmaPlot v12.5. Statistics on pH were

performed on hydrogen ion concentrations, and the results were converted to pH. Linear and non-linear regressions of concentrations against time were run on the seasonal and chronosequence nitrate and methane data. If a relationship did not have a significant linear trend, other non-linear models were considered, such as exponential, Lorentzian, or waveform. If no model had a significant fit to the data, it was considered to have ‘no pattern.’ Exponential and more complex models were chosen over a significant linear model for some of the data based on the Akaike Information Criterion (AIC, Akaike 1973):

Eq. 1

$$AIC = n * \ln(SSerror / n) + 2*K$$

where n is sample size, $SSerror$ is sum of squares error, and K is number of model parameters + 1. The model with a significant model fit ($p < 0.05$) and the lowest AIC score was chosen as the best model. If models had similar AIC values (± 7), we chose the more complex model (Burnham and Anderson 2002).

Results

Temperature, Rainfall, and Groundwater Levels

The study period of Nov 2012–Nov 2013 was slightly wetter (114 cm y^{-1}) than the long-term average of 110 cm y^{-1} (Lee et al. 2001). For the sampling year, peak precipitation ($\sim 24 \text{ cm month}^{-1}$) was in June 2013, which was followed by nearly average rainfall ($\sim 10 \text{ cm month}^{-1}$) in July and Aug (Fig. 2A). The lowest average monthly air temperature ($2.6 \text{ }^\circ\text{C}$) was recorded in January 2013, and the highest ($26.4 \text{ }^\circ\text{C}$) was in July 2013 (Fig. 2B), which follows typical long-term seasonal patterns for

this region (Fisher et al. 2010).

Groundwater temperature and water-table depth exhibited similar seasonal patterns at sites 14b (Fig. 3) and 2a. At these sites, the minimum groundwater depth below the soil surface occurred during the late fall to spring recharge season with water levels only 0.25 m below ground surface in mid-April. The greatest water-table depth was during the late summer and early fall recession period when groundwater depth was approximately 1.6 m below the ground surface. The water-table was closest to the surface during the months of February to April due to low evapotranspiration (ET) in the preceding months, and the water-table was deepest in late summer and early fall due to high summer ET (Fisher et al. 2010). This seasonal pattern agrees with data from other nearby sites in the Choptank River catchment (Fisher et al. 2010), and the only difference between sites 2a and 14b is a slight temperature deviation in the summer. At 2a, for example, the maximum temperature was above 21°C. In contrast, the maximum temperature at 14b was about 19°C, which may be due to differences in shading at the two sites. The temperature and groundwater depth patterns at 2a and 14b mirror groundwater conditions occurring regionally (Fisher et al. 2010, Fox et al. 2014).

General Groundwater Chemistry

Specific conductivity and pH varied by site, but there was no systematic seasonal variability of these parameters. The mean pH values ranged from 4.1 to 7.1 (Table 2), and most of the piezometers at the same site had similar pH means. The 2a – 2d sites varied the most, ranging from 5.0 to 6.3. Average specific conductivity ranged

from 54 to 1370 $\mu\text{S cm}^{-1}$ across the piezometers (Table 2), and conductivities greater than 700 $\mu\text{S cm}^{-1}$ were found at 3 of the 2a – 2d sites and the 8a and 8b sites. These sites are in the headwaters of tidal, oligohaline Trippe Creek (Fig. 1), and the elevated conductivities at sites 2 and 8 represent slight salinization of the groundwater. All other piezometers had conductivities at or below 300 $\mu\text{S cm}^{-1}$, and groundwater at the two forested sites had conductivities of 54-64 $\mu\text{S cm}^{-1}$ (Table 2).

Seasonal Nitrate Variability

Most of the sites (10 out of 17) did not exhibit systematic seasonal variability in groundwater nitrate concentrations (Table 3). However, seasonal nitrate variations were found at seven of the sites. Two sites (8a and 14b) had low nitrate ($< 0.6 \text{ mg NO}_3^- \text{-N L}^{-1}$) and exhibited a weak linear increase in nitrate over the sampling year ($p < 0.05$, Table 3). These low-nitrate sites showed small seasonal increases in nitrate of 0.06 and 0.34 $\text{mg NO}_3^- \text{-N L}^{-1} \text{ y}^{-1}$ (8a and 14b, respectively, Table 3). Of the 4 sites with elevated nitrate concentrations ($> 1.0 \text{ mg N L}^{-1}$), all but one site (9a) had a seasonal nitrate pattern of exponential decay during the sampling season ($p < 0.05$, Table 3, Fig. 4). Site 2a had the largest exponential decay coefficient of -4.59 (Fig. 4B), and the largest percent decrease in nitrate concentration (85%) was found at site 3a (Fig. 4C). The 3a site also had the lowest starting nitrate concentration of the 3 exponential decay sites. Nitrate data from 2c and 3b followed a seasonal sine wave pattern ($p < 0.05$, Table 3). These 2 sites have low to moderate nitrate concentrations ($< 1.2 \text{ mg NO}_3^- \text{-N L}^{-1}$), but their peak nitrate concentration was in the winter/spring months during maximum recharge conditions (Fig. 3).

Nitrate Chronosequence

The longer an area has been out of agricultural production, the lower the annual average groundwater nitrate concentrations (Fig. 5). The agricultural site on Harleigh Farms (Ag) had an average groundwater nitrate concentration of $11.3 \text{ mg NO}_3^- \text{-N L}^{-1}$ (filled circle at $x = 0$), similar to other farms in this region (open squares at $x = 0$, Fisher et al. 2010, Fox et al. 2014). The average groundwater nitrate concentration for all agricultural sites was $9.68 \text{ mg NO}_3^- \text{-N L}^{-1}$. Values of groundwater nitrate $< 10 \text{ mg NO}_3^- \text{-N L}^{-1}$ are associated with hydric soils (water-saturated, with little interstitial oxygen), with large accumulations of excess N_2 in groundwater due to denitrification (Lee et al. 2001, Fox et al. 2014). In contrast, values of groundwater nitrate $> 10 \text{ mg NO}_3^- \text{-N L}^{-1}$ in agricultural areas are associated with better drained soils, with small accumulations of excess N_2 in groundwater (Fox et al. 2014). The ~ 100 -year-old forested site at Harleigh Farms and the additional ~ 30 -year-old forested site on the nearby Marshy Hope Creek both have very low groundwater nitrate ($< 0.05 \text{ mg NO}_3^- \text{-N L}^{-1}$), consistent with low values of nitrate concentrations in streams draining forested areas reported by Clark et al. (2000).

Data from the forested and active agricultural sites provides the end points for a chronosequence study of groundwater nitrate over time after cessation of agriculture. Using the other Harleigh Farms sites as a proxy for varying time periods out of intensive agriculture, there was a significant exponential decrease ($p < 0.0001$) in groundwater nitrate (Fig. 5). Based on the exponential fit, only 3-5 years are necessary for nitrate at the top of the unconfined aquifer to decrease to $< 0.5 \text{ mg NO}_3^- \text{-N L}^{-1}$. The exponential coefficient (2.1 y^{-1}) in Fig. 5 implies a rapid turnover rate

(2.1 times per year) of water in the top of the surface unconfined aquifer, resulting in rapid decreases in nitrate concentrations after the cessation of fertilizer applications. The AIC test rejected the 3-parameter exponential model with an asymptote ($y = y_0 + ae^{-bx}$, with y representing nitrate, x is time after cessation of fertilizer, a and b representing coefficients), and we used a 2-parameter exponential model with no asymptote ($y = ae^{-bx}$). This is consistent with the very low nitrate concentrations reported above for forested systems, and the y-intercept, equivalent to the average nitrate concentration in groundwater of active grain production, is $\sim 8.0 \text{ mg NO}_3^- \text{-N L}^{-1}$, a value commonly observed locally (Table 2, Fox et al. 2014). An exception to the general pattern is the 9a site, which has nitrate concentrations well above the regression line possibly due to this site's close proximity ($< 10 \text{ m}$) to an active agriculture site (Fig. 1, Table 1). Site 9a appears to be receiving some of the nitrogen being applied to the adjacent, actively farmed field (Fig. 1), and we did not include site 9a in the regression shown in Fig. 5.

Seasonal Methane Variability

Dissolved methane was detectable ($> 1.5 \text{ nM}$) in 7 of the 16 Harleigh piezometers sampled for methane and in all of the supplemental sites (Table 2). At the sites with detectable concentrations, methane was variable but above the atmospheric equilibrium concentrations of $\sim 2.7 \text{ nM CH}_4$. Peak methane concentrations occurred in late summer or early fall in all but 1 of the 7 Harleigh piezometers with detectable methane, coinciding with the deepest groundwater depths (Fig. 6) and highest temperatures (Fig. 3). Although methane data were only collected for a portion of the sampling season, the seasonal pattern coincides with that found in other reports on

methane in groundwater in the Choptank basin (Fox 2011). The water in piezometer 8b had the highest average and peak methane, with concentrations nearly reaching 60 μM CH_4 in August and September 2013 (Fig. 6). This level corresponds to more than 20,000 times greater than atmospheric equilibrium.

Methane Chronosequence

There was no significant relationship between groundwater methane concentrations and time out of production (Fig. 7). Only four sites, all with hydric soils, had average dissolved methane in groundwater concentrations greater than 0.50 μM methane (Table 2). Three Harleigh Farms sites and the MHF1 supplemental forested site with hydric soils had elevated methane concentrations that exceeded 10 μM , with no obvious pattern in the chronosequence (Fig. 7). All other Harleigh Farms sites and the supplemental sites dominated by agriculture had methane concentrations $<0.5 \mu\text{M}$ with no clear chronosequence pattern. However, for all locations combined, nitrate was inversely correlated ($p < 0.05$) with methane concentrations, and methane only accumulated in groundwater to concentrations $> 2 \mu\text{M}$ CH_4 when nitrate was less than 0.1 mg $\text{NO}_3^- \text{-N L}^{-1}$ (Fig. 8).

Discussion

Temporal Variations in Nitrate

Our hypothesis of decreasing groundwater nitrate concentrations with increasing time out of grain production was supported by the data. We found that groundwater nitrate concentrations in a chronosequence analysis were exponentially reduced from approximately 11 mg $\text{NO}_3^- \text{-N L}^{-1}$ to much lower concentrations ($<0.5 \text{ mg NO}_3^- \text{-N L}^{-1}$)

in ~3-5 years in the top of the surficial aquifer (Fig. 5). The initial response time of 3-5 years for groundwater nitrate concentrations to drop significantly is consistent with groundwater nitrate data from the studies by Tomer et al. (2010) and Schilling and Jacobson (2010).

The most likely mechanisms for nitrate-attenuation (Fig. 9) in this study are: the cessation of fertilizer applications and dilution of older groundwater nitrate by new, lower-nitrate recharge. All of the post-agricultural sites have low nitrate concentrations and a history of fertilizer cessation. Groundwater residence times for the current study area were not determined, but in a nearby 50 km² watershed in the upper Choptank basin, median groundwater residence times are about 8 years (Sutton et al. 2009). This median groundwater residence time is consistent with the time scale (3-5 years) of the observed reduction of groundwater nitrate concentrations in this study (Fig. 5) because we sampled the top 2 m of the unconfined surface aquifer of about 10 m thickness (Lindsey et al. 2003). The top 2 m is the first part of the groundwater system to be influenced by changes in land use and management.

Seasonal patterns provide further evidence for nitrate-attenuation mechanisms. Local soil processes at the conservation sites may alter nitrate in groundwater. In the winter, low evapotranspiration increases the local groundwater recharge with precipitation having low nitrate concentrations, causing dilution of older groundwater that has high nitrate levels from previous fertilizer applications. In the warm summer months, groundwater recharge decreases except during large storms (Fig. 3), but biological nitrogen processing (e.g., denitrification) may increase with temperature, which may also lead to decreases in nitrate concentrations. Due to

the experimental design and resources available for this study, microbial nitrate attenuation (denitrification and other biological reduction processes) was not measured but based on the water table and the presence of hydric soils, it can be surmised that in sites with wetland hydrology (8a, 8b, 14c), denitrification may have played an important role in nitrate reduction (Lee et al. 2001, Fox et al. 2014). The other, non-hydric sites most likely had a more diverse combination of factors causing the observed reductions in nitrate concentrations.

We can use the seasonal patterns of nitrate concentrations observed at the sites to explore the importance of some of the factors controlling groundwater nitrate concentrations. Three of the four sites with elevated nitrate concentrations ($>1 \text{ mg NO}_3^- \text{-N L}^{-1}$) exhibited exponential decreases over the sampling year (Table 3). This seasonal, exponential decrease in nitrate concentrations (Fig. 4) paralleled the chronosequence pattern (Fig. 5), but on a finer time scale of months. This suggests that our monthly sampling was able to resolve the process of new, low-nitrate groundwater diluting and/or displacing older groundwater enriched with nitrate from previous surface fertilization.

We note that the Harleigh Farms site in active grain production (Ag) exhibited exponential decay during the sampling period (Table 3, Fig.4A and 10B). We argue that this is a short-term fluctuation associated with seasonal variations in recharge and farm management activities similar to those observed in longer term studies such as the example for CFC1, a supplementary site, shown in Fig. 10A. Multiple 12-month blocks of data could be used to show exponential decreases or increases in Fig. 10A (or no change), but this kind of seasonal variability is fundamentally different from

that shown in Fig. 4B and C for sites 2a and 3a. In these data, nitrate concentrations intermediate between agriculture and forest (see Fig. 5) declined rapidly towards those typical of forest groundwater; in contrast, the fluctuations at the Harleigh Farms Ag site (Fig. 4A) decreased but remained in the range typical of agricultural groundwater. For these reasons, we argue that the data in Fig. 4B and 4C for sites 2a and 3a represent dilution and displacement of older groundwater with high nitrate concentrations by newly recharging groundwater with low nitrate concentrations, whereas the data in Fig. 4A represent short term fluctuations in nitrate at the Ag site on Harleigh Farms similar to those observed in the longer record for CFC1 (Fig. 10A).

The seasonal and long-term chronosequence patterns shown in Figs. 4 and 5 provide evidence for dilution and/or vertical displacement of older groundwater (Fig. 9). New, low-nitrate recharge and biological attenuation can be important processes responsible for the general decrease in groundwater nitrate in the surficial unconfined aquifer over time after cessation of surface fertilization. Although we have no evidence for biological nitrogen uptake by surface vegetation, there were 1-2 m tall stands of warm season grasses and wetland plants at these sites growing in the surface soils. Typical nitrogen uptake rates by large vegetation stands are 1.6-35 g NO_3^- -N $\text{m}^{-2} \text{y}^{-1}$ (Jung et al. 1990, Tufekcioglu et al. 2003, McLaughlin et al. 2004, Silveira et al. 2007), and these must have influenced nitrate in recharging groundwater (Fig. 9).

Our data indicate that the impacts of effective management practices designed to reduce groundwater nitrate should be detectable within 3-5 years in the top of the surficial, unconfined aquifer. We suggest that this should be the acceptable range of

time over which conservation practices (e.g., stream buffers, winter cover crops on agricultural fields, etc.) can be evaluated as controls on nitrogen (primarily nitrate) losses to groundwater. The scale of conservation practices has to be large enough ($> 100 \text{ m}^2$) that uncertainty in groundwater flow paths does not obscure the conservation effect. Routine testing can be completed using a simple, drive-point piezometer. If no effects are detectable in the top of the groundwater aquifer within 3-5 years, it is likely that the conservation practice is not effective or insufficiently implemented. In contrast, the effects of conservation practices on nitrate concentrations in streams may take longer to be realized with median groundwater ages of 8-27 years in watersheds of the Choptank River basin (Sutton et al. 2009, Sanford and Pope 2013).

Groundwater Nitrate Model

We used the conceptual model in Fig. 9 as a framework for a mathematical model of groundwater nitrate in our chronosequence. The goals of this effort were (1) to test whether the model could reproduce the observed changes in groundwater nitrate presented here, using additional data for parameters obtained from the literature, and (2) to estimate the importance of the processes in Fig. 9.

There are multiple processes influencing groundwater nitrate concentrations following a major change in land management. The processes include surface N application rate (A , $\text{g NO}_3^- \text{-N m}^{-2} \text{y}^{-1}$), volumetric soil denitrification rate (D , $\text{g NO}_3^- \text{-N m}^{-3} \text{y}^{-1}$), surface plant uptake rate (U , $\text{g NO}_3^- \text{-N m}^{-2} \text{y}^{-1}$), and groundwater export (turnover) based on local water yields (E , m y^{-1}). If we set the initial concentration of groundwater nitrate at time 0 to be approximately what we observed in the chronosequence for current agricultural conditions (Fig 5), $[\text{NO}_3^-]_0 = 11.2 \text{ mg NO}_3^- \text{-N}$

L^{-1} , the annual change in groundwater nitrate concentrations ($d[NO_3^-]/dt$, g NO_3^- -N $m^{-3} y^{-1}$) can be used to predict the nitrate concentration in a future year t ($[NO_3^-]_t$) as a function of these processes using Eq. 2:

$$\frac{d[NO_3^-]}{dt} = \frac{A}{z * \theta} - [D * \frac{[NO_3^-]_t}{[NO_3^-]_0} - \frac{U * \frac{[NO_3^-]_t}{[NO_3^-]_0}}{z * \theta} - \frac{E[NO_3^-]_t}{z * \theta}] \quad \text{Eq. 2}$$

where z is aquifer depth (m), θ is soil porosity ($m^3 m^{-3}$), and all other terms are defined above. We set the average aquifer depth (z) at 10 m based on Denver and Nardi (2016), and we used an average soil porosity (θ) of $0.4 m^3 m^{-3}$ (Brady and Weil 1999). In this formulation we have made both D and U linearly scaled to the nitrate concentrations in groundwater for simplicity, but other, more complex scaling (e.g., hyperbolic) is possible.

Surface N applications (A) include both fertilizer inputs plus atmospheric deposition. In year 0, prior to conversion to conservation practice, fertilizer inputs were set at $15 g NO_3^-$ -N $m^{-2} y^{-1}$ ($150 kg N ha^{-1} y^{-1}$), and atmospheric deposition was assumed to be $1 g NO_3^-$ -N $m^{-2} y^{-1}$ ($10 kg N ha^{-1} y^{-1}$), rates typical of regional values (Scudlark et al. 1998, Staver and Brinsfield 2001, McCarty et al. 2008). In years following conversion to conservation practice, N inputs included only atmospheric deposition.

The model was calibrated by initially using values for model parameters from the range of literature values (Table 4) that resulted in approximate steady state of groundwater nitrate concentrations. We used $D = 1.57 g NO_3^-$ -N $m^{-3} y^{-1}$, $U = 6.35 g NO_3^-$ -N $m^{-2} y^{-1}$, and $E = \sim 0.27 m y^{-1}$ (based upon annual water yields) when fertilizer inputs were $15 g N m^{-2} y^{-1}$ (Fig. 11A). We parameterized E using local annual water

yields (m y^{-1}) from the nearby USGS gauge near Greensboro MD, with a reduction for overland flow (0.33 of water yield, Koskelo et al. in review) to estimate an average groundwater infiltration rate of 0.27 m y^{-1} . This is effectively a groundwater turnover rate per unit area ($\text{m}^3 \text{ m}^{-2} \text{ y}^{-1}$) normalized by the volume of groundwater per unit area in the surface unconfined aquifer ($z * \theta, \text{m}^3 \text{ m}^{-2}$). The annual groundwater recharge based on observed water yields is shown in Fig. 11A. An initial surface rate of plant uptake (U) of $6.35 \text{ g NO}_3\text{-N m}^{-2} \text{ y}^{-1}$ was based on several references for grasses growing in cultivated fields (Table 4). The reported range of rates was 1.6-35.2 $\text{g NO}_3\text{-N m}^{-2} \text{ y}^{-1}$, and 6.35 is a median value for fertilized sites. The use of $U = 6.35 \text{ g NO}_3\text{-N m}^{-2} \text{ y}^{-1}$ and fertilizer application rate of $15 \text{ g N m}^{-2} \text{ y}^{-1}$ results in a crop N use efficiency of 42%, which is typical of North American agricultural fields (Cassman et al. 2002) We assumed that U in subsequent years following conversion was linearly proportional to the concentration of nitrate for that year ($[\text{NO}_3^-]_t / [\text{NO}_3^-]_0$).

For denitrification (D), due to the large range of reported values for D in the literature ($0.01\text{-}38 \text{ g NO}_3\text{-N m}^{-3} \text{ y}^{-1}$, Table 4), D was determined after U and E were chosen and a value of D was selected from the literature range to establish approximate steady state of groundwater nitrate during fertilized years. A value of $1.57 \text{ g NO}_3\text{-N m}^{-3} \text{ y}^{-1}$ for D is reasonable for a fertilized field based on reported values given in Table 4 and results in approximate steady state groundwater nitrate (Fig. 11A).

When we eliminated fertilizer additions, the model produced an exponential time series of nitrate concentrations (Fig. 11B) similar to our observations in Fig. 5.

The model projection (Fig. 11B) prior to 1998 includes the calibration data used in Fig. 11A and then shows an exponential decrease in groundwater nitrate after cessation of fertilizer application ($A=0$) and conversion to conservation planting. The decay coefficient in the model is -0.40, whereas the observed chronosequence at Harleigh Farms exhibited an exponential decrease in nitrate concentrations with a decay coefficient of -2.13 (Fig. 5). As parameterized above, the modeled nitrate concentration decreased similarly but only about 18% as rapidly as our observations in the chronosequence, and we could easily match the rates of decay by increasing one of the loss rates (D or U) or decreasing z or θ . However, in the absence of direct measurements of these parameters at Harleigh Farms to constrain the parameters within the broad ranges shown in Table 4, we felt the similarity of the model and the observed results provided conceptual support for the processes that resulted in the rapid decreases in groundwater nitrate concentrations at Harleigh Farms following conversion of intensive grain production with fertilization to conservation plantings (Fig. 9).

Model projections were run to determine parameter sensitivity and goodness of fit to the empirical data. Parameter values for soil denitrification (D) and plant uptake (U), and groundwater export (E) were varied by $\pm 10\%$ to indicate the sensitivity of $d[\text{NO}_3\text{-N}]/dt$ in eq. 2 to changes in D , U , and E . Given the nominal values selected above, D was the parameter with the greatest effect on $d[\text{NO}_3\text{-N}]/dt$ per unit change in D (3.5), and this was most obvious in year 1 after cessation of fertilization. U and E were similar in their effect on $d[\text{NO}_3\text{-N}]/dt$, but E was the least sensitive parameter, with the least effect on $d[\text{NO}_3\text{-N}]/dt$ per unit change in E (0.9).

These model results suggest that soil denitrification is the most important loss term of the three (D, U, E), and that surface plant uptake (U) and groundwater turnover (E) have smaller impacts on groundwater nitrate concentrations.

Temporal Variations in Methane

We hypothesized that the land use change from heavily fertilized grain production to conservation plantings would result in an increase in dissolved methane. With the decreased abundance of nitrate as an alternate electron acceptor for anaerobic respiration in soil, we expected to see an inverse relationship between groundwater nitrate and methane concentrations. Our data support this hypothesis (Fig. 8), but there was no consistent pattern in methane accumulation in relation to time since active grain production (Fig. 7). Nevertheless, Fig. 8 shows that the availability of nitrate as an alternative electron acceptor exerts considerable control over methane accumulation in groundwater, either by favoring nitrate-based respiration (e.g., denitrification) or by direct oxidation of methane to carbon dioxide by anaerobic oxidation of methane coupled to denitrification (AOM-D, Raghoebarsing et al. 2006).

The only sites that had considerable methane accumulation ($> 0.5 \mu\text{M CH}_4$) were those with hydric soils and seasonal flooding (sites 8b, 14c, 14d, and MHF1, Table 2). Although any groundwater methane concentrations greater than atmospheric equilibrium (2.7 nM CH_4) create a diffusion gradient through the soil to the atmosphere, the much faster process of methane ebullition is of greater concern and usually requires $> 50 \mu\text{M CH}_4$ (Baird et al. 2004). Methane ebullition is a possible risk at the conservation sites with hydric soils. Like Morse et al. 2012, our study found that methane is highly variable, and concentrations are highest in the

wettest sites and during the warmest months with the deepest water-tables. The seasonal patterns at sites 8b, 14c, and 14d indicate that methane levels peak in the summer (June-August, Fig. 6) under the conditions of high groundwater temperatures (19°C, Fig. 3), a deep water-table (Fig. 3), and low nitrate concentrations (Fig. 8). These conditions may lead to enhanced methanogenesis and clearly result in increases in methane concentrations in groundwater (Fig. 6). However, these temporally restricted accumulations of methane may not produce sufficient methane fluxes to the atmosphere to outweigh the benefits of wetland areas such as wildlife habitat and denitrification potential (Jordan et al. 2003, Zedler 2003).

A relationship was found between low nitrate concentrations and high methane accumulation (Fig. 8), but this only provides information about a single electron acceptor. Methanogenesis is associated with less energy production than the reduction of nitrate, iron, manganese, and sulfate in anaerobic respiration (Reeburgh 2007). In order for significant methane accumulation to occur, the groundwater and saturated soils need to be at least partially depleted of nitrate, oxidized iron and manganese, and sulfate. In this study, the other electron acceptors were not measured, and we have no evidence concerning their role in methane accumulation. In conclusion, our study has shown that the use of agricultural land retirement for conservation practices such as stream buffers or wetland development can effectively reduce groundwater nitrate levels at the top of the unconfined aquifer within a few years, with only marginal risks of methane ebullition to the atmosphere.

Acknowledgements

I would like to thank my co-authors, Timothy Rosen, Dr. Thomas Fisher, Tucker Moorshead, and Drew Koslow, on the publication from this chapter. This work was published in *Agriculture, Ecosystems and Environment* in 2017 (<http://dx.doi.org/10.1016/j.agee.2017.07.026>).

I'd also like to thank Judy Denver and Allen Place for helpful discussions, and Emily Harris, Elle O'Brien, Hasan Wilson, and Ryan Saba for field assistance. I thank Chip Akridge and Clay Robinson of Harleigh Farms for providing full cooperation and access to Harleigh Farmland and land records, and I thank Mike Scofield at MD DNR for access to the Marshy Hope Forested reference site (MHF1).

This work was funded by the Chesapeake Bay Trust (Grant 11734), National Geographic Society (Grant 9051-11), NSF DDIG (Award No. DEB-1311302), NSF Coastal SEES Program (Award No. 1325553), and Horn Point Laboratory Bays and Rivers Fellowship.

Tables and Figures

Tables

Table 1. Sampling locations for groundwater nitrate and methane in Talbot County, MD in areas with varying time since intensive grain production (fertilized corn, wheat, and soy). Soil hydrologic group is defined by percolation rate and varies from sandy, well-drained soils (A) to heavy loams that are very poorly drained (D), and the hydric attribute is “Y” (yes) or “N” (no). CFC1, EFAg2, HFF1, and BNDS1 are supplemental agricultural sites located in the adjacent Caroline County, MD. MHF1 is a forested site in Dorchester County, MD. Abbreviations: CREP=Conservation Reserve Enhancement Program, CRP=Conservation Reserve Program, CP23=wetland program.

Site	Time since production, y	Piezometer depth, m	Soil type	Hydrologic group	Hydric attribute	Land use	Distance to agriculture, m
Harleigh Farms							
Ag	0	2.3	Mattapex	C	Y	Grain production	0
2a	2	2.1	Lenni Loam	D	Y	CREP	1
2b	2	1.4	Lenni Loam	D	Y	CREP	10
2c	2	2.6	Lenni Loam	D	Y	CREP	37
2d	2	1.1	Lenni Loam	D	Y	CREP	37
3a	3	2.8	Crosiadore Silt Loam	C	Y	CREP	300
3b	3	2.1	Crosiadore Silt Loam	C	Y	CREP	297
8a	8	1.1	Elkton Silt Loam	D	Y	Wetland	226
8b	8	2.0	Elkton Silt Loam	D	Y	Wetland	202
9a	9	1.9	Mattapex	D	Y	CP23	43
14a	14	2.0	Othello Silt Loam	D	Y	CRP	306
14b	14	2.1	Othello Silt Loam	D	Y	CRP	306
14c	14	0.9	Othello Silt Loam	D	Y	CRP	371
14d	14	2.0	Crosiadore Silt Loam	C	Y	CRP	352
16a	16	3.0	Crosiadore Silt Loam	C	Y	CRP	>600
16b	16	3.3	Crosiadore Silt Loam	C	Y	CRP	>600
Forest	100	2.1	Hambrook-Sassafras	B	N	Forest	327
Supplemental Sites							
CFC1	0	2.5	Sassafras Sandy Loam	A	N	Grain Production	0
EFAg2	0	2.9	Sassafras Loam	B	N	Grain Production	0
HFF1	0	1.8	Woodstown Sandy Loam	B	N	Grain Production	0
BNDS1	0	2.8	Bayboro Silt Loam	D	Y	Grain Production	0
MHF1	30	1.2	Pone Mucky Sandy Loam	B/D	Y	Forest	>1000

Table 2. Summary of average groundwater chemistry \pm standard error for the November 2012-November 2013 sampling period.

Site	pH	Specific conductivity, $\mu\text{S cm}^{-1}$	Nitrate, mg NO_3^- -N L^{-1}	Methane, μM
Harleigh Farms				
Ag	4.67 \pm 0.06	298 \pm 9	11.27 \pm 0.39	0.00 \pm 0.00
2a	5.76 \pm 0.07	155 \pm 6	2.81 \pm 0.30	0.00 \pm 0.00
2b	4.98 \pm 0.08	1369 \pm 26	0.03 \pm 0.01	0.00 \pm 0.00
2c	6.27 \pm 0.07	830 \pm 31	0.30 \pm 0.05	0.00 \pm 0.00
2d	6.21 \pm 0.04	996 \pm 7	0.21 \pm 0.08	0.00 \pm 0.00
3a	4.10 \pm 0.05	267 \pm 15	1.12 \pm 0.23	0.00 \pm 0.00
3b	4.26 \pm 0.06	182 \pm 8	0.70 \pm 0.09	0.00 \pm 0.00
8a	7.11 \pm 0.15	1161 \pm 43	0.01 \pm 0.00	0.15 \pm 0.03
8b	6.99 \pm 0.09	783 \pm 28	0.05 \pm 0.01	25.49 \pm 9.43
9a	5.63 \pm 0.16	192 \pm 7	1.93 \pm 0.20	0.00 \pm 0.00
14a	5.03 \pm 0.05	83 \pm 4	0.15 \pm 0.01	0.00 \pm 0.00
14b	5.19 \pm 0.07	65 \pm 4	0.25 \pm 0.04	0.02 \pm 0.02
14c	5.56 \pm 0.05	222 \pm 34	0.01 \pm 0.00	14.10 \pm 5.27
14d	5.44 \pm 0.11	142 \pm 19	0.01 \pm 0.00	2.41 \pm 1.16
16a	6.02 \pm 0.27	182 \pm 48	0.18 \pm 0.03	0.08 \pm 0.06
16b	5.91 \pm 0.31	301 \pm 77	0.08 \pm 0.01	No Data
Forest	4.72 \pm 0.03	64 \pm 4	0.03 \pm 0.01	0.03 \pm 0.02
Supplemental Sites				
CFC1	5.24 \pm 0.06	257 \pm 8	14.34 \pm 0.42	0.02 \pm 0.00
EFAg2	4.96 \pm 0.04	198 \pm 3	5.80 \pm 0.29	0.40 \pm 0.12
HFF1	5.88 \pm 0.09	235 \pm 16	4.72 \pm 0.76	0.28 \pm 0.20
BNDS1	4.85 \pm 0.03	258 \pm 8	12.27 \pm 0.32	0.06 \pm 0.02
MHF1	4.16 \pm 0.13	54 \pm 5	0.02 \pm 0.01	20.24 \pm 4.52

Table 3. Seasonal variability in nitrate concentrations over the November 2012- November 2013 field season. Slope values are for linear regressions. k is the exponential decay coefficient of an exponential decline model (Exp. Dec.). The maximum is the month of maximum nitrate concentrations for the sites with sine wave models. The r^2 and p values relate to the fit of the seasonal nitrate data to the models.

Site	Model	Maximum Nitrate, mg NO ₃ ⁻ -N L ⁻¹	Slope, y ⁻¹	k, y ⁻¹	Maximum	r ²	p
Ag	Exp. Dec.	14.10		-4.15		0.82	<0.005
2a	Exp. Dec.	5.38		-3.60		0.93	<0.0001
2b	No Pattern	0.10					>0.05
2c	Sine Wave	0.55			Spring	0.79	0.0286
2d	No Pattern	0.50					>0.05
3a	Exp. Dec.	2.67		-2.43		0.94	<0.0001
3b	Sine Wave	1.16			Winter	0.89	<0.0001
8a	Linear	0.04	0.06			0.84	0.0003
8b	No Pattern	0.12					>0.05
9a	No Pattern	3.93					>0.05
14a	No Pattern	0.22					>0.05
14b	Linear	0.54	0.34			0.50	0.0063
14c	No Pattern	0.04					>0.05
14d	No Pattern	0.02					>0.05
16a	No Pattern	0.31					>0.05
16b	No Pattern	0.29					>0.05
Forest	No Pattern	0.10					>0.05

Table 4. Denitrification and N uptake rates from literature for parameters D and U.

Parameter	Denitrification rates, $\text{g N m}^{-3} \text{y}^{-1}$	Well depth, m	Mediate nitrate, mg N L^{-1}	Location	Site description	Reference
D	0.18	1	3.5	Rhode Island	Riparian Buffer, Mod. Well Drained	Hanson et al. 1994
	0.40	1	4.1	Rhode Island	Riparian Buffer, Poorly Drained	Hanson et al. 1994
	0.96	1	0.2	Rhode Island	Riparian Buffer, Very Poorly Drained	Hanson et al. 1994
	0.15	0.5-2.5	26	Colorado	Agriculture	McMahon and Böhlke 1996
	14-38	3-28	0.05-36	British Columbia, Washington	Agriculture	Tesoriero et al. 2000
	0.22	~300	0.10-22	Minnesota	Agriculture	Böhlke et al. 2002
	0.01	Variable	Variable	Nebraska	Agriculture	Böhlke et al. 2007
	0.14-1.40	Variable	Variable	8 US Sites	Variable	Tesoriero and Puckett 2011
Parameter	N uptake rates, $\text{g N m}^{-2} \text{y}^{-1}$		Grass type	Fertilization rate, $\text{kg N ha}^{-1} \text{y}^{-1}$	Reference	
U	1.6-9.7		Warm-Season Grasses	0-75	Jung et al. 1990	
	1.6		Switch Grass	Adjacent to fertilized fields	Tufekcioglu et al. 2003	
	1.6-18.8		Warm-Season Grasses	371	McLaughlin et al. 2004	
	7.7-35.2		Bermuda Grass	45-135	Silveira et al. 2007	

Figures

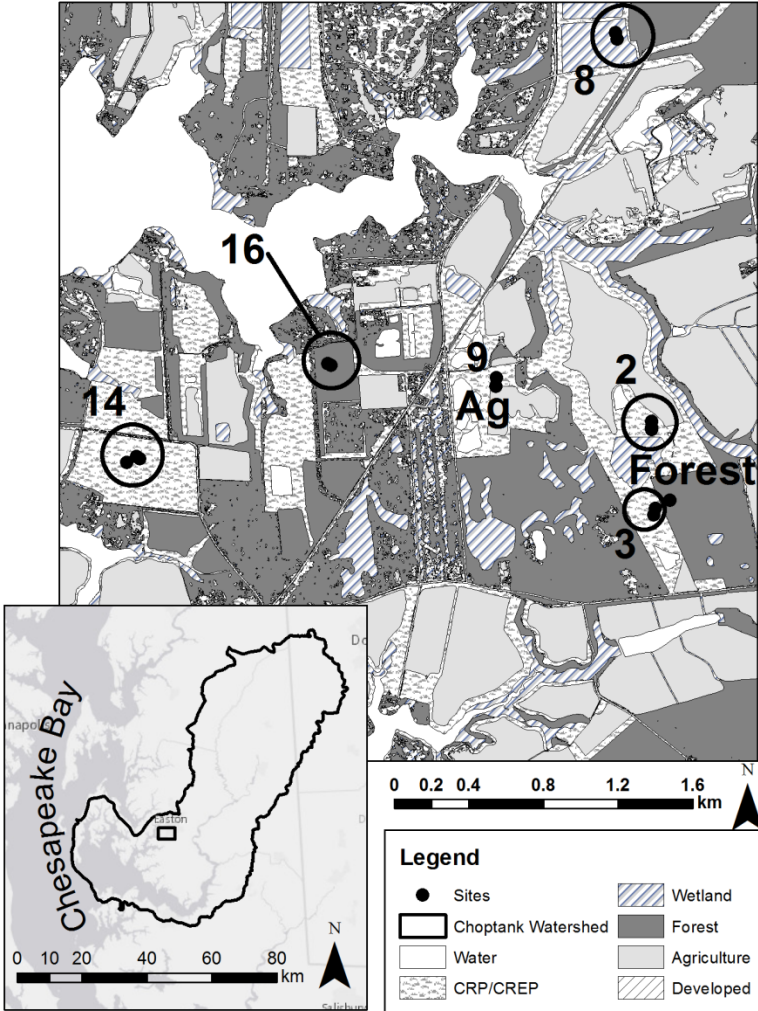


Figure 1. Map of study sites located within the Choptank Basin (inset).

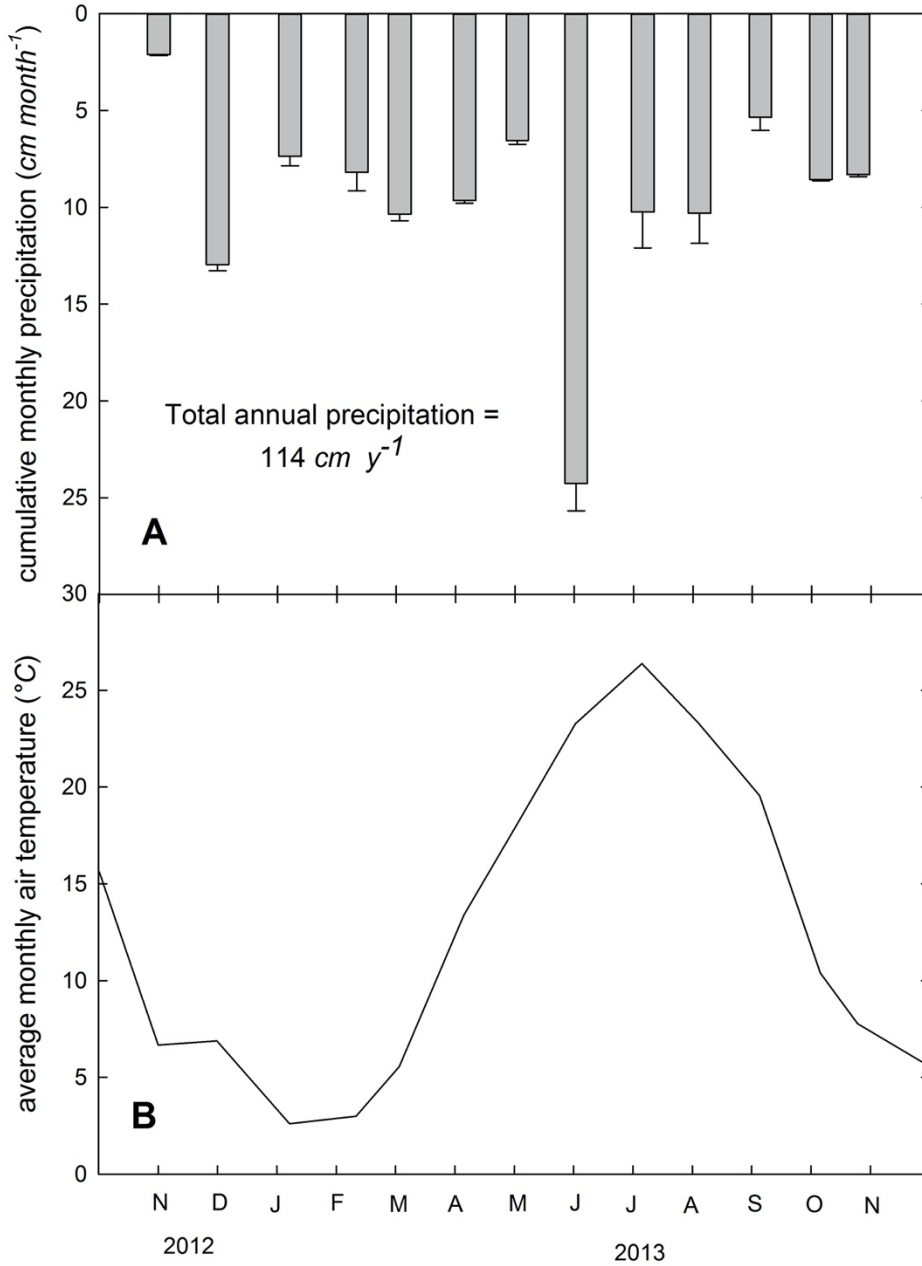


Figure 2. Average cumulative monthly precipitation (panel A) from 3 Talbot County, MD NOAA sites (NOAA NCDC 2014) and average daily air temperature (panel B) data for Trappe, MD (Weather Underground 2014).

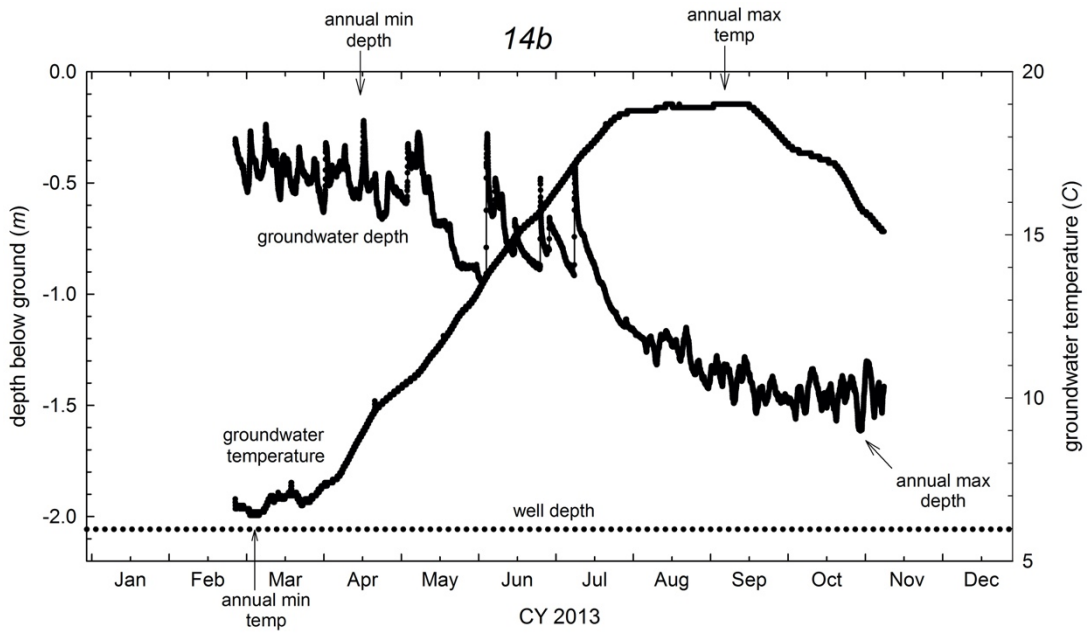


Figure 3. Groundwater temperature and depth below ground for site 14b during calendar year 2013.

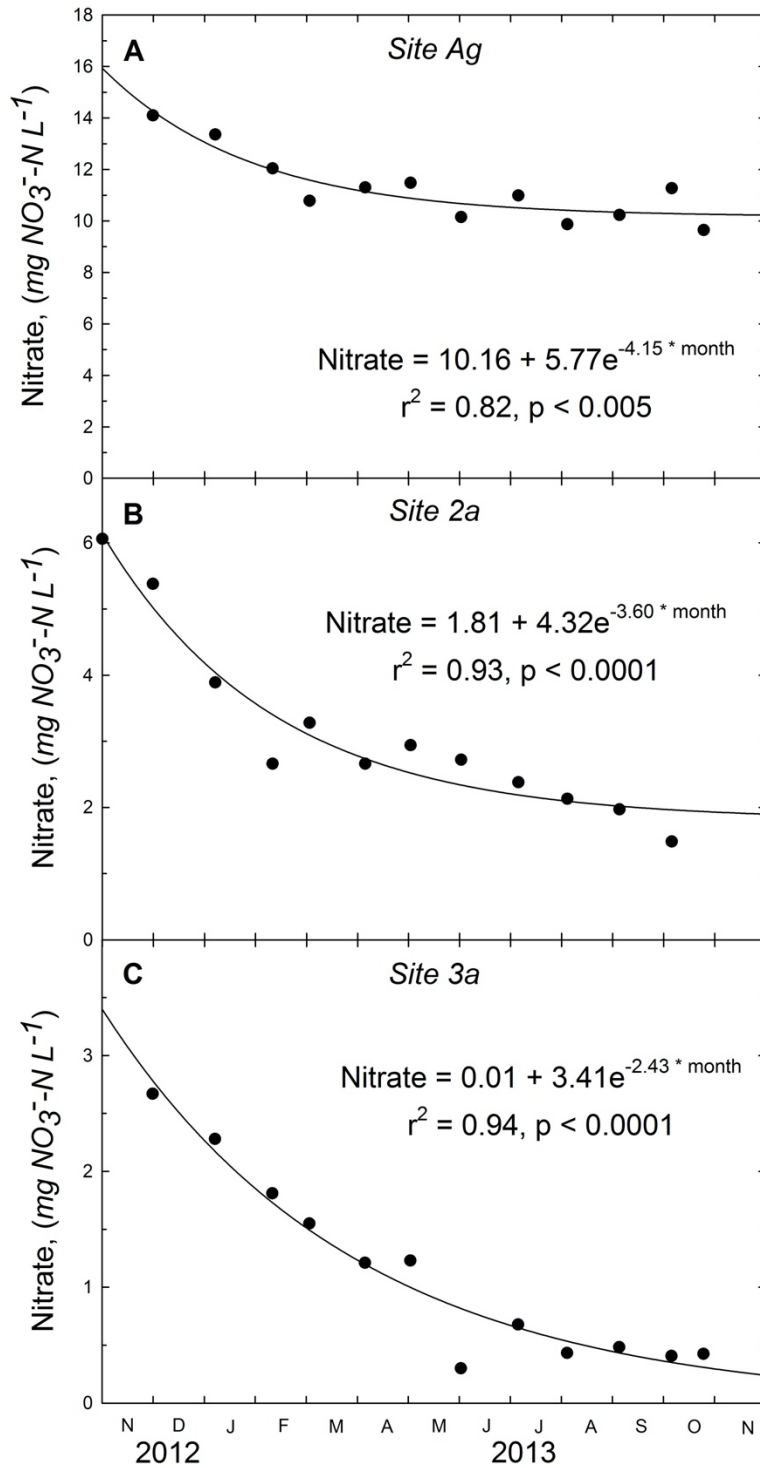


Figure 4. Seasonal nitrate variability at three high nitrate sites (Ag, 2a, 3a). All three of these sites had significant exponential decreases in groundwater nitrate concentrations.

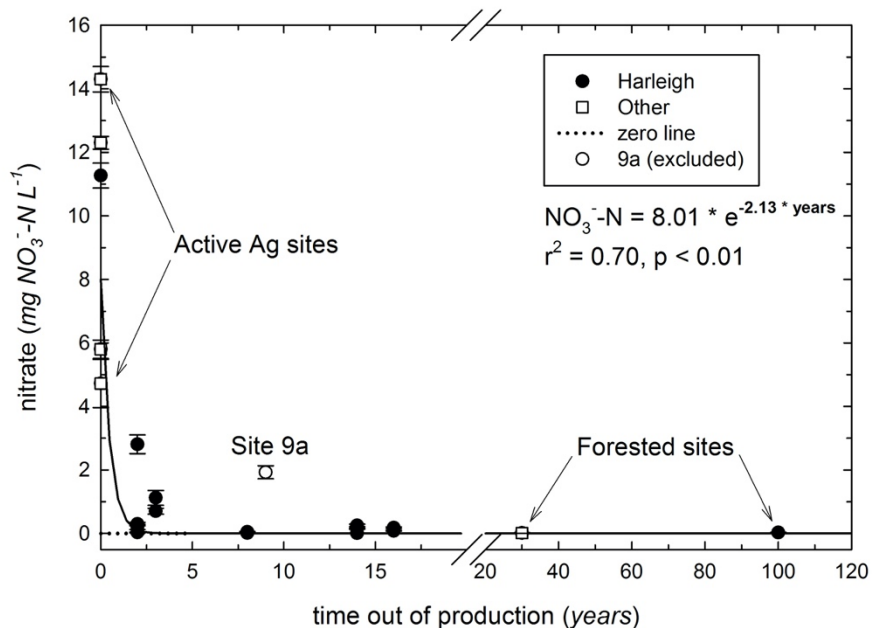


Figure 5. Groundwater nitrate concentrations under fields with variable time away from crop production (chronosequence). There is a significant exponential decrease in nitrate concentrations over time. The closed circles are annual average for chronosequence sites at Harleigh Farms. The open squares represent multi-year means for sites outside of the study location. The open circle is site 9a, which was excluded from the regression due to the downslope proximity to an area of active agriculture.

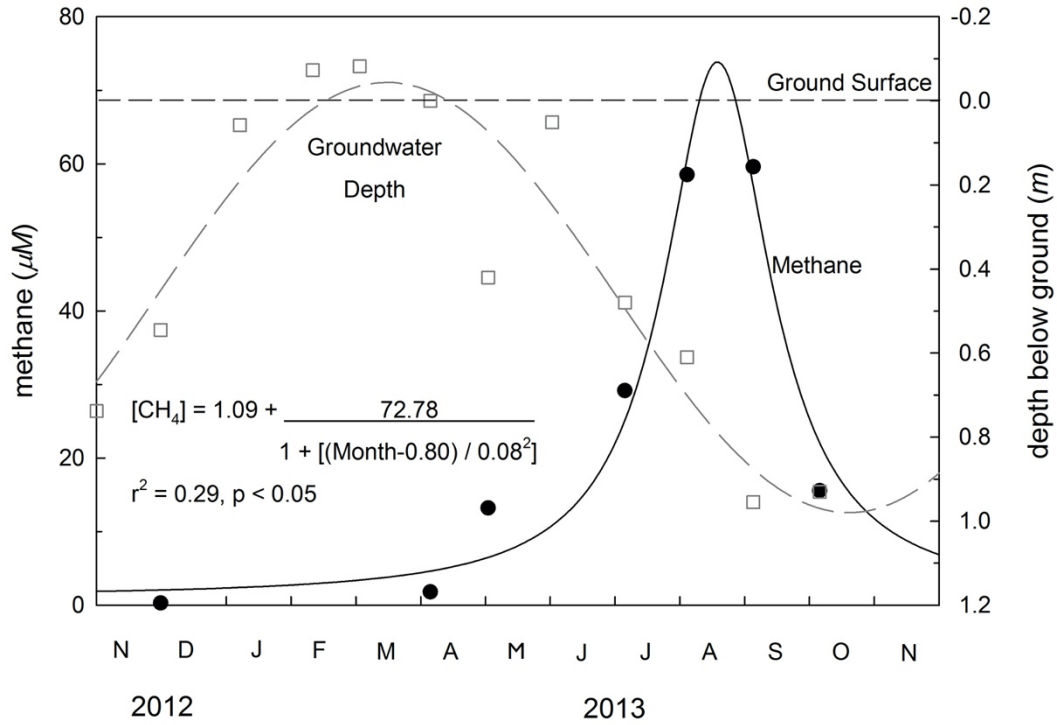


Figure 6. Seasonal variability of dissolved methane in wetland piezometer 8b. In the winter months, groundwater level was above the ground surface. There is a significant peak in methane concentrations in late summer when groundwater depth is approaching its deepest point.

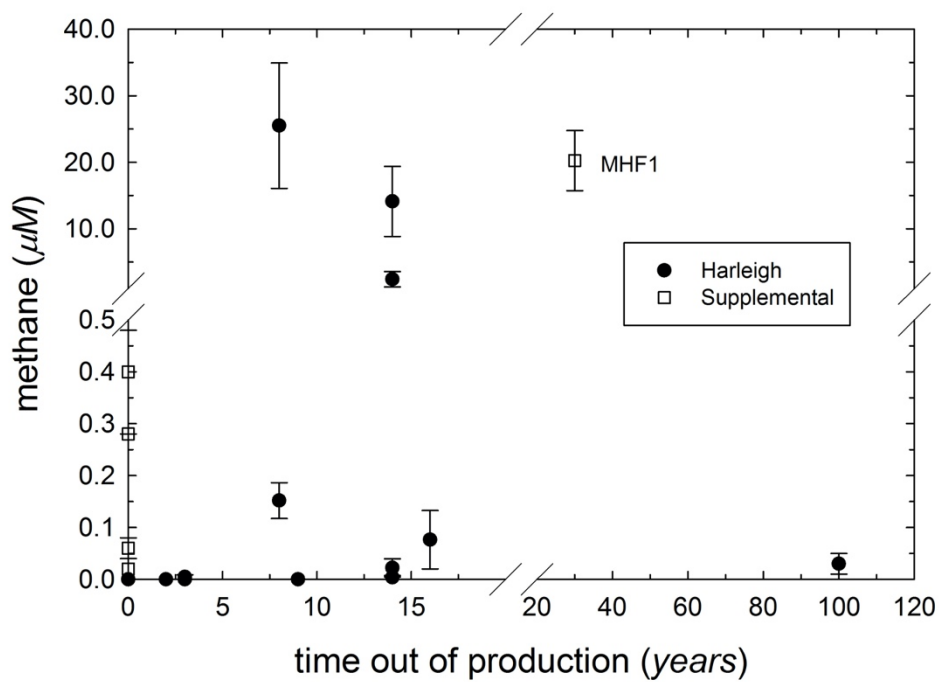


Figure 7. Groundwater methane concentrations on plots with variable time away from intensive grain production (chronosequence). There is no pattern of groundwater methane concentrations in relation to time out of crop production. Sites with high methane accumulation ($> 1 \mu\text{M}$) have hydric soils. The atmospheric equilibrium concentration is $0.003 \mu\text{M CH}_4$.

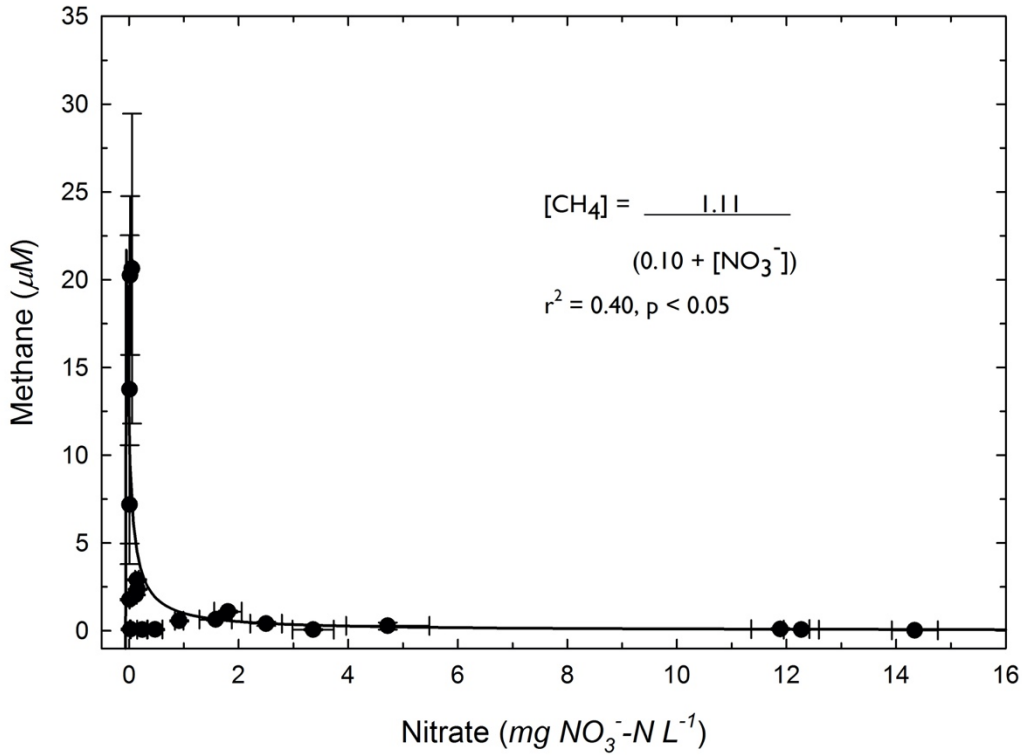


Figure 8. An inverse relationship between average values of groundwater methane and groundwater nitrate concentrations in the Harleigh Farms data.

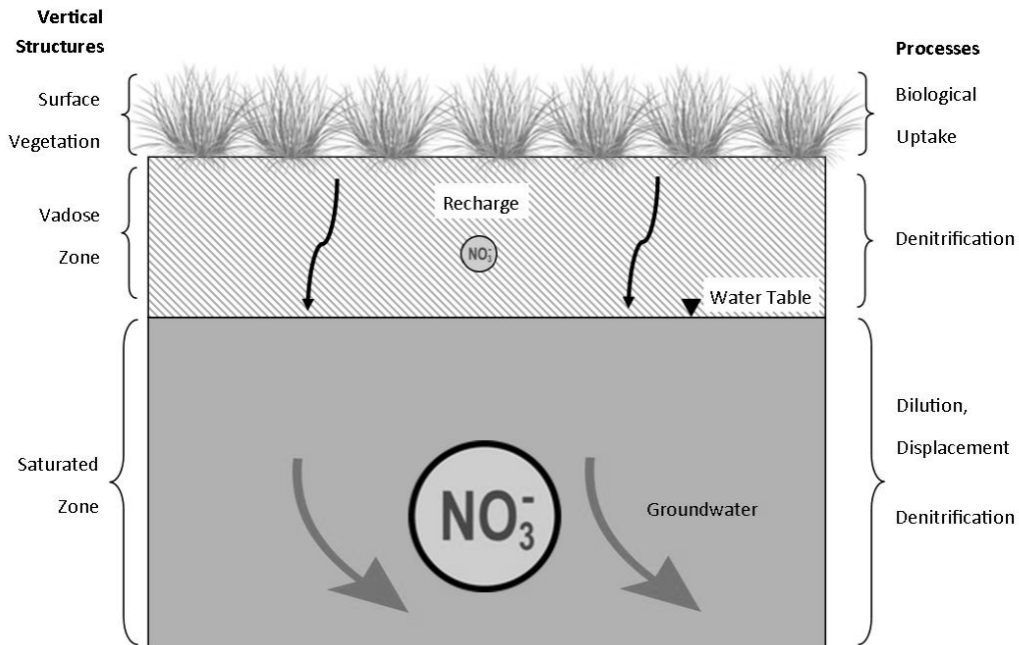


Figure 9. Conceptual model of important processes influencing groundwater nitrate concentrations following cessation of fertilizer applications. Illustration of grasses provided by Tracey Saxby, Integration and Application Network, University of Maryland Center for Environmental Science (ian.umces.edu/imagelibrary/).

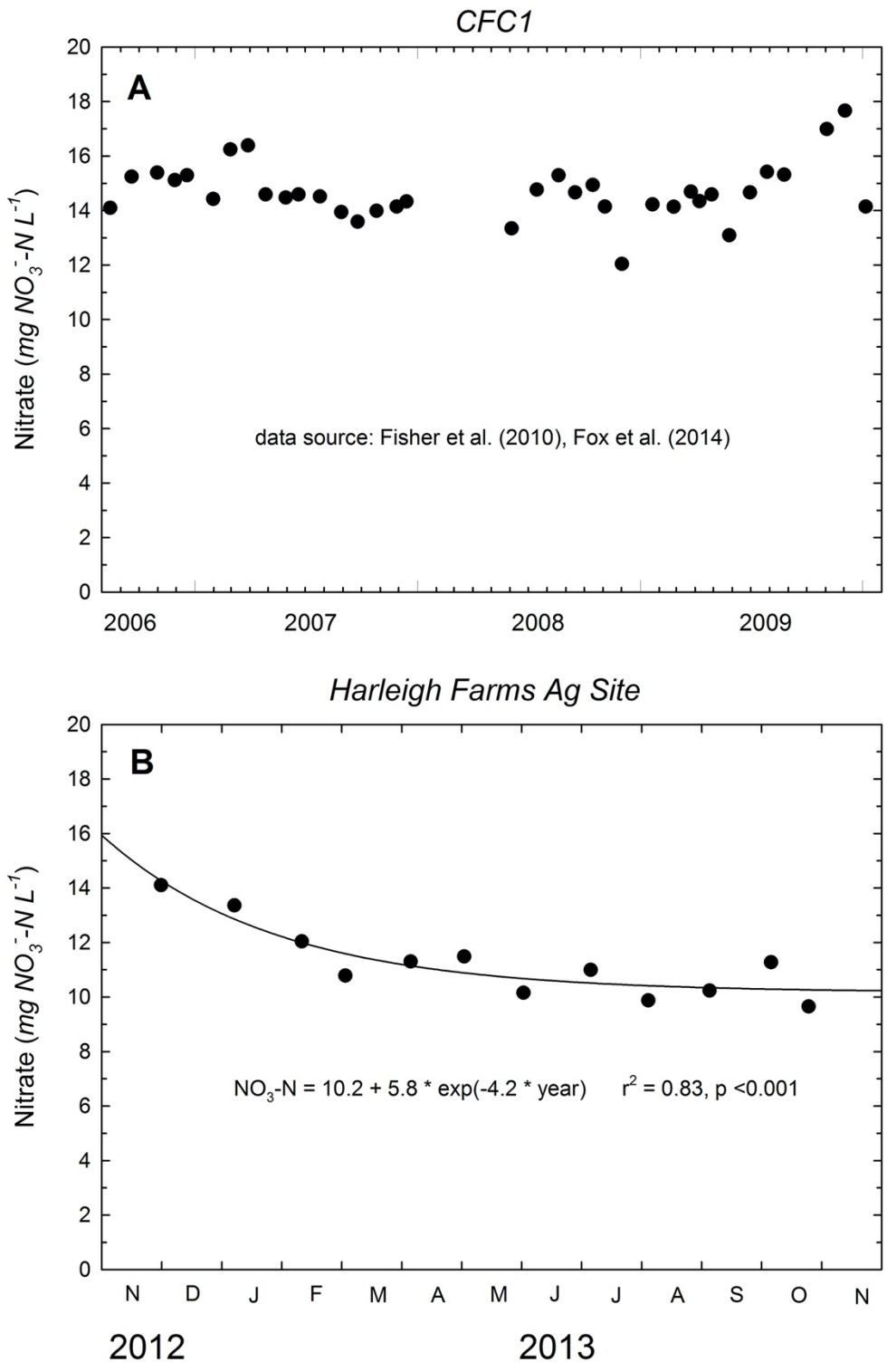


Figure 10. Annual groundwater nitrate concentrations for supplemental agricultural site CFC1 (panel A). Monthly groundwater nitrate concentrations for Harleigh Farms Ag site (panel B).

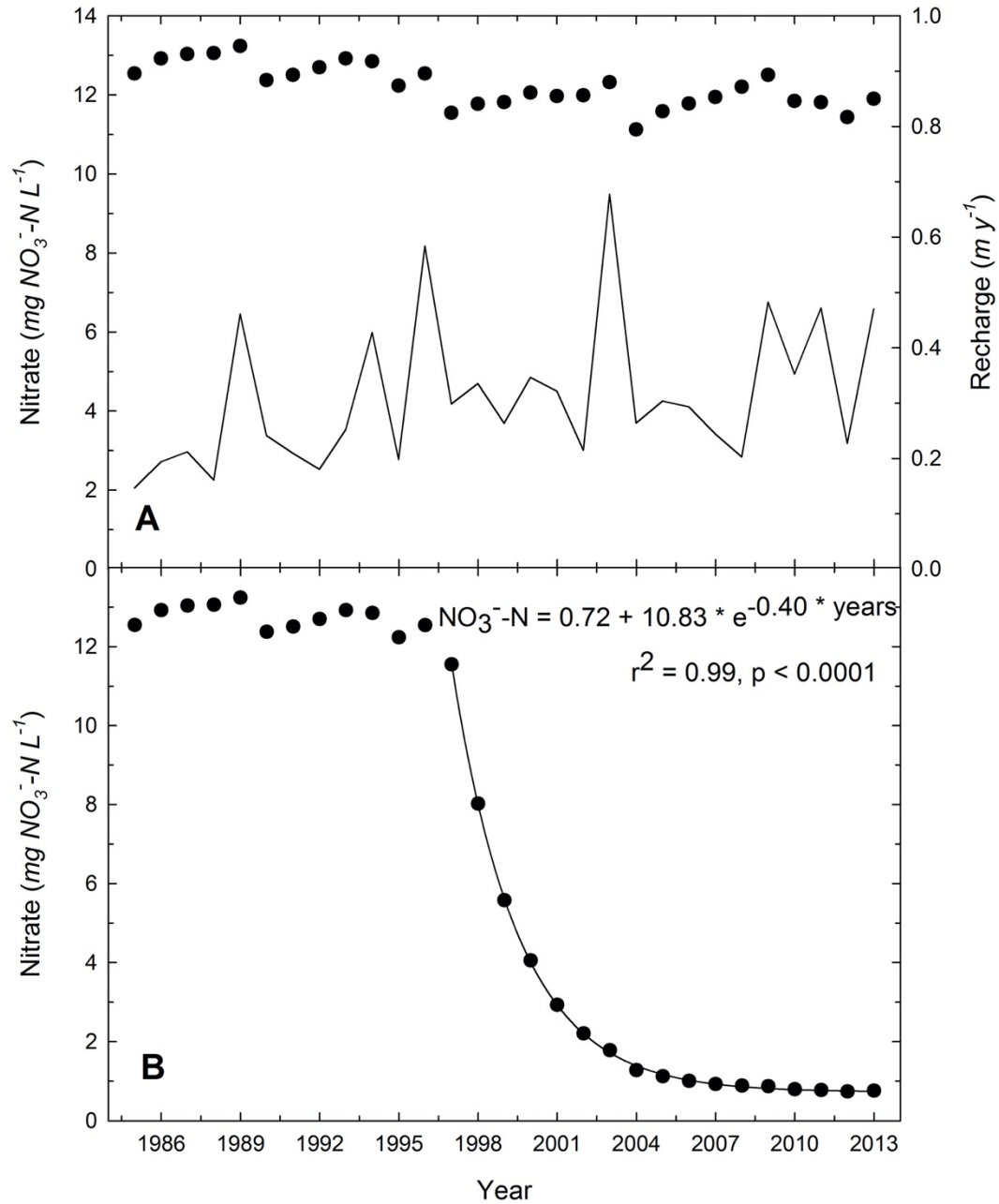


Figure 11. Projected groundwater nitrate concentrations (dots) as predicted by Eq. 2 when fertilization rates are constant at $15 \text{ g N m}^{-2} \text{ y}^{-1}$ and groundwater recharge values (line) for 1985-2013 (panel A). Projected groundwater nitrate concentration as predicted by Eq. 2 when fertilization stops after 1997 (panel B).

Chapter 4: Biogeochemical Investigation of Simultaneous Metabolism of Nitrogen and Methane

Introduction

The classic microbial methane cycle is relatively simple. Methane is formed through methanogenesis under low redox conditions (Vogels et al. 1984) and aerobically oxidized to CO₂ (Hutton and ZoBell 1949). The microbially-mediated oxidation of methane is no longer recognized as this simple because recent studies have found that methane is also oxidized anaerobically using alternative electron acceptors such as NO₃⁻, SO₄⁻², and Fe⁺³ (Raghoebarsing et al. 2006, Reeburgh 2007, Beal et al. 2009). These metabolic processes tie the carbon cycle closely with other important elements (sulfur, manganese, iron, and nitrogen) in terrestrial and aquatic ecosystems. This chapter investigates the potential for anaerobic oxidation of methane (AOM) coupled with denitrification (AOM-D) in forested, wetland, and agricultural soils (Fig 1) to determine if this metabolism is a significant sink for the greenhouse gas methane and the strong eutrophication agents of nitrate and nitrite.

Methanogenesis

Methane is produced biologically via methanogenesis through CO₂ reduction, acetate fermentation, and the reduction of some compounds containing methyl-groups in anaerobic environments (Reeburgh 2007, Liu and Whitman 2008). About 75% of atmospheric methane is a product of methanogenesis (Chen and Prinn 2005).

Wetlands and rice production account for nearly half of methane emissions, with the other half coming from ruminants, termites, biomass burning, landfills, open salt and

freshwaters, and coal and gas production (Chen and Prinn 2005, Conrad 2007, Reeburg 2007). Methanogenesis is a strictly anaerobic process that occurs in anoxic and reduced environments that are devoid of oxygen and other electron acceptors, such as nitrate, sulfate, Mn(IV), and Fe(III) (Conrad 2007).

Methanogens belong to the Archaea domain, viewed as one of the oldest groups of organisms on Earth (Kasting and Seifert 2003). These Archaea are divided into 5 orders, 10 families, and 31 genera (Blaut 1994, Liu and Whitman 2008). Thirteen genera are found in temperate aquatic environments, while the others are adapted to extreme temperatures or pH. Methanogens are abundant in habitats with limited electron acceptors as they are often outcompeted for substrate by bacteria that perform other types of metabolism in more oxidized environments (Liu and Whitman 2008).

Aerobic Methane Oxidation

Aerobic methane oxidation is responsible for the consumption of most methane produced by methanogens (Conrad 2007, Reeburg 2007). Aerobic methane-oxidizing bacteria in soils are responsible for removing a large amount of CH₄ from soils, aquatic sediments, and the atmosphere (Holmes et al. 1999, Reeburg 2007). This process is highly energetically favorable metabolism with a Gibbs free energy of -859 kJ mol⁻¹ CH₄ using O₂ as an electron acceptor (Caldwell et al. 2008). Human society exploits this energy release by burning methane, the dominant component of natural gas, for domestic and industrial uses.

Methanotrophic bacteria belong to the Proteobacteria. This taxon is divided into 3 types: I, II, and X, and these groups are distinguished by carbon assimilation

pathways, internal membrane structure, and a few other characteristics (King 1990, Conrad 2007). Type I methanotrophs are Gammaproteobacteria that assimilate carbon via the ribulose monophosphate pathway (RMP) and Type II methanotrophs are Alphaproteobacteria that assimilate carbon via the serine pathway (King 1990, Conrad 2007). Type II methanotrophs also have complete nitrogenase enzymes, which are responsible for fixing N_2 to NH_3 (King 1990). Type X methanotrophs are unique in that they are Gammaproteobacteria that assimilate carbon via RMP and the serine pathway, have nitrogenase enzymes, and can perform CO_2 fixation (King 1990).

AOM Coupled to Sulfate Reduction

AOM was first discovered with sulfate as the electron acceptor (Reeburgh 2007). This process is barely energetically favorable (Gibbs free energy of -14 kJ mol^{-1} CH_4), but it is also considered to be responsible for the majority of methane oxidation in oceans (Shima and Thauer 2005, Reeburgh 2007, Beal et al. 2009). It has been determined that AOM coupled to sulfate reduction is performed by a consortium of an anaerobic methanotrophic (ANME) archaea and a sulfate reducing bacterium (SRB, Boetius et al. 2000). The archaea were found to grow around aggregates of SRB (Boetius et al. 2000), and there are three phylogenetically different groups of ANME: ANME-1, ANME-2, and ANME-3. ANME-1 and ANME-2 are related to the methanogenic archaea of the Methanosarcinales (Orphan et al. 2002) and are associated with SRB of the *Desulfosarcina/Desulfococcus* group (Boetius et al. 2000). ANME-3 is related to *Methanococcoides* and is associated with the same SRB

as groups 1 and 2 (Beal et al. 2009). Each of these anaerobic methanotroph groups have been found independent of one another as well as together (Orphan et al. 2002).

The mechanism for AOM coupled to sulfate reduction is still unknown. The dominant hypothesis is that AOM is a reversal of methanogenesis, and this mechanism is aptly named 'reverse methanogenesis' (Hallam et al. 2004). Although reverse methanogenesis has not been confirmed, studies have shown that ANME tend to share many of the methanogenesis genes that methanogens possess (Hallam et al. 2004). In the reverse methanogenesis process, methane is converted into carbon dioxide, the opposite of methanogenesis. Sulfate dependent AOM is important in the marine environment, particularly near methane seeps and hydrates and is responsible for the majority of methane oxidation in the oceans (Reeburgh 2007).

AOM Coupled to Manganese or Iron Reduction

More recently, Beal et al. (2009) found that AOM can be coupled to manganese (birnessite) and iron (ferrihydrate) reduction (Gibbs free energy of -556 and -270 kJ mol⁻¹ CH₄, respectively). The microbial diversity of the sediment incubations reported in Beal et al. (2009) included ANME-1, 2, 3 and various bacteria capable of manganese reduction. Manganese-dependent AOM is potentially carried out by ANME-1 and/or *Methanococoides*/ANME-3 with a bacterial partner, or by a sole bacterium (Beal et al. 2009). Ettwig et al. (2016) found that Archea of the order *Methanosarcinales* couple Fe³⁺ and Mn⁴⁺ to AOM. The mechanisms for iron- and manganese-dependent AOM are still elusive, but the microbes that take part in this metabolism are found in many ecosystems (Ettwig et al. 2016).

AOM Coupled to Denitrification

AOM coupled to denitrification (AOM-D) is an interesting avenue of methane oxidation, and many new studies have investigated the microbes and mechanisms involved in this metabolism. AOM-D can be driven by nitrite or nitrate by 2 known microbes: *Candidatus Methyloirabilis oxyfera* (*M. oxyfera*; Ettwig et al. 2010) and *Candidatus Methanoperedens nitroreducens* (*M. nitroreducens*; Haroon et al. 2013). *M. oxyfera* belongs to the NC10 phylum bacteria and performs a novel ‘intra-aerobic’ pathway of nitrite reduction, in which oxygen is produced from nitrite for the oxidation of methane (Ettwig et al. 2010). *M. nitroreducens* is affiliated with ANME-2d archaea and may use reverse methanogenesis to perform methane oxidation (Haroon et al. 2013, Cui et al. 2014, Arshad et al. 2015).

M. oxyfera is reported to be mesophilic with regard to temperature and pH and exhibits slow growth (doubling time 1-2 weeks). The intra-aerobic metabolism used by *M. oxyfera* is termed nitrite-dependent anaerobic methane oxidation, or n-damo (Zhu et al. 2010). *M. oxyfera*'s metabolism is novel to science, and it presents new pathways of AOM and denitrification. N-damo does not use reverse methanogenesis as methane oxidation is performed by cleaving oxygen from nitric oxide (NO) during denitrification. The proposed denitrification pathway is similar to canonical denitrification until the production of NO by nitrite reductase. A proposed enzyme, nitric oxide dismutase (Wu et al. 2012), produces N₂ and O₂ gases (Ettwig et al. 2010, Wu et al. 2012, Luesken et al. 2011). This process not only exhibits a fascinating metabolic pathway, but it could also be an important form of methane oxidation in freshwater (Hu et al. 2014).

Like *M. oxyfera*, *M. nitroreducens* is capable of oxidizing methane while reducing nitrogenous compounds and prefers mesophilic conditions (temp. 22-35°C, pH 7-8). While reverse methanogenesis has been hypothesized as a potential metabolic pathway for AOM, *M. nitroreducens* are the first microbes to be found to have the complete genome required for reverse methanogenesis. The genes for nitrate reduction to nitrite were present in *M. nitroreducens*, but this methanotroph lacks the ability to perform denitrification in its entirety (Haroon et al. 2013). Instead, the nitrite converted to ammonium (rather than N₂) within *M. nitroreducens*, or is further reduced by a symbiotic organism (Arshad et al. 2015, Haroon et al. 2013). This organism was discovered in a bioreactor, so we currently have little information about its occurrence in nature (Haroon et al. 2013).

AOM as a Potential Methane Sink

Aerobic methane oxidation is often considered the dominant methane sink, but AOM research is highlighting the potential for this process to be an important sink in marine sediments (Reeburg 2007), coastal environments (Egger et al. 2016, Rooze et al. 2016, Shen et al. 2016), freshwater sediments (Raghoebarsing et al. 2006, Nordi and Thandrup 2014), wetlands (Hu et al. 2014, Segarra et al. 2015), soils (Bannert et al. 2012, Gauthier et al. 2015), and even wastewater (Haroon et al. 2013, Wang et al. 2017). AOM coupled to sulfate reduction is prevalent in marine sediments (Hinrichs and Boetius 2002, Reeburg 2007), but AOM-D and iron-mediated AOM may have important roles in coastal and estuarine sediments (Egger et al. 2015, Rooze et al. 2016, Shen et al. 2016). AOM rates may even increase with estuarine eutrophication (Egger et al. 2015).

The microbial consortium believed to perform AOM-D was first found in freshwater sediments (Raghoebarsing et al. 2006), and AOM-D was confirmed as being the dominant AOM process in freshwater pond and wetland sediments (Nordi and Thandrup 2014, Hu et al. 2014). AOM in wetlands could also rival AOM rates in marine environments, consuming up to 200 Tg methane a year, about 50% of wetland methane emissions (Segarra et al. 2015). Unsaturated soils are a well-documented methane sink (via aerobic methane oxidation, Mancinelli 1995), while saturated soils are associated with methane production (Chen and Prinn 2005, Conrad 2007, Reeburg 2007), but AOM has been found in anaerobic soil micro-sites (Bannert et al. 2012), anaerobic pond shoreline soils, and peatland soils (Gauthier et al. 2015). Nitrate, iron, and sulfate were found to be a potential electron acceptor for AOM in soils (Bannert et al. 2012, Gauthier et al. 2015). Currently, few biogeochemical models take AOM in soils into account when budgeting methane production and consumption from soils (Gauthier et al. 2015). With the growing understanding of the methane sink provided by AOM, it has been proposed that AOM-D could be used in wastewater treatment plants to rid wastewater of methane and nitrogen simultaneously (Wang et al. 2017).

Methane Production and Oxidation in Soils and Groundwater

In soils and aquifers, there are several pathways for the production and fate of methane (Fig 1). First, methane is produced deep in the anoxic region of groundwater after other electron acceptors have been depleted. In this case, methane then diffuses upward through the soil and is oxidized anaerobically through AOM-D or aerobically after entering the vadose zone. The other potential pathway is the occurrence of

methanogenesis in anaerobic micro soil aggregates (Grundmann et al. 2001) with no other electron acceptors. The methane then diffuses out of the soil aggregates into areas with nitrate, nitrite, and other electron acceptors. AOM could also occur in anaerobic groundwater with aerobic oxidation occurring in the vadose zone.

Hypotheses and Experimental Design

Agricultural soils are rich in nitrate (Fisher et al. 2018), so this study focuses on the potential for AOM-D in agricultural soils and groundwater on the coastal plain of Maryland. This chapter investigates AOM-D from a biogeochemical viewpoint rather than using molecular methods to identify microbial populations, as is common in most AOM studies. This study uses soil incubations and *in-situ* methods. Two hypotheses are tested: (1) AOM is present in soils and detectable using biogeochemical methods and (2) nitrite is the primary electron acceptor in the AOM reactions.

To test these two hypotheses, a complete design of soil amendments are added to soil incubations. The four treatments include: ‘control’, ‘nitrite’, ‘methane’, and ‘both’. Nitrite is chosen over nitrate due to the energetic favorability of nitrite for AOM-D (Shima and Thauer 2005, Raghoebarsing et al. 2006, Ettwig et al. 2008, Zhu et al. 2010, Hu et al. 2011). After testing these soil amendments on soil cores, the experimental work shifts to *in situ* soil enrichments under more realistic conditions.

Methods

Study Sites

Sampling took place on the coastal plain of Eastern Shore, Maryland. Samples were collected from 3 sites: 'Forest,' 'Wetland,' 'Row Crops.' The row crop site refers to farmland that is in a corn and soybean rotation. The slurry row crop site is from a different farm than for the core incubation data due to the inability to secure permission for research after the sale of the first property. Since we were unable to get access to the original row crop site, we used another farm for the soil cores used in the intact core experiments. The row crop samples were taken from a wet spot within the 2 corn fields. The forest site is within the watershed of a first order stream that runs through a completely forested small watershed. Wetland samples were collected from a wetland adjacent to a corn field.

Sampling Methods

Soil cores were collected from the sites using a 2-inch diameter soil core sampler with an inner Plexiglas sleeve (AMC model 404.05). Six-inch intact soil cores were collected in the Plexiglas sleeves, capped, and transported back to the lab on ice. The cores were stored at 4°C for no more than 2 weeks before lab incubations began. Before incubations began, deionized water was added to intact soil cores to bring the soil to field capacity (wet, but not losing water).

Soil Slurry Incubations

Soil slurries were conducted using aggregated soil cores. Initial soil slurries incubations (Fig 2) were performed to collect preliminary information on soil metabolism. Soils were thoroughly mixed and 10 g of wet soil was added to 100 mL serum bottles (Bannert et al. 2012). The serum bottles were crimp sealed and covered with aluminum foil to inhibit photosynthesis. Each bottle was purged twice with N₂ over a 24-hour period. The bottles were over-pressurized with 10 mL of N₂. An initial analysis of methane concentrations was done before any additions were made to the soil slurries.

The hypothesis was tested in triplicate using a complete design of soil additions: control, nitrite, methane, and both (Fig 2). The ‘control’ soils were not treated with soil amendments. Soil nitrite concentrations were below detection levels previous to the amendments. The ‘nitrite’ soils were treated with 100 μL of sodium nitrite. The ‘methane’ soils were treated with 100 μL of pure methane. The ‘both’ soils were treated with 100 μL of sodium nitrite and 100 μL of pure methane. This complete design of soil additions was applied to soil from the forested, wetland, and row crop sites. Methane was added at the start of the incubation. Headspace methane concentrations were measured every 2-3 days using a GC-FID. Sodium nitrite was added on day 10 to the ‘nitrite’ and ‘both’ treatments. Headspace methane was measured until day 18.

Soil Core Incubations

Intact soil core incubations were performed using quart-sized Mason jars fitted with an air-tight septum for gas sampling (Fig 2). Deionized water was added to intact soil cores to bring the soil to field capacity. Mason jar incubators were purged with N₂ and checked for anoxic conditions using oxygen sensors (PyroScience Oxygen Sensor Spots TROXSP5) to monitor oxygen concentrations with a fiber optic O₂ meter (PyroScience FireSting O₂ FSO2-4) until O₂ was < 0.02 %. Incubation chambers were tested for air tightness using the oxygen sensors. Percent oxygen decreased exponentially during a successful purge and remained < 0.02 % (Fig 3A). If the chamber was not airtight, a linear increase in oxygen was observed (Fig 3B). Methane and/or nitrite were added in a complete design of soil additions, as done in the slurries (Fig 2). The soil cores were amended with 100 µL of pure methane and/or 100 µL of sodium nitrite. Methane was added at the start of the incubation. Headspace methane concentrations were measured every 2-3 days using a GC-FID.

After running each soil type incubation 1-2 times, follow-up incubations were conducted to assess how depth of soil impacted patterns of methane consumption or production. Soil cores were divided into 3 parts: 'top' (0-2.5 cm deep), 'mid' (2.5-7.5 cm deep), and 'bottom' (7.5 to 10 cm deep). Soils were collected intact, transported to the lab, and then cut into segments. The 'top' segment represented the O horizon (humus), while the 'mid' and 'bottom' segments represented the A horizon (top soil). While the entire core came from the vadose zone, the 'bottom' segment was typically the wettest. Segmented incubations were done with forested soils and soils from a ditch along-side the row crop site. Methane and nitrite were added to these core

incubations. Nitrite was added roughly midway in these incubations. Since previous incubations showed rapid changes in concentrations, these incubations were run for only 1-3 days, rather than a week or longer. Headspace methane was analyzed for both soils, and carbon dioxide was analyzed for the crop ditch as well. Headspace carbon dioxide was analyzed using a GC-FID with a methanizer. Patterns of methane and carbon dioxide production or consumption were assessed pre- and post-nitrite additions to the segmented soil cores.

In-Situ Additions

Seven piezometers were installed at the forested site as part of a closely spaced piezometer nest (CSPN, Fig 4). The center of the screen for each piezometer was about 1 meter below ground. The central piezometer acted as the injection piezometer, while the surrounding six piezometers were used to detect the tracer as it passed through the soil in groundwater. Initially, to test for hydraulic continuity, trials were conducted by adding 1 L of a 1,000 $\mu\text{S cm}^{-1}$ sodium chloride solution to the injection piezometer. A Solinst LTC Levellogger was used to detect changes in conductivity as the salt tracer passed through the collection piezometer.

Statistics

Graphics and statistics were done using SigmaPlat v12.5. Linear and non-linear regressions were run for each laboratory experiment. Treatment averages were fit with 3-parameter exponential growth curve ($y = y_0 + ae^{bx}$, where y is methane and x is time) or 3-parameter exponential decay curve ($y = y_0 + ae^{-bx}$). Analyses of variation (ANOVA) of the growth coefficients were run for each site. Statistical

significances are denoted as: NS (not significant), MS (marginally significant), * (significant), ** (highly significant). A test of oxygen levels in incubation chambers was run with linear and non-linear (exponential decay) run on the oxygen concentrations.

Results

Soil Slurry Incubations

In order to determine the presence of AOM-D, a specific pattern of headspace methane concentrations would be expected for soil slurries and soil core incubation (Fig 5). The initial soil slurry incubations all exhibited net methane production, but patterns for methane production varied between soil sources and treatments (Fig 6). In forested soils, average headspace methane concentrations significantly increased exponentially in all treatments, except for '+ CH₄', which was marginally significant ($p = 0.0761$, Table 1). The rate of methane increase varied, but there were no significant differences between the growth coefficients of the forest soil treatments. Although methane increased exponentially in all of these treatments in the forested soils, the maximum methane accumulation ($\sim 25 \mu\text{M}$) was the lowest in comparison to the other two soil types.

In wetland soils, significant 3-parameter exponential increases were found in all treatments (Fig 6). The highest accumulation of methane ($\sim 60 \mu\text{M}$) was found in the '+ CH₄' treatment. Like in the forested soils, there were no significant differences between the growth coefficients of the wetland soil treatments (Table 1).

In row crop soils, all treatments had significant exponential increases in methane except for 'both' (Fig 6). Interestingly, the control and '+ CH₄' had similar patterns of growth and reached max methane accumulations of ~ 50 μM. The '+ NO₂⁻' treatment had low CH₄ accumulation, as did the 'both' treatment. There was a significant difference in growth with the addition of nitrite (ANOVA, p = 0.005, Table 1).

Soil Core Incubations

The soils core incubations mostly displayed similar behavior to the soil slurry incubations. There was significant 3-parameter exponential growth in all of the forest soil treatments from Nov 2014 (Table 2). The most methane accumulated in the control and '+ NO₂⁻' treatments (~ 50-85 μM), with much less accumulating in the '+ CH₄' and 'both' treatments (~ 10 μM, Fig 7). There was a significant difference in growth with the addition of methane (two-way ANOVA, p = 0.007, Table 2). The November 2015 forest soil core incubations displayed very different behavior from the 2014 trials (Fig 7). Only one 2015 forest soil core treatment had significant changes in headspace methane concentrations. The '+ CH₄' treatment exhibited 3-parameter exponential decay (Table 2). There were no significant changes in the other treatments, so no comparisons could be made between treatments.

The wetland soil core incubations had the highest accumulations of headspace methane. The '+ NO₂⁻' treatment peaked at ~ 450 μM, but the '+ CH₄' only accumulated ~ 100 μM methane. Each of the 4 treatments had significant exponential growth of methane (Figure 8, Table 2). The '+ NO₂⁻' growth coefficients were

significantly higher than the '+ CH₄' and 'both' treatments (one-way ANOVA, 0.038, Table 2).

The row crop soil core incubations exhibited 3-parameter exponential growth in methane concentrations for all treatments in the February 2015 and September 2015 trials. In February, the '+ CH₄' and 'both' treatments accumulated the most methane at ~ 250 μM methane, but each of these treatments had large variabilities amongst the triplicates (Fig 9). Due to the large standard errors, there were no significant differences amongst the growth coefficients of the February data (Table 2). Similar results were found in September. The primary difference in the two data sets is that the September '+ NO₂⁻' treatment accumulated the highest methane concentrations (along with 'both') at ~ 125 μM methane (Fig 9). Again, there were no significant differences in growth coefficients (Table 2).

Segmented soil core incubations were run for forested soil and soil from a ditch along-side the row crop site (Fig 10). Cores were segmented into 3 parts: 'top' (0-2.5 cm deep), 'mid' (2.5-7.5 cm deep), and 'bottom' (7.5-10 cm deep). Methane and nitrite was added to each core segment, but nitrite was added about halfway through the incubation so that changes in headspace gas concentrations could be analyzed pre- and post-nitrite additions. The forest soils were monitored for changes in methane concentrations. The only significant changes in methane concentrations were in the 'top' soil segment before nitrite was added. There was a significant upward linear trend ($y = y_0 + ax$), but the slope was relatively small at 0.022 μM CH₄ h⁻¹ ($p = 0.0055$, Fig 10). Headspace methane and carbon dioxide were analyzed for the soil from the row crop ditch. There were no significant changes in methane

concentrations pre- or post-nitrite additions to these soil core segments. There were significant, exponential increases in the ‘top’ and ‘bottom’ carbon dioxide concentrations ($p = 0.0011$ and $p = 0.0123$, respectively, Fig 10).

In-Situ

The *in-situ* test with sodium chloride was conducted 6 times with no success in intercepting the tracer plume. In each trial, the injection piezometer showed a spike in conductivity, temperature, and belowground depth when the sodium chloride was added. Temperature and depth belowground returned to normal levels rapidly, while the sodium chloride signal in the conductivity lasted longer. No changes in conductivity were found in the tracer piezometers. In the example given in Fig 11, the sodium chloride tracer was added on April 2, 2014 and there was a resulting peak in temperature, conductivity, and depth below ground in the injection piezometer. While temperature and depth returned to normal levels within the day of adding the tracer, initial conductivity peaked at over $600 \mu\text{S cm}^{-1}$, dropped to about $250 \mu\text{S cm}^{-1}$ until day 5, and then exponentially decreased to ambient levels ($0\text{-}50 \mu\text{S cm}^{-1}$) by day 11. The temperature, conductivity, and depth all stayed at normal levels in the tracer piezometers (Fig 11).

Discussion

Soil Slurry Incubations

The soil slurry incubations presented interesting patterns in the data (Fig 6). Each of the soil types had increases in headspace methane concentrations, indicating net methane production (methanogenesis > methane oxidation). This was not surprising considering the anaerobic conditions, but it is also indicative of healthy methanogen communities in environments that are not always associated with methane emissions (such as forested soils). While all of the soils had increases in methane, patterns between the treatments varied. In order to compare the treatments, exponential growth coefficients were compared via ANOVA analyses. If AOM-D is detected, it would be assumed that the pattern between the growth coefficients would be: '+ CH₄' > control > 'both' > '+ NO₂⁻' (Table 3). If AOM-D was occurring, then the presence of nitrite would stimulate methane oxidation, slowing the growth of headspace methane concentrations.

In forested soils, the highest methane accumulation was found in '+ CH₄' and 'both,' which also had higher methane starting points (Fig 6). The control and '+ NO₂⁻' growth coefficients (b) were higher than 'CH₄' and 'both,' but there were no significant differences between the growth coefficients (Table 1). Although no significant differences were found, a comparison of growth coefficients reveals a pattern of (Table 3). This pattern of growth does not support the expected pattern for the presence of AOM-D.

In wetland soils, the highest methane accumulation was found in the '+ CH₄' treatment (Fig 6). There were no significant differences between the growth

coefficients (Table 1). It was expected that '+ CH₄' would have the greatest rate of increase in methane accumulation, but the other treatments were too close together in ending methane concentrations, that no conclusions can be drawn from this data set on the presence of AOM-D (Table 3).

The crop soil data had a pattern that was closest to what is expected if AOM-D is present (Fig 6, Table 3). The control and '+ CH₄' treatments had the highest methane accumulations, which is indicative of AOM-D, since the nitrite-added treatments should have less methane accumulation due to the oxidation of methane through AOM-D. The 'both' data did not have an exponential increase in methane concentrations, so there is no reported growth coefficient for this treatment (Table 1). The favorable data from the crop soil inspired more soil incubation experiments, but later experiments were done with intact soil cores rather than soil slurries.

Soil Core Incubations

It was expected that the soil core results would resemble the slurry results. Instead, the results were also highly variable and patterns varied amongst soil types and date. For example, the forested soil incubations were run in November 2014 and November 2015 with differing results (Fig 7). The November 2014 data showed net methanogenesis and each treatment had significant exponential increases in methane concentrations (Table 2). The control and the '+ NO₂⁻' treatments had the highest rate of methane accumulation (Fig 7), with the control accumulating the most methane. This pattern is indicative of AOM-D, since the presence of nitrite resulted in less methane accumulation (potentially due to enhanced oxidation). The methane-added treatments were less indicative of AOM-D and have low methane

accumulation relative to the other treatments (Fig 7). Contrary to this early data set, the November 2015 data showed net methane oxidation (Fig 7). This soil incubation was distinct from all other incubations, and it is unclear what caused the net methane oxidation rather than methanogenesis as there were few differences between the seasons. The '+ CH₄' treatment had significant exponential decay, but the other treatments did not have significant trends (Table 2). Due to the lack of observable trends in the 'both' treatment and no changes in the control and 'nitrite' treatments, no conclusions can be drawn about the hypotheses from this set of soil core incubations. When comparing the soil core incubations with the forest soil slurry incubation, the slurry had the opposite pattern of methane accumulation as the 2014 soil incubation and could not be compared to the 2015 soil incubation due to net methane oxidation in the latter (Table 3).

In wetland soil core incubations, all treatments had significant exponential increases in methane concentrations (Table 2, Fig 8), indicating net methanogenesis. The pattern of headspace methane growth, though, contradicts the hypothesis of AOM-D being found in these soils (Table 3). The '+ NO₂⁻' treatment has significantly more methane accumulation than the control. The 'both' treatment's methane growth is also greater than that for '+ CH₄', but this difference is not significant (Table 2). This pattern of methane accumulation differs from the slurry (Table 3), but again, the data does not support that AOM-D is present in the wetland soils that were tested in this experiment.

The crop soil incubations also exhibited net methanogenesis (Fig 9), but the patterns of methane accumulation differed from the trials in February 2015 and

September 2015 (Table 3). In February, the '+ CH₄' and 'both' treatments accumulated the most methane. In September, the control, '+ CH₄', and '+ NO₂⁻' each accumulated about 100 μM methane, while the 'both' treatment only accumulated about 25 μM methane. None of the methane growth rates were significantly different, and the patterns of methane accumulation did not match that of the crop soil slurry data (Table 3, Fig 6). Therefore, although the crop soil slurry showed evidence in favor of AOM-D in the soils, the soil core incubations did not support this hypothesis.

Inconsistent soil core results induced questions about the usefulness of the methods that were devised. A major question was whether the incubators were air-tight. This was addressed by using Pyro Science oxygen sensors to monitor oxygen concentrations in the incubations. Most of the cores were found to have good air-tight seals after being purged with N₂ (Fig 12). Incubators that were leaking had gradual increases in O₂ (Fig 14). Any incubators that showed increases in oxygen levels were assumed to not be air-tight and were excluded from data analyses.

Due to the concern that the potential nitrite oxidation signal was overwhelmed by high rates of methanogenesis, soil incubations were run with smaller, segmented cores and methane levels were sampled for 2-3 days rather than a week or longer as was done in previous incubations (Fig 10). Increasing the sampling frequency determined if the nitrite was rapidly consumed by AOM-D initially. This rapid assessment was used in the core segment trials to determine if AOM-D was localized to one vertical region. On the faster timescale, only minor changes in methane concentrations were found (Fig 10). There was also no difference in the methane

concentration changes in the core segments, although the ‘top’ and ‘bottom’ crop core segments had exponential increases in CO₂, indicative of active soil metabolism in these samples.

Overall, there is no significant evidence for AOM-D in these trials. High rates of methanogenesis may have obscured evidence for methane oxidation by nitrite. This information could potentially be found using an isotope dilution study, but the high variability between soils cores would make this method difficult to interpret. The heterogeneity of soil makes using intact soil cores challenging as it is hard to get reproducible results. Nitrogen transformations are commonly studied using soil core incubations with the acetylene inhibition of nitrification method (Parkin et al. 1984, Ryden et al. 1987, Hatch et al. 1990, Jarvis et al. 2001). The use of a methyl-coenzyme m reductase (*mcrA*) gene inhibitor, such as 2-bromoethanesulphonate (BES), could be used to inhibit methanogenesis, but BES has also been shown to inhibit AOM-D at low concentrations (Haroon et al. 2013).

In-Situ

The *in-situ* approach to this study is promising in theory but requires resources that were outside the scope of this project. Groundwater flow patterns within the top 1-2 m of the soil are difficult to predict and can require sampling from multiple horizontal and vertical locations to receive a targeted tracer plume. *In-situ* soil experiments have been successfully performed in large fields with more than 15 multilevel sampling devices that reach to nearly 14 m belowground (Smith et al. 1991). In this dissertation, the goal was to keep the sampling piezometers close enough that the

plume could not be missed; however, I was not successful in capturing the sodium tracer (Fig 11).

The ultimate fate of multiple tracer plumes is unknown, but there are 2 potentials. The first is that the plumes were small enough to travel between the piezometer (0.5 m spacing between them). If this was the case, then the piezometers would need to be closer together. The second potential for the fate of the tracer plume is that the groundwater traveled below the sampling piezometers. The piezometers were hand-augured and could only be placed as deep as the unsaturated zone. Once the auger reached saturated groundwater, the hole began to collapse so that the auger could not dig deeper. The placement of deeper piezometers would need to be performed with more advanced drilling equipment that was outside the scope of this project. Research of this nature could still be successful with the proper resources to install many closely-spaced piezometers 1-2 meters into the ground.

Hypotheses

In this study, two hypotheses were tested: (1) AOM is present in soils and detectable using biogeochemical methods and (2) nitrite is the primary electron acceptor in the AOM reactions. The core incubations mostly had net methanogenesis, which does not support the first hypothesis. Only one set of soil incubation cores had net methane oxidation in anaerobic conditions. There was little or no support for nitrite as the primary electron acceptor in AOM (hypothesis 2). Overall, there was not enough evidence for these two hypotheses to be supported.

This study is a cautionary tale on using these methods for this type of analysis. Soil core incubations are difficult to control and assess, and there are concerns about

experimental manipulation. To avoid coring and handling artifacts, I attempted to do true *in situ* soil incubations using the CSPN approach. However, groundwater flow is difficult to predict, so groundwater tracers can be hard to capture. With further time and in-depth engineering, these methods could be improved and could provide evidence for these or other hypotheses.

Acknowledgements

The work for this chapter was funded by National Geographic Society (Grant 9051-11), NSF DDIG (Award No. DEB-1311302), NSF Coastal SEES Program (Award No. 1325553), and Horn Point Laboratory Bays and Rivers Fellowship.

Tables and Figures

Tables

Table 1. Slurry data statistics for Fig 5. Each set of treatment averages were fit with a 3-parameter exponential growth curve ($y = y_0 + ae^{bx}$, where y is methane and x is time). Analyses of variation (ANOVA) of the growth coefficients were run for each site. Statistical significances are denoted as: NS (not significant), MS (marginally significant), * (significant), ** (highly significant).

Site	Treatment	Equation	r ²	P	ANOVA
Forest	Control	$y = -0.02 + 0.0011e^{0.4982x}$	0.9999	<0.0001**	NS
	+ NO ₂ ⁻	$y = -0.08 + 0.0066e^{0.4292x}$	0.9997	<0.0001**	
	+ CH ₄	$y = 18.55 + 1.2112e^{0.0853x}$	0.5862	0.0761 (MS)	
	+ Both	$y = 13.22 + 0.1313e^{0.2531x}$	0.9646	0.0006**	
Wetland	Control	$y = -2.17 + 1.3255e^{0.1656x}$	0.9912	<0.0001**	NS
	+ NO ₂ ⁻	$y = -0.76 + 0.4050e^{0.2244x}$	0.9986	<0.0001**	
	+ CH ₄	$y = 17.11 + 1.1241e^{0.2013x}$	0.9788	0.0002**	
	+ Both	$y = 12.80 + 1.1859e^{0.1445x}$	0.9477	0.0012**	
Crops	Control	$y = -71.54 + 69.1289e^{0.0320x}$	0.9490	0.0003**	0.005**
	+ NO ₂ ⁻	$y = -2.32 + 1.9694e^{0.1207x}$	0.9959	<0.0001**	
	+ CH ₄	$y = -10.39 + 24.7494e^{0.0571x}$	0.9892	<0.0001**	
	+ Both	N/A	N/A	N/A	

Table 2. Soil core incubation data statistics for Fig 6, 7, 8. Each set of treatment averages were fit with a 3-parameter exponential growth curve ($y = y_0 + ae^{bx}$, where y is methane and x is time) or 3-parameter exponential decay curve ($y = y_0 + ae^{-bx}$). Analyses of variation (ANOVA) of the growth coefficients were run for each site. Statistical significances are denoted as: NS (not significant), MS (marginally significant), * (significant), ** (highly significant).

Site	Treatment	Equation	r ²	P	ANOVA
Forest Nov 2014	Control	$y = -3.75 + 3.6227e^{0.3402x}$	0.9998	<0.0001**	0.007**
	+ NO ₂ ⁻	$y = -0.95 + 0.9278e^{0.4185x}$	0.9999	<0.0001**	
	+ CH ₄	$y = 2.65 + 0.5226e^{0.2380x}$	0.9995	0.0002**	
	+ Both	$y = 2.75 + 0.4974e^{0.3615x}$	0.9995	0.0005**	
Forest Nov 2015	Control	No Pattern	N/A	N/A	N/A
	+ NO ₂ ⁻	No Pattern	N/A	N/A	
	+ CH ₄	$y = 0.25 + 1.8134e^{-0.4656x}$	0.9729	0.0021**	
	+ Both	No Pattern	N/A	N/A	
Wetland	Control	$y = -18.77 + 21.3712e^{0.2446x}$	0.9988	0.0006**	0.038*
	+ NO ₂ ⁻	$y = -45.59 + 50.9003e^{0.2315x}$	0.9950	0.0025**	
	+ CH ₄	$y = -3.76 + 4.9033e^{0.3103x}$	0.9972	0.0308*	
	+ Both	$y = -5.26 + 6.7687e^{0.3290x}$	0.9978	0.0273*	
Crops Feb 2015	Control	$y = -194 + 201.31e^{0.0182x}$	0.9991	0.0004**	NS
	+ NO ₂ ⁻	$y = -46.76 + 50.9003e^{0.0757x}$	0.9563	0.0218*	
	+ CH ₄	$y = 27.82 + 26.6448e^{0.1749x}$	0.9128	0.0436*	
	+ Both	$y = -510 + 562.46e^{0.0236x}$	0.8928	0.0536 (MS)	
Crops Sept 2015	Control	$y = -37.74 + 471.19e^{0.0899x}$	0.9999	<0.0001**	NS
	+ NO ₂ ⁻	$y = -262 + 275.09e^{0.0281x}$	0.9932	0.0034**	
	+ CH ₄	$y = -1.81 + 7.3114e^{0.1493x}$	0.9997	0.0002**	
	+ Both	$y = -23.00 + 27.2192e^{0.1496x}$	0.9974	0.0013**	

Table 3. Comparison of growth coefficients for soil incubations. The expected pattern when AOM-D is present is shown first. Growth coefficients are taken from the average exponential growth models in Tables 1 and 2. ANOVA significance p-values can be found in Tables 1 and 2.

Soil Treatment	Pattern	ANOVA
Indicative of AOM-D	+ CH ₄ > control > both > + NO ₂ ⁻	**
Soil Slurry Incubations		
Forest	+ CH ₄ > both > + NO ₂ ⁻ > control	NS
Wetland	control > + CH ₄ > both > + NO ₂ ⁻	NS
Crops	control > + CH ₄ > +NO ₂ ⁻	**
Soil Core Incubations		
Forest-Nov 2014	control > + NO ₂ ⁻ > both > + CH ₄	**
Forest-Nov 2015	N/A	N/A
Wetland	+ NO ₂ ⁻ > control > both > + CH ₄	*
Crops-Feb 2015	both > control > + NO ₂ ⁻ > + CH ₄	NS
Crops-Sept 2015	control > + NO ₂ ⁻ > both > CH ₄	NS

Figures

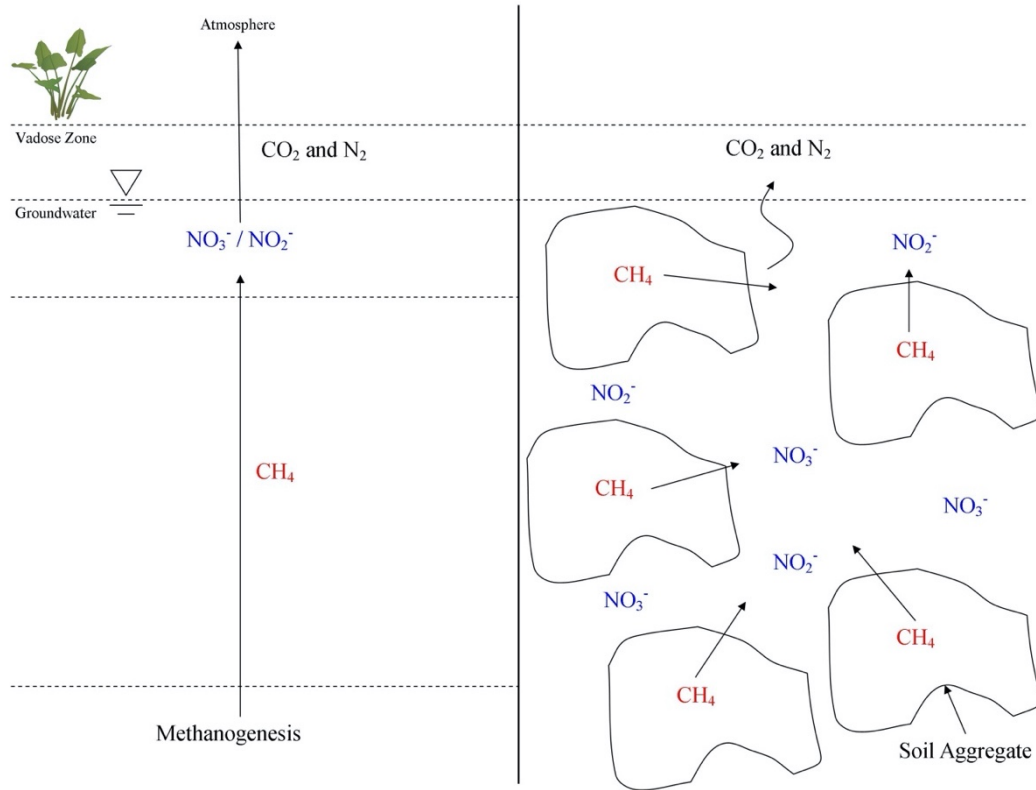
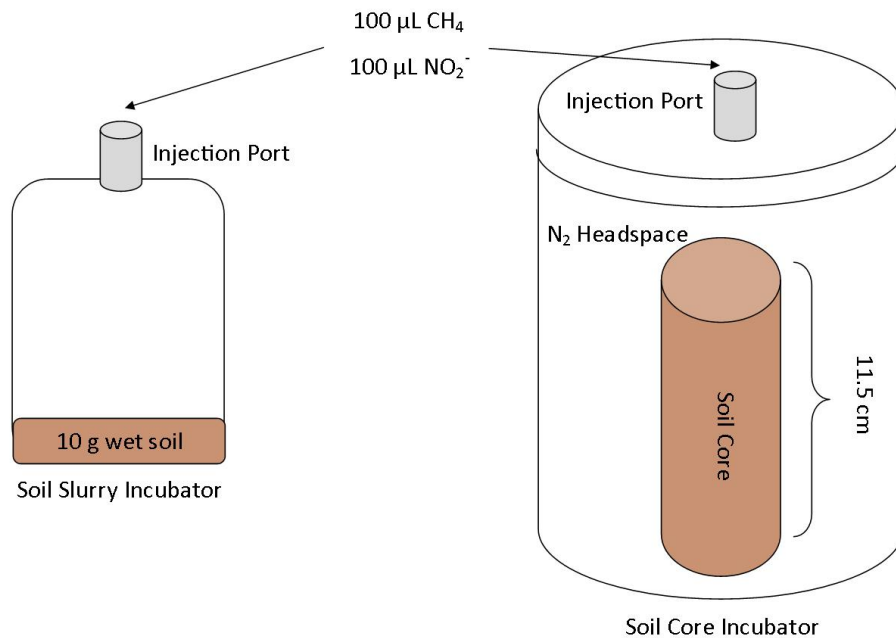


Figure 1. The left panel shows methane produced deep in groundwater and bubbling up into the zone of nitrate and nitrite above, where AOM-D produced CO₂ and N₂. The right panel shows methanogenesis and denitrification in aggregates within saturated soil matrix. In this scenario methane diffused laterally from within anoxic aggregates to groundwater containing nitrate/nitrite. AOM-D occurs in groundwater to produce CO₂ and N₂. Methane does not accumulate in groundwater except when nitrate is less than 10 μM. Arrow Arum figure is from Tracey Saxby, IAN Image Library (Ian.umces.edu/imagelibrary/).



Soil Incubation Block Design		NO ₂ ⁻	
		-	+
CH ₄	-	Control	+ NO ₂ ⁻
	+	+ CH ₄	Both

Figure 2. Conceptual diagram of experimental design for soil incubations. Four treatments were run in triplicate: ‘control,’ ‘+ NO₂⁻,’ ‘+CH₄,’ and ‘both.’ Soils were first run as slurries (10 g wet soil) in serum bottles (soil slurry incubators) and then run as complete soil cores in Mason jars (soil core incubators). For each incubator, soil was added, the incubators were sealed, and an N₂ headspace was injected into the incubator. Methane and or nitrite was added to the treatments that required additions.

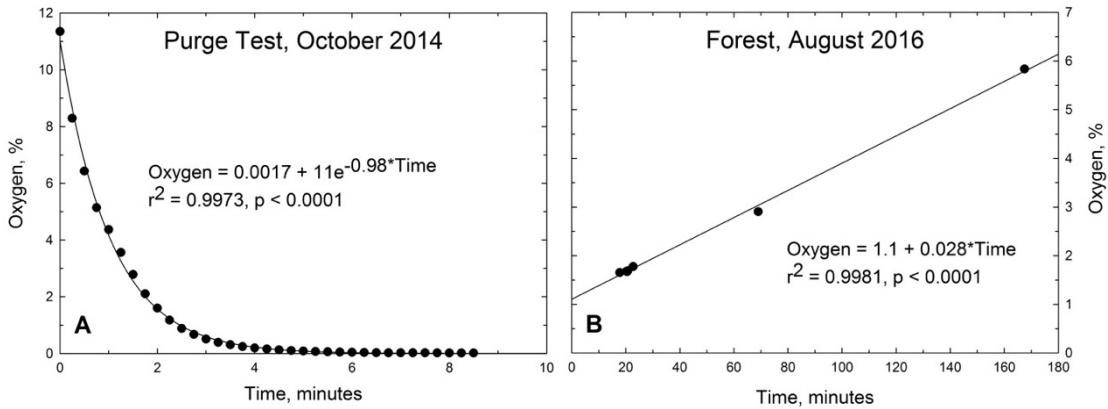


Figure 3. Time sequence of oxygen levels in incubation chambers. Panel A is from a purge test in October 2014. This panel shows the drop in oxygen levels after the chamber while a chamber was purged with N₂ gas. Panel B is from a segmented forest soil incubation that had a chamber lid with leaks. This panel shows the gradual increase in oxygen levels over time.

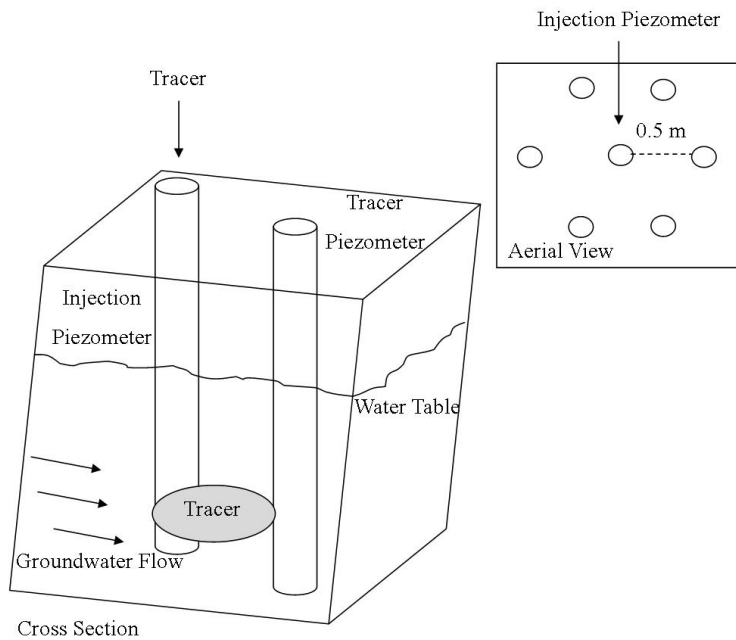


Figure 4. Diagram of a closely spaced piezometer nest (CSPN).

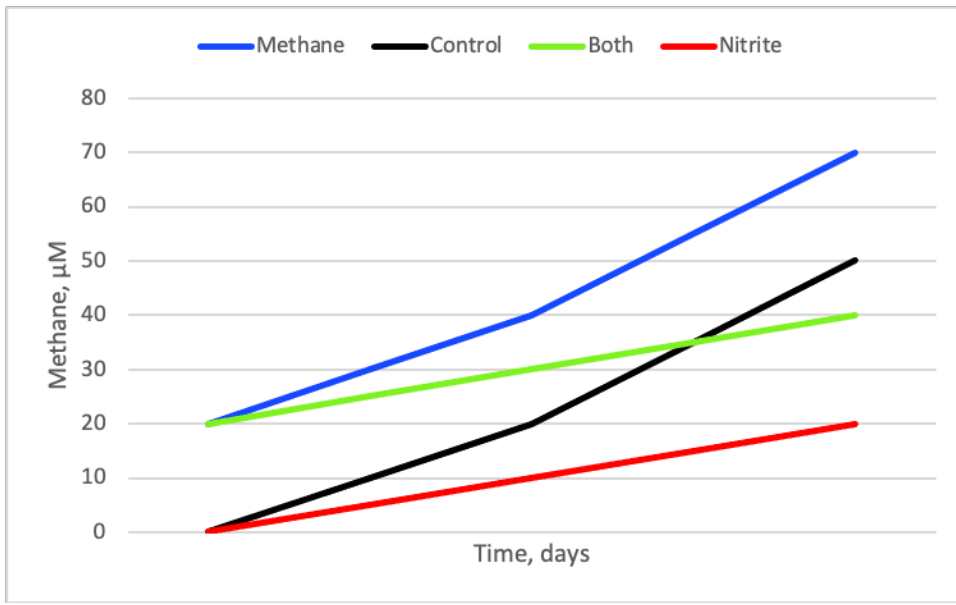


Figure 5. Expected pattern of results for soil slurry and core incubations if AOM-D is present in the samples.

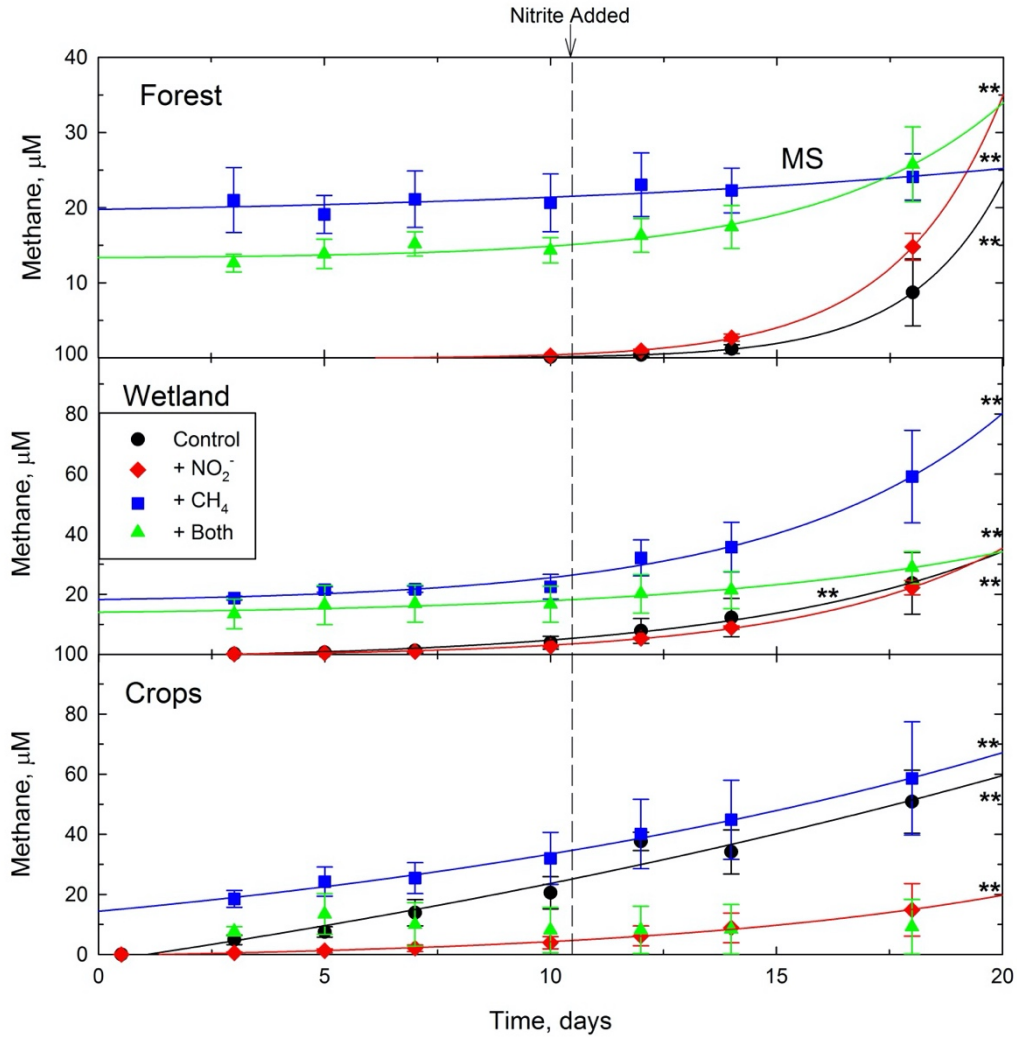


Figure 6. Average headspace methane concentrations for forested, wetland, and row crop soil slurry incubation experiments. Nitrite was added to the '+ NO₂⁻' and '+ both' treatments after day 10. Data are plotted with 3 parameter exponential growth trend lines and data without trend lines have no significant change in headspace methane concentrations. Significance of trend lines is noted with MS, *, or **. All equations for trend lines are given in Table 1.

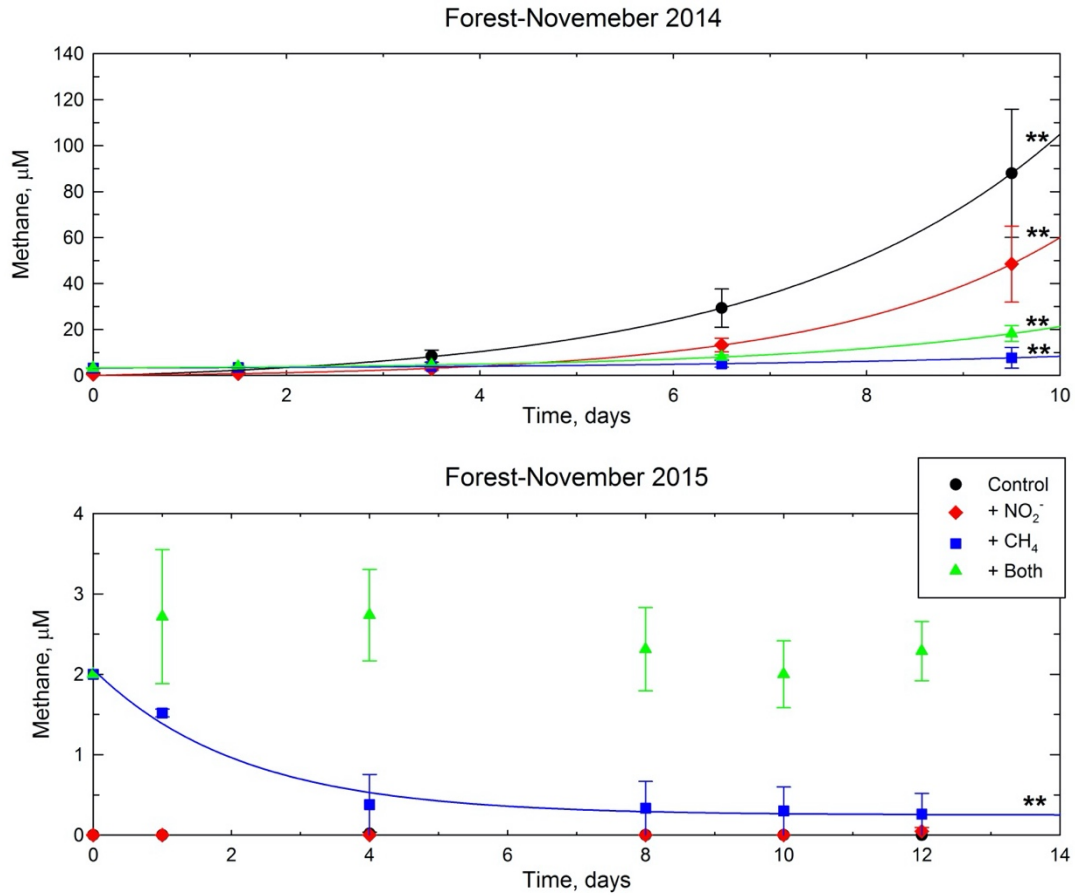


Figure 7. Average headspace methane concentrations for forest soil core incubations. The top panel is from Nov. 2014 and the bottom panel is from Nov. 2015. Data are plotted with 3 parameter exponential growth (or decay) trend lines and data without trend lines have no significant change in headspace methane concentrations. Significance of trend lines is noted with MS, *, or **. All equations for trend lines are given in Table 2.

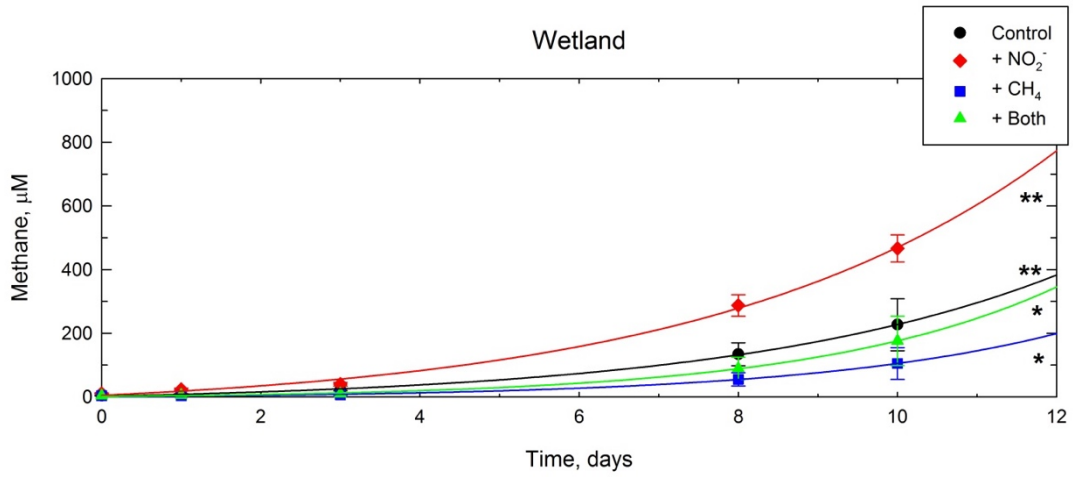


Figure 8. Average headspace methane concentrations for wetland soil core incubations. Data are plotted with 3 parameter exponential growth trend lines. Significance of trend lines is noted with MS, *, or **. All equations for trend lines are given in Table 2.

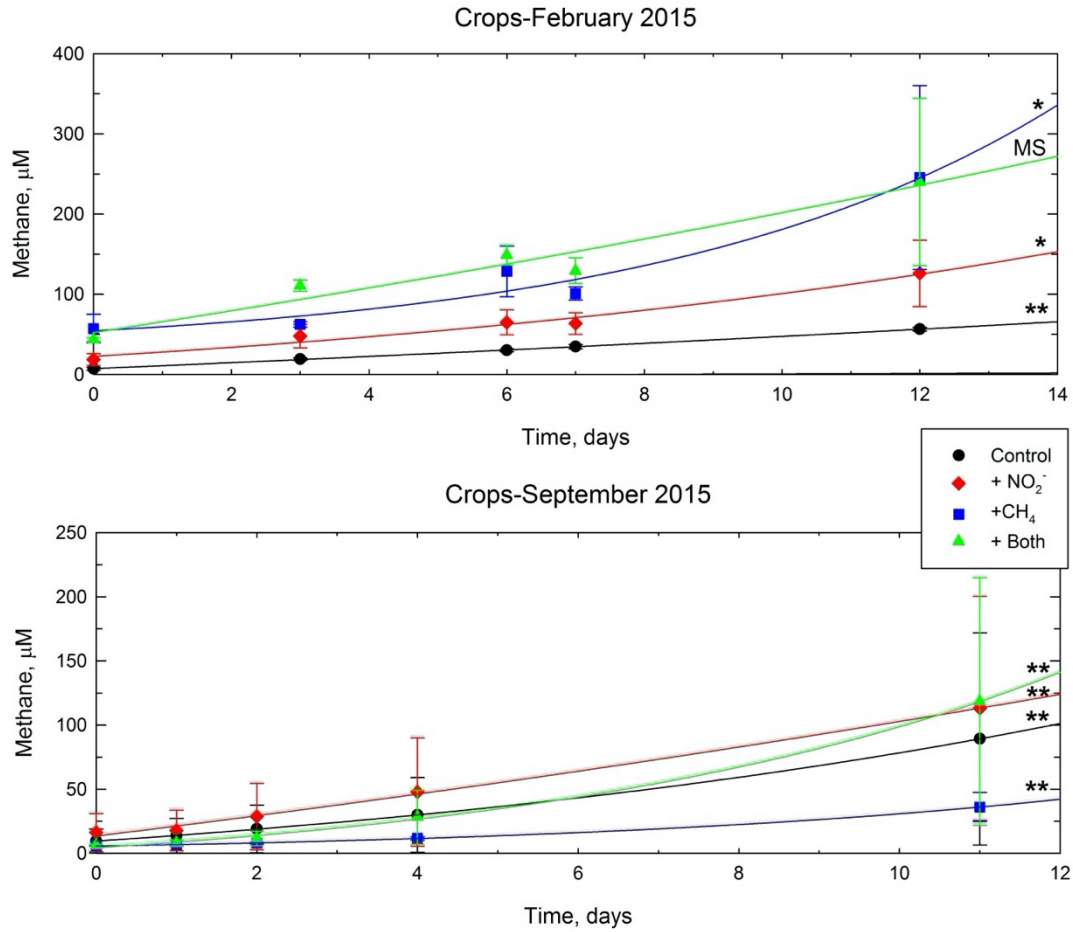


Figure 9. Headspace methane concentrations for crops soil incubations. The top panel is from Feb. 2015 and the bottom panel is from Sept. 2015. Data are plotted with 3 parameter exponential growth trend lines. Significance of trend lines is noted with MS, *, or **. All equations for trend lines are given in Table 2.

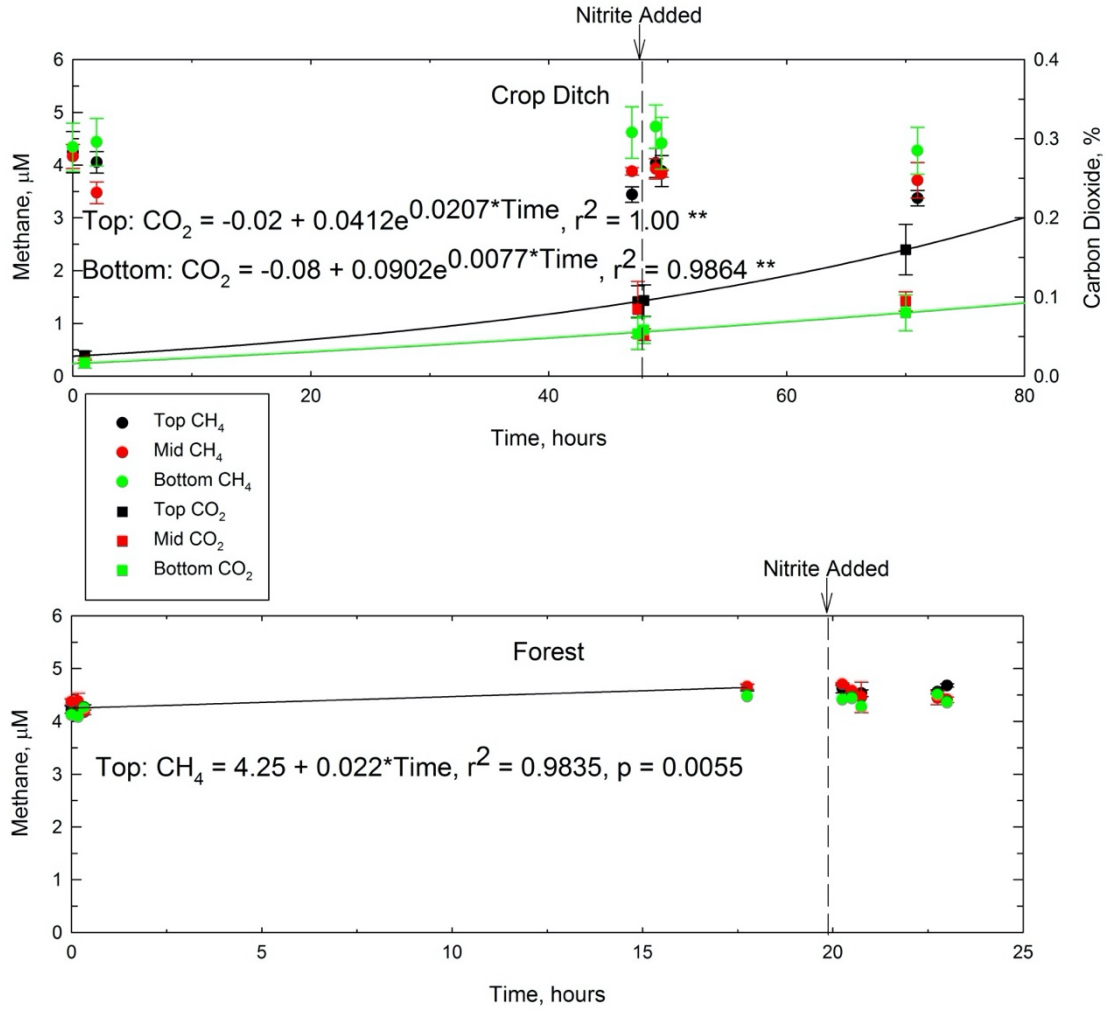


Figure 10. Headspace methane (circles) and carbon dioxide (squares) for segmented soil cores from the agricultural ditch (top) and headspace methane concentrations for segmented soil cores from the forested site. The segments are top (0-2.5 cm deep, black), mid (2.5-7.5 cm deep, red), and bottom (7.5-10 cm deep, green). Equations for significant patterns headspace gas concentrations are given.

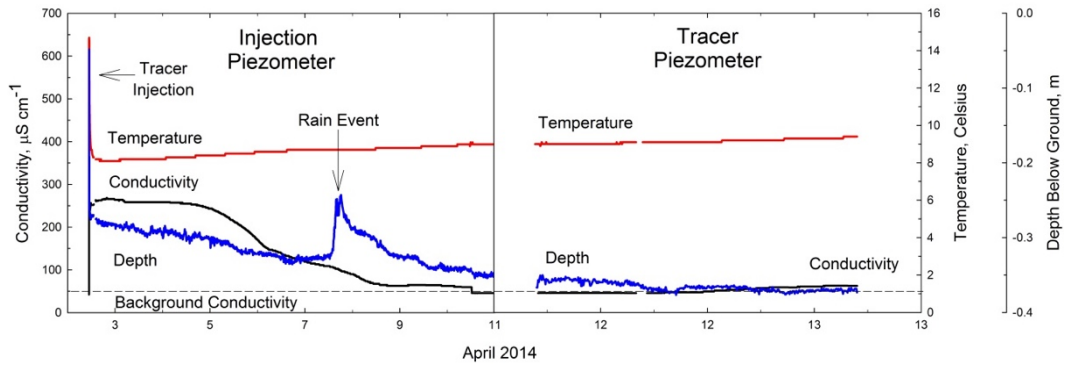


Figure 11. Groundwater conductivity (black), temperature (red), and depth below ground (blue) for the injection piezometer (left) and the tracer piezometer (right) after the injection of a sodium chloride tracer plume into a CSPN at the forested site.

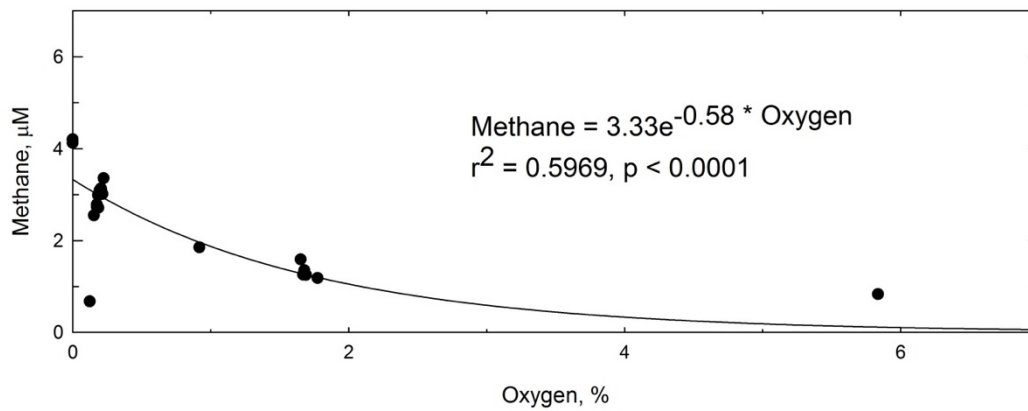


Figure 12. Methane and oxygen levels for 3 forested soil core incubations with leaking incubator lids.

Bibliography

- Achtnich, C., Bak, F., & Conrad, R. (1995a). Competition for electron donors among nitrate reducers, ferric iron reducers, sulfate reducers, and methanogens in anoxic paddy soil. *Biology and Fertility of Soils*, 19, 65-72.
- Achtnich, C., Schuhmann, A., Wind, T., & Conrad, R. (1995b). Role of interspecies H₂ transfer to sulfate and ferric iron-reducing bacteria in acetate consumption in anoxic paddy soil. *FEMS Microbiology Ecology*. 16, 61-69.
- Akaike, H. (1973). Information theory as an extension of the maximum likelihood principle, in: Petroy, B.N., Csaki, F. (Eds.), Second International Symposium on Information Theory. Akademiai Kiado, Budapest, pp. 267-281.
- Arshad, A., Speth, D.R., de Graaf, R.M., Op den Camp, H.J.M., Jetten, M.S.M., & Welte C.U. (2015). A metagenomics-based metabolic model of nitrate-dependent anaerobic oxidation of methane by *Methanoperedens*-like Archaea. *Frontiers in Microbiology*, 6, 1-14.
- Audet, J., Bastviken, D., Bundschuh, M., Buffam, I., Feckler, A., Klemedtsson, L., ...& Wallin, M.B. (2019). Forest streams are important sources for nitrous oxide emissions. *Global Change Biology*, DOI: 10.1111/gcb.14812.
- Baedecker, M.J., & Back, W. (1979). Modern marine sediments as a natural analog to the chemically stressed environment of a landfill. *Journal of Hydrology*, 43, 393-414.

- Baedecker, M.J., Cozzarelli, I.M., Eganhouse, R.P., Siegel, D.I., & Bennett, P.C. (1993). Crude oil in a shallow sand and gravel aquifer-III. Biogeochemical reactions and mass balance modeling in anoxic groundwater. *Applied Geochemistry*, 8, 569-586.
- Baird, A.J., Beckwith, C.W., Waldron, S., & Waddington, J.M. (2004). Ebullition of methane-containing gas bubbles from near-surface *Sphagnum* peat. *Geophysical Research Letters*, doi:10.1029/2004GL021157.
- Bannert, A., Bogen C., Esperschütz, J., Koubová, A., Buegger, F., Fischer, D.,...Schloter, M. (2012). Anaerobic oxidation of methane in grassland soils used for cattle husbandry. *Biogeosciences*, 9, 3891-3899.
- Barnes, R.O., & Goldberg, E.D. (1976). Methane production and consumption in anoxic marine sediments. *Geology*, 4(5), 297-300.
- Bastviken, D., Tranvik, L.J., Downing, J.A., Crill, P.M., & Enrich-Prast, A. (2011). Freshwater methane emissions offset the continental carbon sink. *Science*, 331, 50.
- Baulch, H.M., Dillon, P.J., Maranger, R., & Schiff, S.L. (2011). Diffusive and ebullitive transport of methane and nitrous oxide from streams: Are bubble-mediated fluxes important? *Journal of Geophysical Research*, 116, 1-15.
- Beal, E.J., House, C.H., & Orphan, V.J. (2009). Manganese- and iron-dependent marine methane oxidation. *Science*, 325(5937), 184-187.
- Beckert, K.A., Fisher, T.R., O'Neil, J.M., & Jesien, R.V. (2011). Characterization and comparison of stream nutrients, land use, and loading patterns in Maryland coastal bay watersheds. *Water Air Soil Pollution*, 221, 255-273.

- Berner, R.A. (1980) *Early Diagenesis: A Theoretical Approach*. Princeton, New Jersey: Princeton University Press.
- Blaut, M. (1994). Metabolism of methanogens. *Antonie van Leeuwenhoek*, 66, 187-208.
- Boetius, A., Ravenschlag, K., Schubert, C.J., Rickert, D., Widdel, F., Gieseke, R.A.,...& Pfannkuche, O. (2000). A marine microbial consortium apparently mediating anaerobic oxidation of methane. *Nature*, 407, 623-626.
- Böhlke, J.K., Wanty, R., Tuttle, M., Delin, G., & Landon, M. (2002). Denitrification in the recharge area and discharge area of a transient agricultural nitrate plume in a glacial outwash sand aquifer, Minnesota. *Water Resources Research*, doi:10.1029/2001WR000663.
- Böhlke, J.K., Verstaeten, I.M., & Kraemer, T.E. (2007). Effects of surface-water irrigation on sources, fluxes, and residence times of water, nitrate, and uranium in an alluvial aquifer. *Applied Geochemistry*, 22, 152-174.
- Brady, N.C., & Weil, R.R. (1999). *The Nature and Properties of Soils*. Prentice Hall, Upper Saddle River.
- Bunnell-Young, D.E., unpublished. Dynamics of methane and nitrogen in agricultural watersheds in the northern Choptank River Basin, MD. MS Thesis, Marine-Estuarine-Environmental Science Program, University of Maryland.
- Burnham, K.P., & Anderson, D.R. (2002). *Model Selection and Multimodel Inference: A Practical Information-Theoretic Approach*, Second Ed. Springer-Verlag, New York, pp.70.

- Cai, C., Leu, A.O., Xie, G.-J., Guo, J., Feng, Y., Zhao, J.-X.,...& Hu, S. (2018). A methanotrophic archaeon couples anaerobic oxidation of methane to Fe (III) reduction. *The ISME Journal*, 12(8), 1929-1939.
- Caldwell, S.L., Laidler, J.R., Brewer, E.A., Eberly, J.O., Sandborgh, S.C., & Colwell, F.S. (2008). Anaerobic oxidation of methane: mechanisms, bioenergetics, and the ecology of associated microorganisms. *Environ. Sci. Technol.*, 42(18), 6791-6799.
- Campeau, A., & Del Giorgio, P.A. (2014). Patterns in CH₄ and CO₂ concentrations across boreal rivers: Major drivers and implications for fluvial greenhouse emissions under climate change scenarios. *Global Change Biology*, 20, 1075-1088.
- Canfield, D.E., Thamdrup, B., & Hanson, J.W. (1993). The anaerobic degradation of organic matter in Danish coastal sediments: iron reduction, manganese reduction, and sulfate reduction. *Geochim. Cosmochim. Acta*, 57(16), 3867-3883.
- Canfield, D.E., Glazer, A.N., & Falkowski, P.G. (2010). The evolution and future of Earth's nitrogen cycle. *Science*, 330(6001), 192-196.
- Cassman, K.G., Dobermann, A., & Walters, D.T. (2002). Agroecosystems, nitrogen-use efficiency, and nitrogen management. *Ambio*, 31, 132-140.
- Chapelle, F.H., Zelibor, J.L., Grimes, D.J., & Knobel, L.L. (1987). Bacteria in deep coastal plain sediments of Maryland: A possible source of CO₂ to groundwater. *Water Resources Research*, 23(8), 1625-1632.

- Chen, Y.-H. & Prinn, R.G. (2005). Atmospheric modeling of high- and low-frequency methane observations: Importance of interannually varying transport. *Journal of Geophysical Research*, 110, doi:10.1029/2004JD005542.
- Christensen, T.H., Bjerg, P.L., Banwart, S.A., Jakobsen, R., Heron, G., & Albrechtsen, H.-J. (2000). Characterization of redox conditions in groundwater contaminant plumes. *Journal of Contaminant Hydrology*, 45, 165-241.
- Clark, G.M., Mueller, D.K., & Mast, M.A. (2000). Nutrient concentrations and yields in undeveloped stream basins of the United States. *Journal of American Water Research Association*, 36, 849-860.
- Conrad, R. (2007). Microbial ecology of methanogens and methanotrophs. In D. Sparks (Ed.), *Advances in Agronomy* (pp. 1-63). Massachusetts: Academic Press.
- Crawford, J.T., Stanley, E.H., Spawn, S.A., Finlay, J.C., Loken, L.C., & Striegl, R.G. (2014). Ebullitive methane emissions from oxygenated wetland streams. *Global Change Biology*, 20(11), 3408-3422.
- Cui, M., Ma, A., Qi, H., Zhuang, X., & Zhuang, G. (2014). Anaerobic oxidation of methane: an “active” microbial process. *Microbiology Open*, doi: 10.1002/mbo3.232.
- Davidson, E.A., David, M.B., Galloway, J.N., Goodale, C.L., Haeuber, R., Harrison, J.A.,...& Ward, M.H. (2012). Excess nitrogen in the U.S. environment: trends, risks, and solution. *Issues in Ecology*, 15, 1-16.

- DelSontro, T., Boutet, L., St. Pierre, A., del Giorgio, P.A., & Prairie, Y.T. (2016). Methane ebullition and diffusion from northern ponds and lakes regulated by the interaction between temperature and system productivity. *Limnology & Oceanography*, 61(S1), S62- S77.
- Denver, J.M., Ator, S.W., Debrewer, L.M., Ferrari, M.J., Barbaro, J.R., Hancock, T.C., Brayton, M.J., & Nardi, M.R. (2004). Water quality in the Delmarva Peninsula, Delaware, Maryland, and Virginia, 1999–2001. *U.S. Geological Survey Circular*, 1228, 26 pps.
- Denver, J.M., & Nardi, M.R. (2016). Thickness of the Surficial Aquifer, Delmarva Peninsula, Maryland and Delaware. U.S. Geological Survey. Data release <http://dx.doi.org/10.5066/F7610XFT>.
- Demars, B.O., Thompson, J., & Manson, J.R. (2015). Stream metabolism and the open diel oxygen method: Principles, practice, and perspective. *Limnology & Oceanography: Methods*, 13, 356-374.
- Dubrovsky, N.M., Burow, K.R., Clark, G.M., Gronberg, J.M., Hamilton, P.A., Hitt, K.J.,...& Wilber, W.G. (2010). The quality of our nation's waters-nutrients in the nation's streams and groundwater, 1992-2004. *US Geol. Surv. Circ*, 1350, 174 pps.
- Egger, M., Rasigraf, O., Sapart, C.J., Jilbert, T., Jetten, M.S.M., Röckman, T., Slomp, C.P. (2015). Iron-mediated anaerobic oxidation of methane in brackish coastal sediments. *Environmental Science & Technology*, 49 (1), 277-283.

- Egger, M., Kraal, P., Jilbert, T., Sulu-Gambari, F., Sapart, C.J., Röckmann, T., & Slomp, C.P. (2016). Anaerobic oxidation of methane alters sediment records of sulfur, iron and phosphorus in the Black Sea. *Biogeosciences*, (13), 5333-5355.
- Ettwig, K.F., Shima, S., van de Pas-Schoonen, K.T., Kahnt, J., Medema, M.H., Op den Camp, H.J.,...Strous, M. (2008). Denitrifying bacteria anaerobically oxidize methane in the absence of Archaea. *Environ. Microbiol.*, 10(11), 3164-3173.
- Ettwig, K.F., Butler, M.K., Paslier, D.L., Pelletier, E., Mangenot, S., Kuypers, M.M.M.,...Strous, M. (2010). Nitrite-driven anaerobic methane oxidation by oxygenic bacteria. *Nature*, 464, 543-548.
- Ettwig, K.F., Zhu, B., Speth, D., Keltjens, J.T., Jetten, M.S.M., & Kartel, B. (2016). Archaea catalyze iron-dependent anaerobic oxidation of methane. *PNAS*, 113(45), 12792-12796.
- Fisher, T.R., Peele, E.R., Ammerman, J.W., & Harding Jr., L.W. (1992). Nutrient limitation of phytoplankton in Chesapeake Bay. *Marine Ecology Progress Series*, 82(1), 51-63.
- Fisher, T.R., Hagy III, J.D., Boynton, W.R., & Williams, M.R. (2006). Cultural eutrophication in the Choptank and Patuxent estuaries of Chesapeake Bay. *Limnol. Oceanogr.*, 51, 435-447.

- Fisher, T.R., Jordan, T.E., Staver, K.W., Gustafson, A.B., Koskelo, A.I., Fox, R.J.,...Lang, M.W. (2010). The Choptank Basin in transition intensifying agriculture, slow urbanization, and estuarine eutrophication. In Kennish M.J., Paerl H.W. (eds.) Coastal Lagoons Critical Habitats of Environmental Change, CRC Press, pp 135-165.
- Fisher, T.R., Fox, R.J., Gustafson, A.B., Lewis, J., Millar, N., & Winsten J.R. (2018). Fluxes of nitrous oxide and nitrate from agricultural fields on the Delmarva Peninsula: N biogeochemistry and economics of field management. *Agriculture, Ecosystems and Environment*, 254, 162-178.
- Foley, J.A., DeFries R., Asner G.P., Barford C., Bonan G., Carpenter S.R.,...& Snyder P.K. (2005). Global consequences of land use. *Science* 309, 570-574.
- Follett, J.R., & Follett, R.F. (2001). Utilization and metabolism of nitrogen by humans. In Follett R., Hatfield J.L. (eds.) Nitrogen in the Environment: Sources, Problems and Management. Elsevier Science, New York, pp 65-92.
- Fox, R.J. (2011). Dynamics of metabolic gases in groundwater and the vadose zone of soils on Delmarva. University of Maryland (PhD Dissertation).
- Fox, R.J., Fisher, T.R., Gustafson, A.B., Jordan, T.E., Kana, T., & Lang, M. (2014). Searching for the missing nitrogen: Biogenic nitrogen gases in groundwater and streams. *The Journal of Agricultural Sciences*, 152, 96-106.
- Galloway, J.N., Schlesinger, W.H., Levy II, H., Michaels, A., & Schnoor, J.L. (1995). Nitrogen fixation: Anthropogenic enhancement-environmental response. *Global Biogeochemical Cycles*, 9(2), 235-252.

- Galloway, J.N., Dentener, F.J., Capone, D.G., Boyer, E.W., Howarth, R.W., Seitzinger, S.P.,...& Vörösmarty, C.J. (2004). Nitrogen cycles: past, present, and future. *Biogeochemistry*, 70, 153-226.
- Gardner, J.R., Fisher, T.R., Jordan, T.E., & Knee, K.L. (2016). Balancing watershed nitrogen budgets: accounting for biogenic gases in streams. *Biogeochemistry*, 127, 231-253.
- Gauthier, M., Bradley, R.L., and Simek, M. (2015). More evidence that anaerobic oxidation of methane is prevalent in soils: is it time to upgrade our biogeochemical models? *Soil Biology & Biochemistry*, 80, 167-174.
- Godin, A, McLaughlin, J.W., Webster, K.L., Packalen, M., & Basiliko, N. (2012). Methane and methanogen community dynamics across a boreal peatland nutrient gradient. *Soil Biology & Biochemistry*, 48, 96-105.
- Grundmann, G.L., Dechesne, A., Bartoli, F., Flandrois, J.P., Chassé, J.L., & Kizungu, R. (2001). Spatial modeling of nitrifier microhabitats in soil. *Soil Sci. Soc. Am. J.*, 65, 1709-1716.
- Hallam, S.J., Putnam, N., Preston, C.M., Detter, J.C., Rokhsar, D., Richardson, P.M., & DeLong, E.F. (2004). Reverse methanogenesis: testing the hypothesis with environmental genomics. *Science*, 305 (5689), 1457-1462.
- Hamilton, P.A., Denver, J.M., Phillips, P.J., & Shedlock, R.J. (1993). Water-quality assessment of the Delmarva Peninsula, Delaware, Maryland, and Virginia: Effects of agricultural activities on, and distribution of, nitrate and other inorganic constituents in the surficial aquifer. U.S. Geological Open-File Report. 93-40, 87 p.

- Hanson, G.C., Groffman, P.M., & Gold, A.J. (1994). Denitrification in riparian wetlands receiving high and low groundwater nitrate inputs. *Journal of Environmental Quality*, 23, 917-922.
- Haroon, M.F., Hu, S., Shi, Y., Imelfort, M., Keller, J., Hugenholtz, P., Yuan, Z., & Tyson, G.W. (2013). Anaerobic oxidation of methane coupled to nitrate reduction in a novel archaeal lineage. *Nature*, doi:10.1038/nature12375.
- Hatch, D.J., Jarvis, S.C., & Philipps, L. (1990). Field measurement of nitrogen mineralization using soil core and acetylene inhibition of nitrification. *Plant and Soil*, 124, 97-107.
- Hedin, L.O., von Fischer, J.C., Ostrom, N.E., Kennedy, B.P., Brown, M.G., & Roberson, G.P. (1998). Thermodynamic constraints on nitrogen transformations and other biogeochemical processes at soil-stream interfaces. *Ecology*, 79(2), 684-703.
- Hendriks, D.M.D., van Huissteden, J., Dolman, A.J., & van der Molen, M.K. (2007). The full greenhouse gas balance of an abandoned peat meadow. *Biogeosciences*, 4, 411-424.
- Hinrichs, K.-U., & Boetius, A. (2002). The anaerobic oxidation of methane: new insights in microbial ecology and biogeochemistry. In G. Wefer, D. Billett, D. Hebbeln, B.B. Jørgensen, M. Schlüter, & T.C.E van Weering (Eds.), *Ocean Margin Systems* (pp. 457-477), Berlin, Springer.
- Holland, H.D., Turekian, K.K., & Lollar, B.S. (2011). *Treatise on Geochemistry: Volume 9: Environmental Geochemistry*, Elsevier, 630 pp.

- Holmes, A.J., Roslev, P., McDonald, I.R., Iversen, N., Henriksen, K., & Murrell, J.C. (1999). Characterization of methanotrophic bacterial populations in soils showing atmospheric methane uptake. *Applied and Environmental Microbiology*, 65 (8), 3312-3318.
- Hope, D., Palmer, S.M., Billett, M.F., & Dawson, J.J.C. (2001). Carbon dioxide and methane evasion from a temperate peatland stream. *Limnol. Oceanogr.*, 46(4), 847-857.
- Howarth, R.W., Santoro, R., & Ingraffea, A. (2011). Methane and the greenhouse-gas footprint of natural gas from shale formations. *Climate Change*. 106, 679-690.
- Hu, S., Zeng, R.J., Burow, L.C., Lant, P., Keller, J., & Yuan, Z. (2009). Enrichment of denitrifying anaerobic methane oxidizing microorganisms. *Environmental microbiology reports*, 1(5), 377-384.
- Hu, S. Zeng, R.J., Keller, J., Lant, P.A., & Yuan, Z. (2011). Effect of nitrate and nitrite on the selection of microorganisms in the denitrifying anaerobic methane oxidation process. *Environmental Microbiology Reports*, 3 (3), 315-319.
- Hu, B., Shen, L., Lian, X., Zhu, Q., Liu, S., Huang, Q.,...& He, Y. (2014). Evidence for nitrite-dependent anaerobic methane oxidation as a previously overlooked microbial methane sink in wetlands. *PNAS*, 111 (12), 4495-4500.
- Hütsch, B.W., Webster, C.P., & Powlson, D.S. (1994). Methane oxidation in soil as affected by land use, soil pH and N fertilization. *Soil Biol. Biochem.*, 26(12), 1613-1622.

- Hutton, W. & ZoBell, C.E. (1949). The occurrence and characteristics of methane-oxidizing bacteria in marine sediments. *J. Bacteriolog*, 58, 463-473.
- Huttunen, J.T., Alm, J., Liikanen, A., Juutinen, S., Larmola, T., Hammar, T., Solvola, J., & Martikainen, P.J. (2003). Fluxes of methane, carbon dioxide and nitrous oxide in boreal lakes and potential anthropogenic effects on the aquatic greenhouse gas emissions. *Chemosphere*. 52, 609-621.
- IPCC, 2014: Climate Change 2014: Synthesis Report. Contribution of Working Groups I, II, and III to the Fifth Assessment Report of the International Governmental Panel on Climate Change [Core Writing Team, R.K. Pachauri and L.A. Meyer (eds.)] IPCC, Geneva Switzerland, 151 pp.
- Islas-Lima, S., Thalasso, F., & Gómez-Hernandez, J. (2004). Evidence of anoxic methane oxidation coupled to denitrification. *Water Res.*, 38(1), 13-16.
- Jarvis, S.C., Hatch, D.J., & Lovell, R.D. (2001). An improved soil core incubation method for the field measurement of denitrification and net mineralization using acetylene inhibition. *Nutrient Cycling in Agroecosystems*, 59, 219-225.
- Johnson, K.M., Hughes, J.E., Donaghay, P.L., Sieburth, J.M. (1990). Bottle-calibration static head space method for the determination of methane dissolved in seawater. *Anal. Chem.*, 62(21), 2408-2412.
- Jones, J.B., & Mullholland, P.J. (1998a). Methane input and evasion in a hardwood forest stream: Effects of subsurface flow from shallow and deep pathways. *Limnol. Oceanogr.* 43(6), 1243-1250.

- Jones, J.B., & Mullholland, P.J. (1998b). Influence of drainage basin topography and elevation on carbon dioxide and methane supersaturation of stream water. *Biogeochemistry*, 40, 57-72.
- Jordan, T.E., Whigham, D.F., Hofmockel, K.H., & Pitteck, M.A. (2003). Nutrient and sediment removal by a restored wetland receiving agricultural runoff. *Journal of Environmental Quality*, 32, 1534-1547.
- Jung, G.A., Shaffer, J.A., Stout, W.L., & Panciera, M.T. (1990). Warm-season grass diversity in yield, plant morphology, and nitrogen concentration and removal in northeastern USA. *Agronomy Journal*, 82, 21-26.
- Kampbell, D.H., & Vandegrift, S.A. (1998). Analysis of dissolved methane, ethane, and ethylene in ground water by a standard gas chromatographic technique. *J. Chromatogr. Sci.*, 36, 253-256.
- Kana, T.M., Darkangelo, C., Hunt, M.D., Oldham, J.B., Bennett, G.E., & Cornwell, J.C. (1994). Membrane inlet mass spectrometer for rapid high-precision determination of N₂, O₂, and Ar in environmental water samples. *Analytical Chemistry*, 66(23), 4166-4170.
- Karl, D.M. (2002). Nutrient dynamics in the deep blue sea. *TRENDS in Microbiology*, 10(9), 410-418.
- Kasper, J.W., Denver, J.M., & York, J.K. (2015). Suburban groundwater quality as influenced by turfgrass and septic sources, Delmarva Peninsula, USA. *Journal of Environmental Quality*, 44(2), 642-654.
- Kasting, J.F., & Siefert, J.L. (2003). Life and the evolution of Earth's atmosphere. *Science*, 296, 1066-1068.

- Kaushal, S.S., Groffman, P.M., Mayer, P.M., Striz, E., & Gold, A.J. (2008). Effects of stream restoration on denitrification in an urbanizing watershed. *Ecological Applications*, 18(3), 789-804.
- Kemp, W.M., Boynton, W.R., Adolf, J.E., Boesch, D.F., Boicourt, W.C., Brush, G.,... & Stevenson, J.C. (2005). Eutrophication of Chesapeake Bay: historical trends and ecological interactions. *Marine Ecology Progress Series*, 303, 1-29.
- Kietavaine, R., & Purkamo, L. (2015). The origin, source, and cycling of methane in deep crystalline rock biosphere. *Frontiers in Microbiology*, 6, 1-16.
- King, G. (1990). Ecological aspects of methane oxidation, a key determinant of global methane dynamics. In K.C. Marshall (Ed.), *Advances in Microbial Ecology* (pp. 431-468), Boston, Springer.
- Klüber, H.D., & Conrad, R. (1998). Inhibitory effects of nitrate, nitrite, NO and N₂O on methanogenesis by *Methanosarcina barkeri* and *Methanobacterium bryantii*. *FEMS Microbiology Ecology*, 25, 331-339.
- Knittel, K., & Boetius, A. (2009). Anaerobic oxidation of methane: Progress with an unknown process. *Annu. Rev. Microbiol.*, 63, 311-334.
- Koskelo A.I., Fisher T.R., Sutton A.J., & Gustafson A.B. (in review). Biogeochemical storm response in agricultural watersheds of the Choptank River Basin, Delmarva Peninsula, USA. *Biogeochemistry*. in review.
- Le Mer, J. & Roger, P. (2001). Production, oxidation, emission and consumption of methane by soils: A review. *Eur. J. Soil Biol.*, 37, 25-50.

- Lee, K.-Y., Fisher, T.R., & Rochelle-Newall, E. (2001). Modeling the hydrochemistry of the Choptank River basin using GWLF and Arc/Info: 2. Model Application. *Biogeochemistry*, 56, 311-348.
- Lindsey, B.D., Phillips, S.W., Donnelly, C.A., Speiran, G.K., Plummer, L.N., Böhlke, J.K., Focazio, M.J., Burton, W.C., & Busenberg, E. (2003). Residence times and nitrate transport in groundwater discharging to streams in the Chesapeake Bay Watershed. *Water-Resources Investigations Report 03-4035*. 215 pps.
- Liu, Y., & Whitman, W.B. (2008). Metabolic, phylogenetic, and ecological diversity of the methanogenic Archaea. *Incredible Anaerobes from Physiology to Genomics to Fuel*, 1125 (1), 171-189.
- Lovely, D.R., Chapelle, F.H., & Woodward, J.C. (1994). Use of dissolved H₂ concentrations to determine distribution of microbially catalyzed redox reactions in anoxic groundwater. *Environ. Sci. Technol.*, 28(7), 1205-1210.
- Lowrance, R., Altier, L.S., Newbold, J.D., Schnabel, R.R., Groffman, P.M., Denver, J.M.,...& Todd, A.H. (1997). Water quality functions of riparian forest buffer systems in Chesapeake Bay watersheds. *Environmental Management*, 21, 687-712.
- Luesken, F.A., van Alen, T.A., van der Biezen, E., Frijters, C., Toonen, G., Kampman, C.,...& Jetten, M.S.M. (2011). Diversity and enrichment of nitrite-dependent anaerobic methane oxidizing bacteria from wastewater sludge. *Appl. Microbiol. Biotechnol.*, 92, 845-854.

- Lyngkilde, J., & Christensen, T.H. (1992). Redox zones of a landfill leachate pollution plume (Vejen, Denmark). *Journal of Contaminant Hydrology*, 10, 273-289.
- Mancinelli, R.L. (1995). The regulation of methane oxidation in soil. *Annu. Rev. Microbiol.*, 49, 581-605.
- Martens, C.S., & Berner, R.A. (1977). Interstitial water chemistry of anoxic Long Island Sound sediments: Dissolved gases. *Limnol. Oceanogr.*, 22, 10-25.
- McCarty, G.W., McConnell, L.L., Hapeman, C.J., Sadeghi, A., Graff, C., Hively, W.D., Lang, M.L., Fisher, T.R., Jordan, T., Rice, C.P., Codling, E.E., Whitall, D., Lynn, A., Keppler, J., & Fogel, M.L. (2008). Water quality and conservation practice effects in the Choptank River watershed. *J. Soil Water Conserv.*, 63, 461-474.
- McLaughlin, M.R., Fairbrother, T.E., & Rowe, D.E. (2004). Nutrient uptake by warm-season perennial grasses in a swine effluent spray field. *Agronomy Journal*, 96, 484-493.
- McMahon, P.B., & Böhlke, J.K. (1996). Denitrification and mixing in a stream-aquifer system: effects on nitrate loading to surface water. *Journal of Hydrology*, 105-128.
- Modin, O., Fukushi, K., & Yamamoto, K. (2007). Denitrification as methane as external carbon source. *Water Research*, 41, 2726-2738.
- Morse, J.L., Ardón, M., & Bernhardt, E.S. (2012). Greenhouse gas fluxes in southeastern U.S. coastal plain wetlands under contrasting land uses. *Ecological Applications*, 22, 264-280.

- Ni, X., & Groffman, P.M. (2018). Declines in methane uptake in forest soils. *PNAS*, 115(34), 8587-8590.
- NOAA NCDC. (2014). Monthly Summaries of the Global Historical Climatology Network-Daily (GHCN-D) Dataset C00841. 19 Aug 2014.
- Nordi, K., & Thamdrup, B. (2014). Nitrate-dependent anaerobic methane oxidation in a freshwater sediment. *Geochimica et Cosmochimica Acta*, 132, 141-150.
- Orphan, V.J., House, C.H., Hinrichs, K.-U., McKeegan, K.D., & DeLong, E. (2002). Multiple archaeal groups mediate methane oxidation in anoxic cold seep sediments. *PNAS*, 99 (11), 7663-7668.
- Parkin, T.B., Kaspar, H.F., Sexstone, A.J., & Tiedje, J.M. (1984). A gas-flow soil core method to measure field denitrification rates. *Soil Biol. Biochem.*, 16(4), 323-330.
- Pitz, S., & Megonigal, J.P. (2017). Temperate forest methane sink diminished by tree emissions. *New Phytologist*, 214, 1432-1439.
- Priemé, A., Christensen, S., Dobbie, K.E., & Smith, K.A. (1997). Slow increase in rate of methane oxidation in soils with time following land use change from arable agriculture to woodland. *Soil Biol. Biochem.*, 29(8). 1269-1273.
- Primrose, N.L., Millard, C.J., McCoy, J.L., Dobson, M.G., Sturm, P.E., Bowen, S.E., & Windschitl, R.J. (1997). German Branch targeted watershed project: Biotic and water quality monitoring evaluation report 1990–95. Annapolis (MD): Maryland Department of Natural Resources. Report no. CCWS-WRD-MN-97-03.

- Raghoebarsing, A.A., Pol, A., van de Pas-Schoonen, K.T., Smolders, A.J.P, Ettwig, K.F., Rijpstra, W.I.C.,...& Strous, M. (2006). A microbial consortium couples anaerobic methane oxidation to denitrification. *Nature*, 440, 918-921.
- Reay, W.G. (2004). Septic tank impacts on ground water quality and nearshore sediment nutrient flux. *Ground Water*, 42(7), 1079-1089.
- Reeburgh, W.S. (1976). Methane consumption in Cariaco Trench waters and sediments. *Earth and Planetary Science Letters*, 28, 337-344.
- Reeburgh, W.S. (2007). Ocean methane biogeochemistry. *Chem. Rev.*, 107, 486-513.
- Ritz, S., Dähnke, K., & Fischer, H. (2018). Open-channel measurement of denitrification in large lowland river. *Aquatic Sciences*, 80(11), <https://doi.org/10.1007/s00027-017-0560-1>.
- Rooze, J., Egger, M., Tsandev, I., & Slomp, C.P. (2016). Iron-dependent anaerobic oxidation of methane in coastal surface sediments: potential controls and impacts. *Limnol. Oceanogr.*, 61, 267-282.
- Roy, R., & Conrad R. (1999). Effect of methanogenic precursors (acetate, hydrogen, propionate) on the suppression of methane production by nitrate in anoxic rice field soil. *FEMS Microbiology Ecology*, 28, 49-61.
- Ryden, J.C., Skinner, J.H., & Nixon, D.J. (1987). Soil core incubation system for the field measurement of denitrification using acetylene-inhibition. *Soil Biol. Biochem.* 19(6), 753-757.
- Ryther, J.H. & Dunstan, W.M. (1971). Nitrogen, phosphorus, and eutrophication in the coastal marine environment. *Science*, 171, 1008-1013.

- Sanders, I.A., Heppell, C.M., Cotton, J.A., Wharton, G., Hildrew, A.G., Flowers, E.J., & Trimmer, M. (2007). Emission of methane from chalk streams has potential implications for agricultural practices. *Freshwater Biology*, 52, 1176-1186.
- Sanford, W.E., & Pope, J.P. (2013). Quantifying groundwater's role in delaying improvements to Chesapeake Bay water quality. *Environmental Science and Technology*, 47(23), 13330-13338.
- Schilling, K.E., & Jacobson, P. (2010). Groundwater conditions under a reconstructed prairie chronosequence. *Agriculture, Ecosystems and Environment*, 135, 81-89.
- Schilling, K.E., & Spooner, J. (2006). Effects of watershed-scale land use change on stream nitrate concentrations. *Journal of Environmental Quality*, 35, 2132-2145.
- Schubert, C.J., Vazquez, F., Lösekann-Behrens, T., Knittel, K., Tonolla, M., & Boetius, A. (2011). Evidence for anaerobic oxidation of methane in sediments of a freshwater system (Lago di Cadagno). *FEMS Microbiol. Ecol.*, 76, 26-38.
- Segarra, K.E.A., Schubotz, F., Samarkin, V., Yoshinaga, M.Y., Hinrichs, K.-U., & Joye, S.B. (2015). High rates of anaerobic methane oxidation in freshwater wetlands reduce potential atmospheric methane emissions. *Nature Communications*, DOI: 10.1038/ncomms8477.
- Segers, R. (1998). Methane production and methane consumption: A review of processes underlying wetland methane fluxes. *Biogeochemistry*, 41, 23-51.

- Shen, L., Hu, B., Liu, S., Chai, X., He, Z., Ren, H.,...& Zheng, P. (2016). Anaerobic methane oxidation coupled to nitrite reduction can be a potential methane sink in coastal environments. *Appl. Microbiol. Biotechnol.*, 100, 7171-7180.
- Shima, S., & Thauer, R.K. (2005). Methyl-coenzyme M reductase and the anaerobic oxidation of methane in methanotrophic Archaea. *Current Opinion in Microbiology*, 8, 643-648.
- Shindell, D.T., Faluvegi, G., Koch, D.M., Schmidt, G.A., Unger, N., & Bauer, S.E. (2009). Improved attribution of climate forcing to emissions. *Science*. 326, 716-718.
- Silveira, M.L., Haby, V.A., & Leonard, A.T. (2007). Response of coastal Bermudagrass yield and nutrient uptake efficiency to nitrogen sources. *Agronomy Journal*, 99, 707-714.
- Sivan, O., Adler, M., Pearson, A., Gelman, F., Bar-Or, I., John, S.G., & Eckert, W. (2011). Geochemical evidence for iron-mediated anaerobic oxidation of methane. *Limnol. Oceanogr.*, 56(4), 1536-1544.
- Smith, R.L., Howes, B.L., & Garabedian, S.P. (1991). In situ measurement of methane oxidation in groundwater by using natural-gradient tracer tests. *Applied and Environmental Microbiol.*, 57(7), 1997-2004.
- Smith, V.H., Tilman, G.D., & Nekola, J.C. (1999). Eutrophication impacts of excess nutrient inputs of freshwater marine, and terrestrial ecosystems. *Environmental Pollution*, 100, 179-196.

- Soil Survey Staff, Natural Resources Conservation Service, United State Department of Agriculture, 2015. Soil Survey. <http://websoilsurvey.nrcs.usda.gov/> (accessed 01.06.16).
- Spalding, R.F., & Exner, M.E. (1993). Occurrence of nitrate in groundwater-a review. *Journal of Environmental Quality*, 22, 392-402.
- Stanley, E.H., Casson, N.J., Christel, S.T., Crawford, J.T., Loken, L.C., & Oliver, S.K. (2016). The ecology of methane in streams and rivers: patterns, controls, and global significance. *Ecological Monographs*, 86(2), 146-171.
- Staver, K.W., & Brinsfield, R.B. (2001). Agriculture and water quality on the Maryland Eastern Shore: Where do we go from here? *BioSciences*, 51, 859-868.
- Sutton, A.J., Fisher, T.R., & Gustafson, A.B. (2009). Historical changes in water quality at German Branch in the Choptank River basin. *Water Air Soil Poll*, 199, 353-369.
- Szal, D., & Gruca-Rokosz, R. (2019). Denitrification-dependent anaerobic oxidation of methane in freshwater sediments of reservoirs in SE Poland. *J. of Ecological Engineering*, 20(9), 218-227.
- Tesoriero, A.J., Liebscher, H., & Cox, S.E. (2000). Mechanism and rate of denitrification in an agricultural watershed: Electron and mass balance along groundwater flow paths. *Water Resources Research*, 36, 1545-1559.
- Tesoriero, A.J., & Puckett, L.J. (2011). O₂ reduction and denitrification rates in shallow aquifers. *Water Resources Research*, doi:10.1029/2011WR010471.

- Timmer, P.H.A., Welte, C.U., Koehorst, J.J., Plugge, C.M., Jetten, M.S.M., & Stams, A.J.M. (2017). Reverse methanogenesis and respiration in methanotrophic Archaea. *Archaea*, 2017, <https://doi.org/10.1155/2017/1654237>.
- Tomer, M.D., Schilling, K.E., Cambardella, C.A., Jacobson, P., & Drobney, P. (2010). Groundwater nutrient concentrations during prairie reconstruction on an Iowa landscape. *Agriculture, Ecosystems and Environment*, 139, 206-213.
- Tufekcioglu, A., Raich J.W., Isenhardt, T.M., & Schultz, R.C. (2003). Biomass, carbon, and nitrogen dynamics of multi-species riparian buffers within an agricultural watershed in Iowa, USA. *Agroforestry Systems*, 57, 187-198.
- Valenzuela, E.I., Prieto-Davó, A., López-Lozano, A.H.E., Vega-Alvarado, L., Juárez, K., García-González, A.S.,...& Cervantes, F.J. (2017). Anaerobic methane oxidation driven by microbial reduction of natural organic matter in a tropical wetland. *Appl. and Environ. Microbiol.*, 83(11), 1-15.
- Valiela, I., & Costa, J.E. (1988). Eutrophication of Buttermilk Bay, a Cape Cod coastal embayment: concentrations of nutrients and watershed nutrient budgets. *Environmental Management*, 12(4), 539-553.
- Vitousek, P.M., Aber, J.D., Howarth, R.W., Likens, G.E., Matson, P.A., Schindler, D.W.,...& Tilman, D.G. (1997). Technical report: Human alteration of the global nitrogen cycle: Sources and consequences. *Ecological Applications*, 7(3), 737-750.
- Vogels, G.D., van der Drift, C., Stumm, C.K., Keltjens, J.T., & Zwart, K.B. (1984). Methanogenesis: surprising molecules, microorganisms and ecosystems. *Antoine van Leeuwenhoek*, 50(5-6), 557-567.

- Wang, Y., Wang, D., Yang, Q., Zeng, G., & Li, X. (2017). Wastewater opportunities for denitrifying anaerobic methane oxidation. *Trends in Biotechnology*, 35 (9), 799-802.
- Weather Underground. (2014). La Trappe Creek (KMDTRAPP1), Maryland. www.wunderground.com (accessed 05.04.15).
- Wu, M.L., van Alen, T.A., van Donselaar, E.G., Strous, M., Jetten, M.S.M., & van Niftrik, L. Co-localization of particulate methane monooxygenase and cd_1 nitrite reductase in the denitrifying methanotroph 'Candidatus Methylomirabilis oxyfera.' *FEMS*, 334, 49-56.
- Yavitt, J.B., Lang, G.E., & Sexstone, A.J. (1990). Methane fluxes in wetland and forest soils, beaver ponds, and low-order streams of a temperate forest ecosystem. *Journal of geophysical research*, 95, 463-474.
- Yavitt, J.B., Kryczka, A.K., Huber, M.E., Pipes, G.T., & Rodriguez, A.M. (2019). Inferring methane production by decomposing tree, shrub, and grass leaf litter in bog and rich fen peatlands. *Front. Environ. Sci.*, 7(182), 1-15.
- Zedler, J.B. (2003). Wetlands at your service: reducing impacts of agriculture at the watershed scale. *Frontiers in Ecology and the Environment*, 1(2), 65-72.
- Zhu, G., Jetten, M.S.M., Kusch, P., Ettwig, K.F., & Yin, C. (2010). Potential roles of anaerobic ammonium and methane oxidation in the nitrogen cycle of wetland ecosystems. *Applied Microbiology & Biotechnology*, 86 (4), 1043-1055).